INVESTIGATION OF INERTIAL SUPPORT LIMITS IN WIND TURBINES AND THE EFFECTS IN THE POWER SYSTEM STABILITY

A THESIS SUBMITTED TO
THE GRADUATE SCHOOL OF NATURAL AND APPLIED SCIENCES
OF
MIDDLE EAST TECHNICAL UNIVERSITY

BY

ERENCAN DUYMAZ

IN PARTIAL FULFILLMENT OF THE REQUIREMENTS
FOR
THE DEGREE OF MASTER OF SCIENCE
IN
ELECTRICAL AND ELECTRONICS ENGINEERING

JANUARY 2019

Approval of the thesis:

INVESTIGATION OF INERTIAL SUPPORT LIMITS IN WIND TURBINES AND THE EFFECTS IN THE POWER SYSTEM STABILITY

submitted by **ERENCAN DUYMAZ** in partial fulfillment of the requirements for the degree of **Master of Science in Electrical and Electronics Engineering Department, Middle East Technical University** by,

Prof. Dr. Halil Kalıpçılar _____
Dean, Graduate School of **Natural and Applied Sciences**

Prof. Dr. Tolga Çiloğlu _____
Head of Department, **Electrical and Electronics Engineering**

Assist. Prof. Dr. Ozan Keysan _____
Supervisor, **Electrical and Electronics Engineering, METU**

Examining Committee Members:

Assoc. Prof. Dr. Murat Göl
Electrical and Electronics Engineering, METU _____

Assist. Prof. Dr. Ozan Keysan
Electrical and Electronics Engineering, METU _____

Prof. Dr. Oğuz Uzol
Aerospace Engineering, METU _____

Assist. Prof. Dr. Emine Bostancı
Electrical and Electronics Engineering, METU _____

Assist. Prof. Dr. Tolga İnan
Electrical and Electronics Engineering, Çankaya University _____

Date: _____

I hereby declare that all information in this document has been obtained and presented in accordance with academic rules and ethical conduct. I also declare that, as required by these rules and conduct, I have fully cited and referenced all material and results that are not original to this work.

Name, Last Name: Erencan Duymaz

Signature :

ABSTRACT

INVESTIGATION OF INERTIAL SUPPORT LIMITS IN WIND TURBINES AND THE EFFECTS IN THE POWER SYSTEM STABILITY

Duymaz, Erencan
M.S., Department of Electrical and Electronics Engineering
Supervisor : Assist. Prof. Dr. Ozan Keysan

January 2019, 111 pages

In this study, the inertial support implementation is studied for variable speed wind turbines with a full-scale power electronics. To increase the active power as desired, Machine Side Converter is modified with an additional control loop. In the first part of the thesis, active power of the wind turbine is increased to the limits and the maximum achievable active power is found out to be restricted by the wind speed. It is found that the wind turbine can increase its output power by 40% of rated power in the low and medium wind speeds. Moreover, even though the high speed scenarios gives limited increased power, it does not require any speed recovery state. The probability of different wind speeds and the inertial supports are found according to the wind speed measurement taken from field. In the second part of the thesis, the synthetic inertia implementation is presented by the provision of inertial support which is proportional to rate of change of frequency. The effect of the implementation in the P.M.Anderson test case is observed for different inertia constants. It is discovered that the effect of renewable penetration in the frequency stability is negligible when the synchronous generators are kept in the operation. Nonetheless, frequency stability in

the test system gets more vulnerable to renewable energy penetration when the conventional generators are decommissioned by the economical concerns. In this case, the synthetic inertia implementation with different inertia constants possess the ability to lower RoCoF following a frequency disturbance. Finally, the wind turbine inertial support is evaluated in terms of economics for the energy provider perspective.

Keywords: Power System Frequency Stability, Inertial Support, Synthetic Inertia, Virtual Inertia, Renewable Energy

ÖZ

RÜZGAR TÜRBİNLERİNDE ATALET DESTEĞİNİN SINIRLARININ İNCELENMESİ VE GÜÇ SİSTEMLERİ STABİLİTESİNE ETKİLERİ

Duymaz, Erencan
Yüksek Lisans, Elektrik ve Elektronik Mühendisliği Bölümü
Tez Yöneticisi : Yrd. Doç. Dr. Ozan Keysan

Ocak 2019 , 111 sayfa

Bu çalışmada, tam ölçek güç elektronikli değişken hızlı rüzgar türbinleri için atalet desteği uygulanmıştır. Aktif gücü istenildiği gibi arttırabilmek için Makine Tarafı Kontrolcüsüne kontrol döngüsü eklenmiştir. Bu tez çalışmasının ilk kısmında, rüzgar türbinin aktif gücü sınır noktalarına kadar arttırılmıştır ve ulaşılabilir maksimum gücün rüzgar hızıyla kısıtlandığı gözlenmiştir. Ayrıca, düşük ve orta rüzgar hızlarında rüzgar türbininin aktif gücünü nominal gücünün %40 oranında arttırabildiği gözlenen bulgular arasındadır. Bunun yanında, yüksek rüzgar senaryolarında sınırlı güç artışı gözlense de, generatör hızının toparlanma evresine gerek duymadığı gözlenmiştir. Sahadan alınan rüzgar hızı verilerine göre değişik rüzgar hızı ve atalet desteklerinin olma olasılıkları da hesaplanmıştır. Tezin ikinci kısmında, frekansın değişim hızıyla ortantılı atalet desteği uygulayarak yapay atalet desteği uygulanmıştırç Bu uygulamanın etkileri, değişik atalet sabitleri ile P.M. Abderson test düzeneğinde gözlenmiştir. Buna göre, konvansiyonel senkron makineler operasyonda olduğu sürece, yenilenebilir enerji penetrasyonun frekans stabilitesine olan etkisinin ihmal edilebilir düzeyde olduğu görülmüştür. Ancak, generatörlerin ekonomik kaygılarla operasyondan alın-

dığı durumlarda, yenilenebilir enerji penetrasyonun frekans stabilitesini zayıflattığı gözlenmiştir. Bu durumlar, değişik atalet sabitleriyle uygulanabilen yapay ataletin frekans bozunumlarında sistemin frekans değişim hızını azalttığı sonucuna varılmıştır. Son olarak, rüzgar türbinin atalet desteğinin ekonomik yönü enerji üretici açısından incelenmiştir.

Anahtar Kelimeler: Güç Sistemleri Frekans Stabilitesi, Atalet Desteği, Yapay Atalet, Sanal Atalet, Yenilebilir Enerji

To my family..

ACKNOWLEDGMENTS

Firstly, I would like to express my greatest appreciation to my supervisor, Assist.Prof.Dr. Ozan Keysan for his faith in me. I will be grateful for his endless support, guidance and encouragement.

I would like to thank examining committee members Assoc. Prof. Dr. Murat Göl, Assist. Prof. Dr. Emine Bostancı, Prof. Dr. Oğuz Uzol and Assist. Prof. Dr. Tolga İnan as the second reader of this thesis.

I wish to thank my dearest friends Aysel Akgemci, Doğa Ceylan, Siamak Pourkeivannour, İlker Şahin and the rest of the PowerLab research group.

I would like to share my heartfelt thanks to Ece Büber for her endless support, extreme love and thoughtfulness. She always believed in me and made me feel as special. I am grateful for the entire time that we spent together.

I must also express my gratitude to my family members, Nazikar, Hüseyin and Anılcan for their faith in me, their support and encouragement.

TABLE OF CONTENTS

LIST OF TABLES

TABLES

LIST OF FIGURES

FIGURES

LIST OF ABBREVIATIONS

AC	Alternating Current
AGC	Automatic Generation Control
CDF	Cumulative Distribution Function
DC	Direct Current
DFIG	Doubly Fed Induction Generator
EESG	Electrically Excited Synchronous Generator
FFR	Firm Frequency Response
FSIG	Fixed Speed Induction Generator
FSPC	Full Scale Power Converter
GSC	Grid Side Converter or Controller
HCS	Hill-Climb Search
HV	High Voltage
IGBT	Insulated Gate Bipolar Transistor
LSC	Line Side Converter or Controller
LVRT	Low Voltage Ride-Through
MOSFET	Metal Oxide Semiconductor Field Effect Transistor
MSC	Machine Side Converter or Controller
PDF	Probability Density Function
PI	Proportional-integral
PLL	Phase-Locked Loop
PMSG	Permanent Magnet Synchronous Generator
PSPC	Partial Scale Power Converter
P&O	Perturb&Obserb
PSF	Power Signal Feedback
RES	Renewable Energy System
RoCoF	Rate of Change of Frequency

LIST OF SYMBOLS

C_p	Power Coefficient
f_{grid}	Grid Frequency
H	Inertia Constant
J_{tur}	Turbine Inertia
J_{gen}	Generator Inertia
J_{total}	Total Equivalent Inertia
λ	Tip Speed Ratio
λ_{opt}	Optimal Tip Speed Ratio
β	Pitch or Blade Angle
P_e	Electromechanical Output Power
P_{gen}	Generator Active Power
P_{grid}	Active Power injected to Grid
P_m	Input Mechanical Power
P_{tur}	Turbine Active Power
P_{rated}	Rated Active Power
p	Number of Pole
p_p	Number of Pole Pair
P_{wind}	Aerodynamic Wind Power
S_{base}	Base Apparent Power
ω_m	Generator Speed
ω_{max}	Maximum Generator Speed
T_{Plim}	Torque Limited by Active Power of Wind Turbine
T_{Slim}	Torque Limited by Apparent Power of Wind Turbine

CHAPTER 1

INTRODUCTION

1.1 Global Renewable Energy Status

The share of the renewable energy systems has been reached significant levels. At the end of 2017, the renewable power capacity has reached 2179 GW throughout the world including hydro power plants [2]. Fig. 1.1 shows the installed renewable energy capacity for leading countries at the end of 2016 and 2017. China, USA, Brazil and Germany constitutes almost half of the world total capacity. China has the biggest installed renewable capacity so far and increased its capacity by 73 GW in 2017.

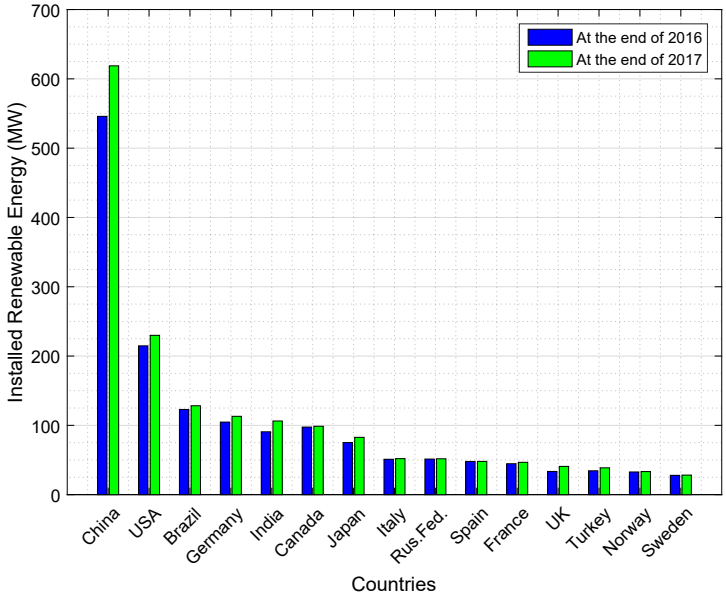

Figure 1.1: Installed Renewable Energy Capacity of Leading Countries [2], [3]

EU countries promotes the renewable energy systems from the very beginning. In

2008, 20 20 by 2020-Europe's Climate Change Opportunity report has been released by EU Commission and two key targets are set for 2020 [11]:

- At least 20 % reduction in greenhouse gases (GHG) by 2020
- Achieving 20% renewable energy share in energy consumption of EU by 2020

In order to accomplish this target, the Renewable Energy Directive is published in 23 April 2009. This directive has set national binding targets for EU countries in order to accomplish the 20% renewable energy target for EU and 10 % target for the renewable energy usage in the transport. [12] As a result, each EU country has been determined their national action plans. In order to achieve the 20 % target, each member state determine their own targets ranging from 10% in Malta to 49% in Sweeden. According to the latest release by Eurostat, renewable share of the EU in energy consumption has reached 17 % in 2016 [13]. Moreover, eleven of EU member states has already achieved their 2020 targets.

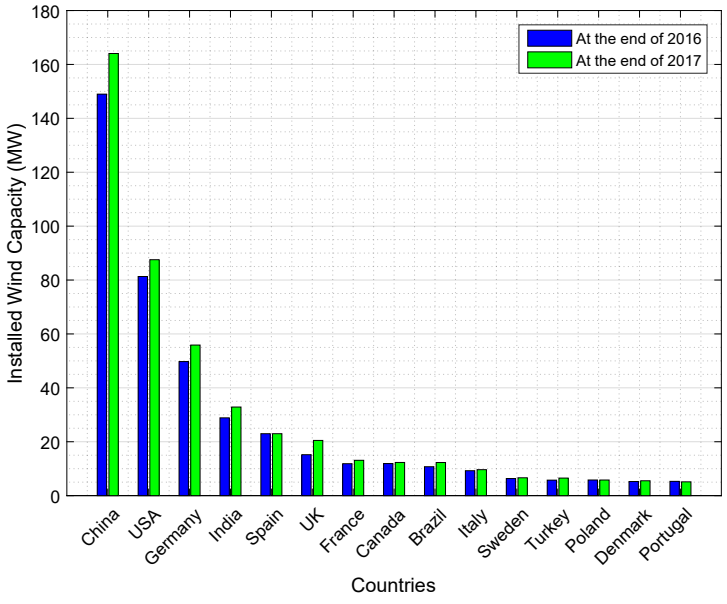

Figure 1.2: Wind Power Capacity of Leading Countries in 2016 [2], [3]

Wind power has the highest share among the renewable energy sources in the installed renewable energy capacity except for hydro power. The wind power capacity at the end of 2017 has reached 514 GW worldwide [2]. The installed wind power capacity

of the leading countries is shown in the Fig. 1.2. As in the case of total installed renewable energy capacity, China and USA have also the highest installed capacities in the wind power capacity.

The share of renewable energy is increasing continuously. Today, the discussion is about whether 100% renewable energy is possible in the upcoming future. In [14], grid integration issues of wind and solar and the lack of sufficient storage technologies are considered as the main barrier for this target meanwhile the major problem seems as the existing energy industry. Nonetheless, a significant renewable share is expected even though the 100% is reality or not. The report published by IRENA (International Renewable Energy Agency) estimates the share of renewable energy in EU as 24% by 2030 which is below proposed target of 27% [15]. Nonetheless, the increase in the renewable energy share will continue in the upcoming future.

1.2 Renewable Energy Problems

It is an undeniable fact that renewable energy systems are advantageous in terms of global warming and carbon dioxide emission. Nonetheless, they also have disadvantages to the system operators due to intermittent energy generation profile. First of all, the term intermittent in the literature is related to the variable and uncontrollable nature of the renewable sources [16]. Since the source of the RES is variable, it is not possible to adjust its output according to the demand. Therefore, the thermal plants have to be in the operation when high wind speeds and solar radiation exist. Moreover, the system requires additional start-ups and rise from partly loaded plants in order to balance the energy in the system because of the uncertainty of RES. These all create additional costs caused by high share of RES in the system [17]. Besides, power grid will face with transmission system issues as overloaded transmission lines, changes on the protection and control in the distribution system, greater level of power-factor control and low voltage ride-through (LVRT) requirements when the RES share is increased in the grid [18].

Another challenge of increasing RES is the problem of power system frequency stability. Since the frequency of the power system depends on the balance between

generation and consumption, grid operators are responsible for adjusting the generation in order to maintain a constant frequency. However, the renewable energy generation is strictly dependent on the renewable source i.e. solar radiation or wind speed. Therefore, renewable systems makes the system operation harder due to their intermittent and uncertain power generation profiles.

Frequency of the grid depends on the balance between supply and demand. As the balance is established, frequency stays constant. However, that is the ideal case. In fact, the load always varies. It is the responsibility of the grid operator to provide continues balance. Consequently, the grid frequency varies around the nominal frequency with small deviations.

However, unintentional generation unit outages or instant load connections cause high deviations in the grid. A generic frequency disturbance is depicted in the Fig. 1.3. In the beginning of the disturbance, frequency falls with a slope that is called Rate of Change of Frequency (RoCoF) until the minimum frequency what is called frequency nadir. Grid RoCoF is limited with the inertia of the generators. The higher grid inertia decreases RoCoF and increases the frequency nadir.

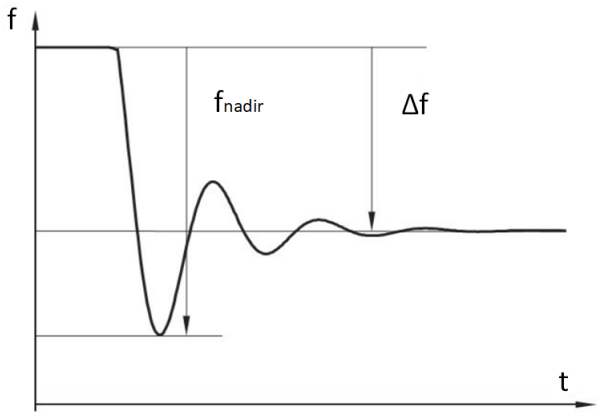

Figure 1.3: A Generic Frequency Disturbance

As the renewable systems with power electronics interface increase in the electricity grid, the grid equivalent inertia decreases. In [19], the reduced grid inertia due to the high DFIG wind turbine penetration is emphasized. Moreover, the results of the reduced grid inertia following a disturbance is listed as:

- increased effective aggregated angular acceleration of synchronous machines which require high restoring forces
- high rate of change of frequency and hence, decreased frequency nadir

It should be noted that this problem is not specific to DFIG wind turbines but renewable energy systems which are connected to grid with power electronics. Conventional synchronous generators rotate at synchronous speed which is proportional to the grid frequency. If the grid frequency decreases, then the synchronous speed also decreases. In this case, the generator active power is increased inherently due to kinetic energy extraction from the generator inertia. The increase in active power provides action time for primary controllers and crucial for frequency stability.

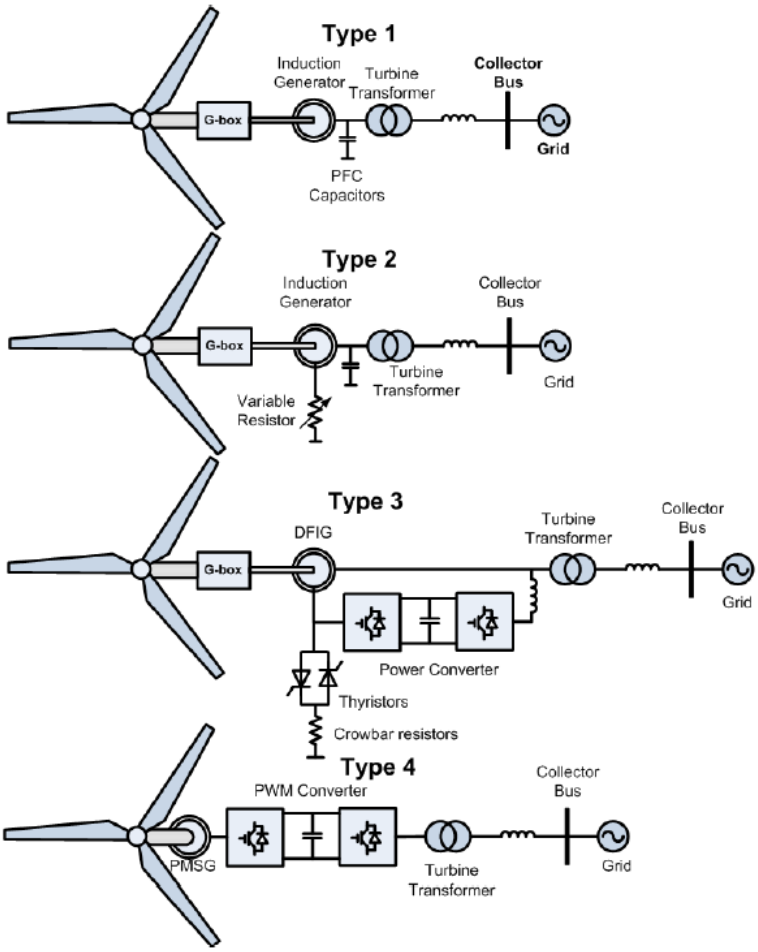

Figure 1.4: Wind Turbine Generator Configurations [4]

Different turbine topologies gives different reactions to the frequency disturbances.

Wind turbine generator topologies are shown in Fig. 1.4. Type-1 turbines are connected to grd with a asynchronous generators. The wind turbine generates active power as turbine rotates faster than synchronous speed. Therefore, the generator operates at the linear part of the torque-slip curve. Hence, the change in the grid frequency causes smaller decrease in the turbine speed. Type-2 is very similar to Type-1 except for the variable resistor which can shift the torque speed curve slightly. Hence, the frequency deviations affects the active power output of Type-1 and Type-2 [4]. Type-3 wind turbines include Doubly-Fed Induction Generator (DFIG). DFIG stator is directly connected to grid meanwhile its rotor is connected to grid with a Partial Scale Power Converter (PSPC). Even though the stator is directly coupled to stator, the power electronics enable wind turbine to operate in a range of speeds. Therefore, the rotor frequency is also decoupled from grid.

Type-4 wind turbines are connected to grid with back-to-back converters i.e. FSPC. AC/DC and DC/AC conversion decouples the grid frequency and the turbine speed. Thanks to this decoupling, Type-3 and Type-4 turbines can operate at the MPPT speed that will capture the maximum power from air. Nonetheless, this results that Type-3 and 4 wind turbines is not affected from the grid frequency deviations. Therefore, these systems have no contribution to the grid inertia despite the system includes significant inertia. Hence, the aggregated grid inertia is reduced with the penetration of wind turbines with power electronics. The comparison for different type of generators is made in [20] and listed in Table 1.1.

Type of the generator	**Inertial Response Behaviour**
Conventional Synchronous Generator	++
Fixed Speed Induction Generator (FSIG)	+
Doubly Fed Induction Generator (DFIG)	-
Variable Speed Wind Turbine Generator (Connected with Full Scale Power Electronics)	None

Table 1.1: Comparison of Different Type of Generators for Inertial Response Behaviour

Another reason for the decrease in the grid inertia is the de-commitment or dispatch

of the conventional sources due to economic concerns. Since the renewable energy systems have the lowest cost for energy production, they are preferred instead of conventional generators im the economical dispatch. As a result, conventional generators are dispatched to a lower generation profile or taken-off from operation.

It should be noted that grid inertia is directly related to the amount of load in the system in addition to the share of RES. Since the amount of online generators fluctuates within time, the grid aggregated inertia also changes. Hence, the scenario in which the system has low demand and also high renewable generation is the most critical one since the lowest grid inertia will be faced in the network.

1.3 Literature Review

Studies regarding inertial support date back to early 2000s. In the study [21], the effect of the increasing wind energy penetration has been investigated. The study concludes that increasing share of wind energy increases the primary reserve requirement for the successful grid operation. The increased frequency deviations, especially in light load conditions (high wind generation with low consumption scenario) can be mitigated in the system as long as the wind generation provides inertia support. Study in [22] states that DFIG wind turbines are de-coupled from power system resulting in no contribution to system inertia. A supplementary loop is proposed for reinstating the machine inertia. Moreover, in [23], performance of the supplementary control loop is evaluated with the comparison of the inertial support of a fixed-speed wind turbine. The proposed control loop has been validated in [24] and compared with the droop control in [25].

It is an undeniable fact that renewable energy systems are the most economical way of producing electrical energy due to absence of any fuel cost. Therefore, they are to be operated in their rated power. However, they have to curtail their power in order to leave a margin for droop control. Droop control by wind energy is also studied in the literature. In [4], the inertial support of different type of wind turbines is compared. It is concluded that the Type-4 wind turbines are able to perform better performance for inertial support due to the power electronics interface. Moreover, combination of

inertial support and droop control produces better results in these wind turbines.

Fast inertial response is studied in the literature as Torque-Limit based inertial support or Stepwise Inertial Control in the studies [26], [27]. Nonetheless, the support is achieved by the operation in the limit torque independent from the size of the disturbance and the support is ended at the pre-defined generator speed. Still, limits of the support for varying wind speed is not studied as well as the restoration of the generator speed is not discussed.

The concept of the synthetic inertia has been widely studied in the literature since it is a method for renewable energy systems to emulate synchronous generators. In [28], the method is implemented a VSC-HVDC transmission systems in order to improve frequency stability of a weak grid. Study [29] focuses on the implementation in the PV systems in a coordination with energy storage systems. In the studies [20], [30], the method is implemented on a variable speed wind turbines. The effects of the synthetic inertia implementation in a full-scale wind turbine is studied in [31].

General Electrics has active power control module called as WindInertia for their wind turbines in order to react the large frequency disturbances. The control module increase the power output of the wind turbine by 10% for 15 seconds [32]. Moreover, the Enercon provides inertial response capability to its turbines by allowing 10% increase in the active power [33]. Nonetheless, solutions of GE and Enercon are independent of the grid RoCoF.

However, the full capacity of the wind turbines for inertial support is not studied in the literature. Practical limits of the inertial support has been studied in [34] by varying the inertia constant to be emulated. However, the practical limits in terms of maximum achievable power and turbine internal parameters are not focused in the study. Moreover, the studies does not compare the two main method of the inertial support namely, fast frequency support and frequency based method. Finally, the studies does not focus on the wind speed for the inertial support capacity.

1.4 Thesis Motivation

Although renewable energy systems are beneficial for environmental concerns and lower energy cost, higher renewable penetration also brings operational challenges for system operators. One of the most important problem that comes with renewable energy is the power system frequency instability. With the high renewable penetration, grid aggregated inertia decreases. As a result, grid is exposed to high rate of change of frequency (RoCoF) for the disturbances. This implies that the power systems successful operation with increasing renewable energy penetration is not achievable unless the decrease in the grid inertia is prevented. Therefore, the main objective of this study is to avoid the decrease in the grid inertia arising with the renewable energy penetration. In this way, the share of renewable energy systems can be increased without the negative effects on the power system operation.

Wind energy systems, especially variable speed wind turbines with full scale power electronics are the most promising renewable energy systems that can contribute to grid frequency stability thanks to their high inertia in their blades and generator and also their back-to-back converters that give ability to control its active power. Wind turbine with full-scale power electronics is the key solution to be used against the decrease in the grid inertia. However, the full capability of a wind turbine with full-scale power electronics has not been discovered yet. This study will explore the full capacity of the wind turbines for the inertial support. The practical limits of the wind turbines is explored under different wind speed scenarios. Another objective of this study is revealing the effects of grid supporting functions in the wind turbines. Besides, the differences between the frequency dependent and independent inertial support mechanisms is investigated especially for weak power systems.

1.5 Thesis Outline

This thesis study focuses on the wind turbine inertial support limits and its effects in power system stability. The thesis starts with a brief summary of the renewable energy status in Chapter 1. By reviewing the share of the renewable energy systems and the targets for upcoming future highlight the importance of the frequency stability

studies.

In the Chapter 2, the frequency concept in power systems is extensively described. Since renewable energy systems are replaced or preferred over the conventional power generation units, the electricity grid is facing with frequency stability issues due to the absence of inertia-less units. Therefore, the behaviour of old-fashion power plants are described under frequency disturbances. Moreover, the frequency regulating mechanisms are presented. Finally, the energy markets are also explained in order to emphasize the role of renewable energy systems.

Chapter 3 presents the modelling of wind turbine used in this study. Since the existing variable speed wind turbines require modification in order to integrate to electricity grid, detailed modelling of these wind turbines is presented. By utilizing synthetic inertia method, a relation between grid frequency and the active power output is constructed.

The limits of the active power increase is investigated in Chapter 4. The ability of increasing its active power output is already presented in the literature. However, the limits of support power is studied for different wind speed scenarios. Maximum achievable active power are studied for varying wind speeds. The real wind speed measurements from site are utilized to find to probability of support power for different wind speeds is calculated. Wind turbine inertial support limits and turbine internal parameters are observed for the non-dynamic frequency response.

Synthetic inertia implementation within a wind farm is studied in the Chapter 5. The effect of synthetic inertia is observed in a dynamic test case with renewable penetration.Test case is modified with different combinations in which the system is penetrated with wind farm with/without generator decommission are studied in this chapter. Frequency response of the test system is tested for different grid configurations as well as different emulated inertia constants.

Chapter 6 presents a basic conclusions for the inertial support implementation which is either frequency dependent or not. Moreover, an economical analysis from an energy provider perspective is given. Two hypothetical payment methods are constructed and compared to estimate which economical motive that can persuade the

energy provider for participating grid supporting methods with renewable energy systems.

CHAPTER 2

POWER SYSTEM FREQUENCY STABILITY

The increasing renewable energy penetration deteriorates the power system frequency stability. One of the most severe effect of renewable energy penetration is the reduction in grid inertia. Grid aggregated inertia is important for the frequency stability. As the frequency falls, a part of the kinetic energy is extracted from the grid inertia and released inherently from synchronous generators to grid. Therefore, as the grid aggregated inertia decreases, the control of the frequency becomes difficult resulting in quick changes in the grid frequency.

In this chapter, the internal dynamics of the power system will be presented in terms of frequency stability. The frequency regulation mechanisms in the grid is presented. Furthermore, the energy market is briefly explained in order to understand the role of renewable energy providers inside the market.

2.1 Synchronous Generator and Synchronous Speed

Synchronous machines produce torque only in synchronous speed. If a transient overspeeding occurs in the rotor, the torque cannot be produced that results in a deceleration. This makes the rotor angular velocity to strictly coupled to the electrical frequency of the stator rotating MMF. This is why these machines are equipped with damper windings which are basically induction machine windings. If the frequency of grid changes, damper windings create a torque which creates a force to synchronize

the speed to the grid frequency.

$$n_s = \frac{120f}{p} \tag{2.1}$$

Relation between grid frequency and the synchronous speed is given in Eq. (2.1) in terms of rpm where n_s is the synchronous speed in rpm, f is the grid frequency in Hz, p is the number of poles of the generator [35].

2.2 Swing Equation

Rotational speed of synchronous machines changes according to the net torque acting on the rotor. Therefore, the speed is maintained constant unless there is a difference between mechanical and electromechanical torque. The equation of motion is given in Eq. (2.2) where J is aggravated moment of inertia of the generator and the turbine in kgm^2, ω_m is the rotor angular velocity in rad/s, T_m and T_e are mechanical and electromechanical torques in Nm. T_a is the accelerating torque in Nm which determines the acceleration or deceleration in the rotor according to its sign.

$$J\frac{d\omega_m}{dt} = T_m - T_e = T_a \tag{2.2}$$

In power system network, the power ratings of the generators in operation and corresponding moment of inertia values varies. Inertia constant is defined as the ratio of kinetic energy stored in the inertia to the power rating of the generator as in Eq. (2.3) where ω_{0m} denotes the rated angular velocity of generator in rad/s and S_{base} is the rated apparent power in VA. H is indicates the time duration in which generator produces its rated apparent power by only using its kinetic energy in the inertia. Thus, H is a better indication of factor for power system frequency stability analysis compared to J. Hence, it is more convenient to use inertia constant, H which varies between 2 and 9 seconds [35].

$$H = \frac{\frac{1}{2}J\omega_{0m}^2}{S_{base}} \tag{2.3}$$

Substituting Eq. (2.3) into Eq. (2.2) and replacing units to per-unit quantities yield the swing equation given in Eq. (2.4) where $\overline{P_m}$ is the input mechanical power in pu and $\overline{P_e}$ is the electromechanical output power in pu. It defines the inherent behaviour

of a synchronous generator against the frequency deviations in the grid. When the grid frequency falls, a subsequent decrease in the rotor is observed. According to the Eq. (2.4), a negative term is found in the left-hand side. This means that rotor electromechanical output power, $\overline{P_e}$ will be increased inherently. It should be noted that the additional energy is not taken from the input mechanical power but it is extracted from the kinetic energy. Moreover, the decreased energy is injected to grid whenever the frequency increases due to the acceleration in the rotor.

$$2H\overline{\omega_m}\frac{d\overline{\omega_m}}{dt} = \overline{P_m} - \overline{P_e} \tag{2.4}$$

2.3 Frequency in Power Systems

The frequency in a power system is related to the speed of the synchronous generators and changes according to the swing equation. The frequency of the each generator is not the same in the network since each generator does not have the same speed. Nonetheless, the fluctuations in the generator speeds are called rotor swings and can be negligible in the steady state. Hence, the network can be assumed as a single generating unit by neglecting small differences between the generator speeds. The swing equation basically investigates the relation between mechanical and electromechanical powers and the rate of change of angular speed of a generator. However, it is also applicable to grid in order to estimate the grid frequency.

$$2H_{sys}\overline{f}_{sys}\frac{d\overline{f}_{sys}}{dt} = \overline{P}_{tm} - \overline{P}_{te} \tag{2.5}$$

If the generators of the grid is considered as a single generator, the inertia of the equivalent generator is aggravated from each generator in the network. In this case, average frequency in the network can be found as in Eq. (2.5) where P_{tm} is the aggravated mechanical input power of the generators meanwhile P_{te} is the aggravated electromechanical output power. In other words, the system frequency depends on the balance between generation and consumption. It should be noted that generation means the input mechanical power of the generators meanwhile the demand is absorbed from the electromechanical output power of the generators. Hence, the difference between these causes either acceleration or deceleration.

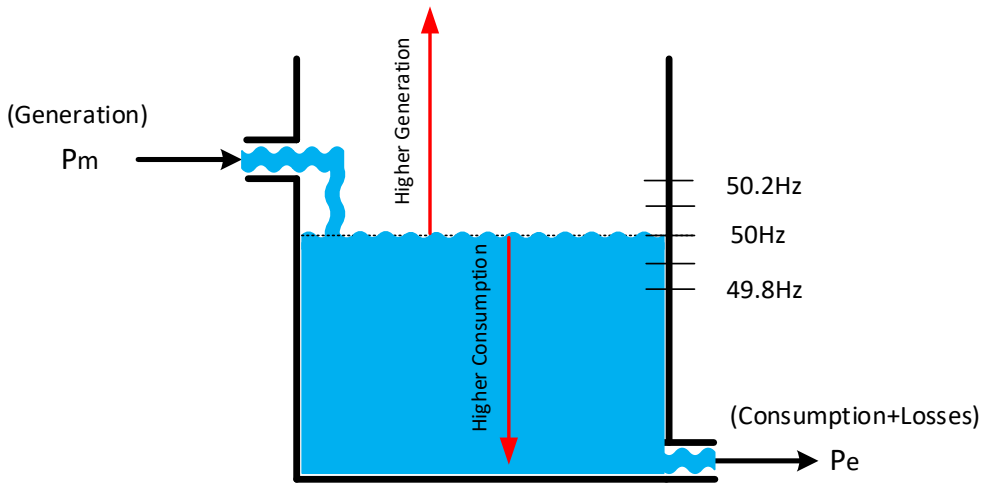

Figure 2.1: Frequency behaviour in electric grid with the water level in a container analogy [5]

The behaviour of the frequency in electric grid is depicted in Fig. 2.1. As it can be seen from the water level in a container analogy, the frequency of the system is dependent on the in-flow and the out-flow. Therefore, in the electricity grid, frequency increases as the aggravated input power is higher than the aggregated output power. Note that, the direction of the frequency is dictated by this balance. Having a constant 49.8Hz frequency does not mean that consumption is higher than generation. If the frequency is constant, then the input mechanical power is equal to output power.

The variation of the grid frequency is depicted for a typical day in Fig 2.2. The frequency deviates continuously during the day. It should be noted that there exists hourly peaks in the frequency. The peaks occur due to the change in the hourly generation shift. Since the generation level is changed for the next hour, the frequency deviates hourly in the grid.

2.4 Frequency Regulating Mechanisms

Having a constant frequency is one of the most important responsibilities of a system operator. In order to have a constant frequency, supply is being adjusted according to the demand continuously. By doing so, the system frequency varies between a band-gap. The variation depends on the disturbances which are generally a sudden

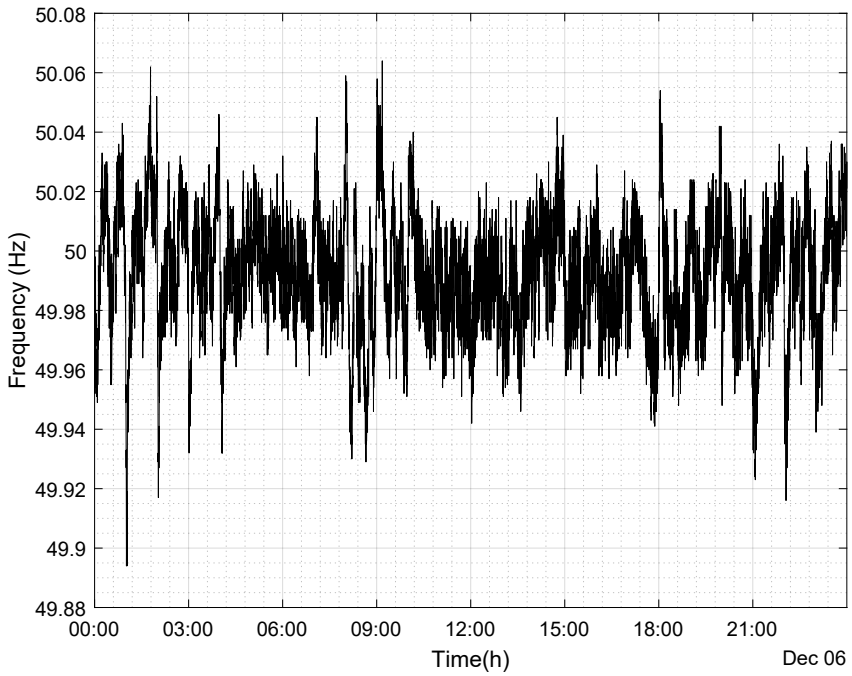

Figure 2.2: Variation of the Frequency in a Typical Day (06 Dec 2018) [6]

generation outage or instant load connection. The size of the disturbance determines the severity of the frequency change and there are three main mechanisms to arrest the frequency changes in the system.

The frequency control services in England and Wales are depicted in Fig. 2.3 for a frequency disturbance. The frequency is maintained between 49.8Hz and 50.2Hz for continuous service. A frequency disturbance event causes frequency to decline. However, the decline in the frequency is arrested with the help of the inertial support of the conventional generators and the primary frequency controllers. The main responsibility of the primary frequency control is arresting the frequency decline. Restoration of grid frequency to nominal is the responsibility of the secondary and tertiary frequency controls.

2.4.1 Primary Frequency Control

Following generator outage or sudden load connection event, frequency starts decreasing. The rate of change of the frequency is dependent on the severity of the event

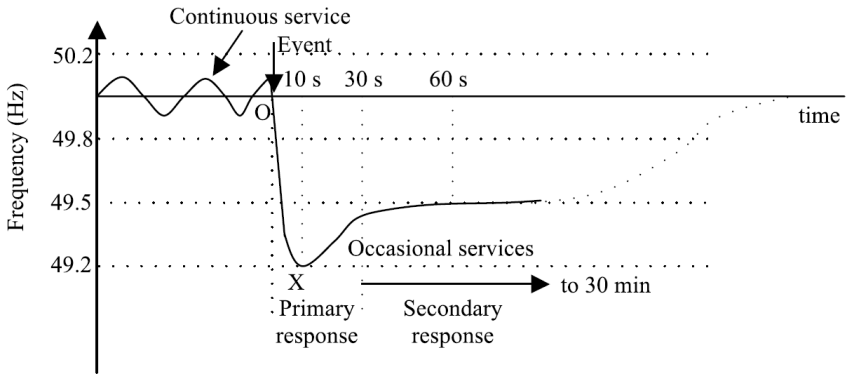

Figure 2.3: Grid Frequency Control in England and Wales [7], [8]

by means of power and the available inertia of the power system. Such frequency disturbance requires increased input power. However, the increase in the input mechanical power should be activated very fast and should be automated. This responsibility is assigned to generating units with primary frequency control. The active power generation of these units is increased or decreased by the governor depending on the network frequency direction. Notice that each generator in the power system does not necessarily perform primary frequency control function. In this case, their active power generation is independent from the network frequency. The contribution to primary frequency control is an responsibility but also a way to sell higher energy to grid operator. The primary frequency control is automated with droop control defined in the generator speed governors. According to droop control, the generator power should be increased according to the frequency deviation from nominal. Therefore, the generating unit does not utilize its whole capacity but rather keeps a capacity which is called as spinning reserve. According to the droop curve, the generation unit should increase its output power no longer than 15 seconds and keep their operation up to 30 minutes [36].

2.4.2 Secondary Frequency Control

The frequency is recovered back to nominal value with the Secondary Frequency Control action. This controller might be a single or multiple centres that monitor the frequency and adjust the generation accordingly. They are also called as Auto-

matic Generation Control (AGC) systems and their action takes a few minutes. The AGC monitors the frequency deviation from the nominal and takes action to recover frequency back to nominal. With the secondary frequency control action, primary controllers decreases their production back to their pre-disturbance value.

2.4.3 Tertiary Frequency Control

The final frequency control mechanism is the Tertiary Frequency Control. If the frequency is not recovered back to nominal value with the secondary controllers, tertiary frequency controllers manually activates the load shedding which is an undesired situation by the network operator. However, it is an emergency case which might result in black-out and requires immediate action.

2.5 Energy Market

Since the energy is generated and distributed by private energy companies, a system operator should be responsible for maintaining a balance in the power network. The frequency is kept inside the operational band in the electricity network by balancing the supply and the demand by intersecting the supply and demand curves inside the different time intervals. In this way, the balance is ensured in the market by day ahead, intra-day and balancing markets.

2.5.1 Day Ahead Market

The load power in a network has a distinct characteristic depending on the day of the week or the hour of the day. By foreseeing the next day demand power variation, the electricity market collects the bids from the energy suppliers and consumers. According to submitted bids, the next day generation price is determined by intersecting the supply and demand price curves. The price of the energy is called Market Clearing Price (MCP). These bids are submitted for the next day and the prices are determined before the corresponding day.

2.5.2 Intra-Day Market

Even though the estimations for the upcoming day load power has superior accuracy with the advanced estimation methods, networks are subjected to unexpected problems such as generator trips, line outages. Therefore, intra-day market contributes the balance of the market between the day ahead market and balancing market. Moreover, it gives the participants almost real-time trading opportunity meanwhile it increases the sustainability of the market. After day ahead market has closed for the corresponding day, the bids are submitted to system. In other words, MCP is already determined for the corresponding day meanwhile the rest of the day prices are not set.

2.5.3 Balancing Market

Primary and secondary control reserves are maintained in the system in order to improve the balance for the instant deviations in the frequency. The frequency is first arrested by the primary controllers and it is restored by the secondary controllers. The generation units that participate primary and secondary control promises a defined generation capacity to these actions. Balancing market is much more different than day ahead and intra-day market since its main goal is the network security rather than electricity trading. The price of the energy in this market called as System Marginal Price (SMP).

The price of the energy changes according to the market type. In the Fig. 2.4, three market prices such as Market Clearing Price (MCP), Weighted Average Price (WAP) and System Marginal Price (SMP) are shown.

2.5.4 Feed-In Tariff

Significant amount of energy produced inside the Turkish electricity network is based on exported sources such as coal and gas. As a result of this, the energy sector is highly dependent on the foreign countries. In order to decrease the dependency on the external sources, the renewable energy sources are supported by government in Turkey. The energy generated by renewable energy systems are bought with the

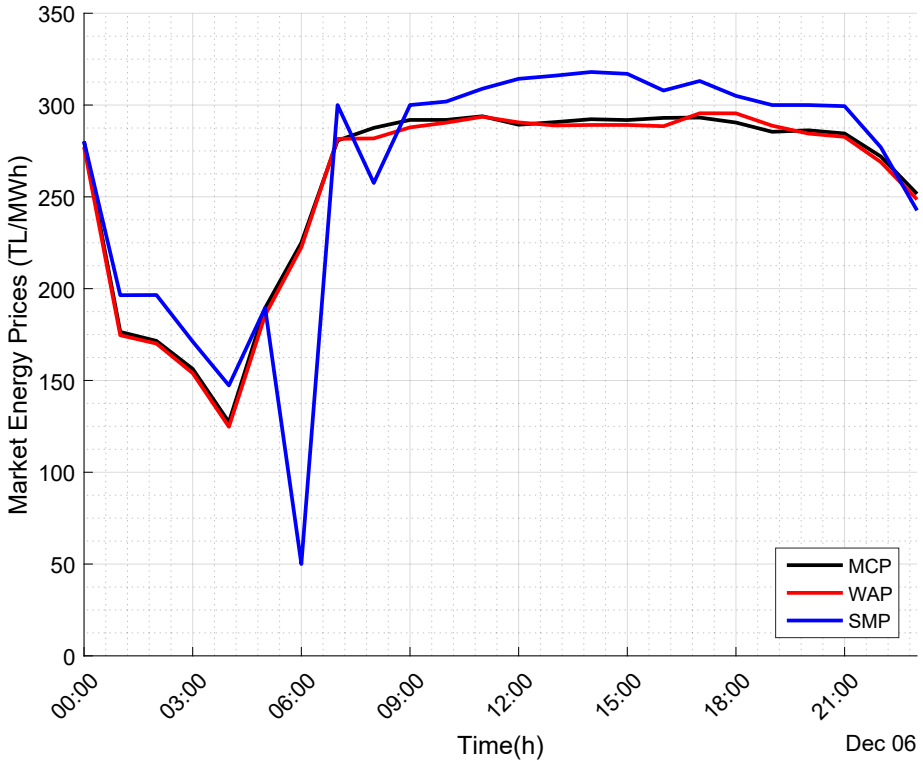

Figure 2.4: Energy Prices on 06 Dec. 2018 [9]

feed-in tariff (FIT) within the pre-determined time interval according to the purchase agreement. This decreases the return of investment due to the fact that all produced energy will be bought during this period with a remarkable price. The feed-in tariff for different renewable energy systems is listed in Table 2.1.

In addition to feed-in tariff, energy provider can benefit from additional incentives as long as some parts of the system is produced inside Turkey. For instance, by preferring the tower of a wind turbine which is a domestic production, an additional price is given to energy provider as local-bonus content. The local-bonus contents for wind turbines are listed in Table 2.2.

With the increasing renewable energy penetration, the power system stability is getting more vulnerable to the disturbances. Since the grid operators are responsible for the successful operation of the grid, they work on grid stability improving. Nonetheless, power system stability is not the responsibility of the energy providers. However, participation of the renewable energy providers is also a necessity to improve

Renewable Energy System	Feed-In Tariff (cent/kWh)
Hydro	7.3
Wind	7.3
Geothermal	10.5
Biomass	13.3
Solar	13.3

Table 2.1: Feed-In Tariff for Renewable Energy Systems in Turkey [1]

Local Content for Wind Turbines	Local Content Incentive (cent/kWh)
Blade	0.8
Generator and Power Electronics	1.0
Turbine Tower	0.6
All Mechanical Parts in Rotor and Nacelle	1.3

Table 2.2: Local Content Incentives for Wind Turbines [1]

frequency stability of the grid. Hence, the grid operators have to come up with a solution to be implemented by the energy providers. Nonetheless, the solution should also be beneficial for the energy providers who is already satisfied with the existing purchase agreement with additional incentives. As long as the renewable energy providers are convinced to implement the solutions, the grid stability can be maintained against the increasing renewable penetration.

2.6 Conclusion

This chapter focuses on the frequency dynamics inside the power grid. The importance of inherited inertial support of the synchronous generators are highlighted. The characteristics of this behaviour is defined with swing equation that can be adopted

to renewable energy systems. The swing equation explains the change in the active powers of the synchronous generators upon a frequency disturbance on the output terminal. However, the internal dynamics of the frequency is also presented to understand the frequency stability.

Frequency regulating mechanisms such as primary, secondary and tertiary control are essential for power systems. Their action sequence are also explained in detail. In addition to technical details, the energy market is also summarized to present a economical perspective.

CHAPTER 3

WIND TURBINE MODELLING

Ancillary services are getting attention especially for renewable energy systems. Participation of renewable energy systems to frequency regulating mechanisms will be a necessity for the successful operation of the power system. Hence, the detailed modelling of renewable energy systems are essential for grid supporting implementations. In this chapter, detailed modelling for wind turbines is investigated. The wind turbine modelling is presented for the wind turbines that are connected to grid with full-scale power electronics.

3.1 Wind Turbines with Full Scale Power Electronics

The share of variable speed wind turbines with full scale power electronics is increasing worldwide due to the high efficiency. Full-scale power electronics enables the turbine to have wide speed range. The wind turbines in this type are able to adjust its speed according to the variation in the wind speed and torque [37]. PMSG wind turbines are one of the most common type of these turbines. Even though the price of the permanent magnet fluctuates with time, the reliability and high efficiency of this type of turbine increase its share in the market. The wind turbine modelling in this study is based on PMSG wind turbines. However, the ability to control the wind turbine output power is not just specific to PMSG wind turbines but the ones with full-scale power electronics.

Fig. 3.1a, 3.1b and 3.1c show the modelling of wind turbine topologies that are connected to grid full-scale back-to-back converter. In wind turbines with full-scale power electronics, stator of the wind turbine generator is not directly connected to

grid. A back-to-back converter is used between generator and the electrical grid to ensure that the turbine speed is independent from the grid frequency. The back-to-back converter is composed of two converters to perform the AC/DC and DC/AC conversion. The converter which is connected to turbine generator is called Machine Side Converter (MSC) meanwhile the one connected to grid is called Grid Side Converter(GSC). Moreover, GSC is connected to grid with a filter in order to filter out high frequency currents due to switching action. Since GE2.75-103 model geared PMSG wind turbine model is used in this study, the turbine topology in Fig. 3.1a is emphasized. The turbine is composed of sub-models such as aerodynamic model, gearbox, PMSG, MSC and GSC. The details of the sub-models are given in the following sections.

3.1.1 Aerodynamic Model

Aerodynamic model is the sub-model that captures power from the wind. The output of this block is the aerodynamic torque that rotates the turbine. However, the wind speed is not the only input. Turbine speed and pitch angle are also the inputs of the system since they affect the mechanical power that is captured from the wind.

The aerodynamic power of wind is given in Eq. (3.1) where ρ_{air} is air density in kg/m^3, R is the blade radius in m abd v_{wind} is the wind speed in m/s. Note that this is the available power of the air that is striking the turbine swept area and it is not possible to extract that amount of energy. Otherwise, the air would be standstill behind the wind turbine [38].

$$P_{wind} = 0.5\rho_{air}\pi R^2 v_{wind}^3 \tag{3.1}$$

The wind turbine captures a fraction of the available wind power that is denominated as power coefficient C_p. Therefore, turbine power captured from wind can be found with the Eq. (3.2).

$$P_{tur} = C_p P_{wind} \tag{3.2}$$

Power coefficient determines the amount of power to be captured from wind and it is a non-linear function of the tip speed ratio, λ and pitch angle, β. Tip speed ratio is a parameter proportional with turbine speed. It can be defined as the ratio of the speed

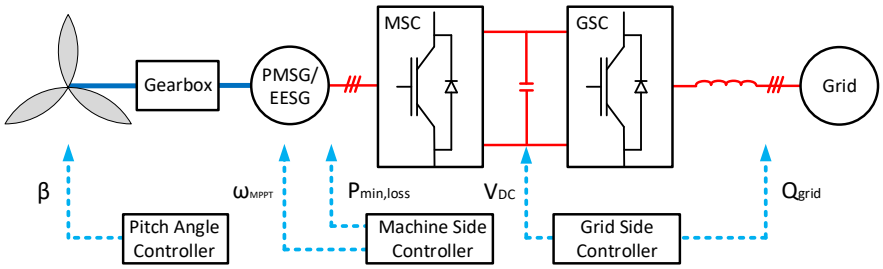

(a) Geared PMSG/EESG Wind Turbine

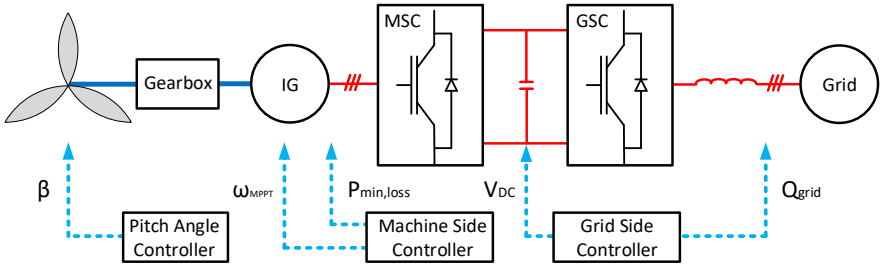

(b) Geared IG Wind Turbine

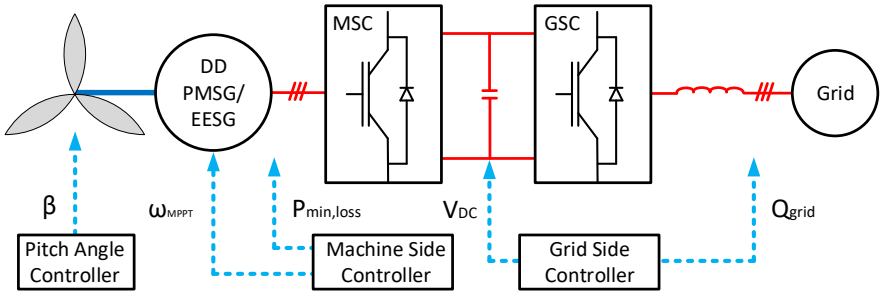

(c) Direct-Drive PMSG/EESG Wind Turbine

Figure 3.1: Wind Turbine Topologies with Full-Scale Power Electronics

in the turbine tip to the wind speed as in the Eq. (3.3). Power coefficient for a specific tip speed ratio and pitch angle can be found with the Eq. (3.4) and (3.5) where c_1 is 0.5176, c_2 is 116, c_3 is 0.4, c_4 is 5, c_5 is 21 and c_6 is 0.0068 [39].

$$\lambda = \frac{\omega_{tur} R}{v_{wind}} \tag{3.3}$$

$$C_p(\lambda, \beta) = c_1(c_2/\lambda_i - c_3\beta - c_4)e^{-c_5/\lambda i} + c_6\lambda \tag{3.4}$$

$$\frac{1}{\lambda_i} = \frac{1}{\lambda + 0.08\beta} - \frac{0.035}{\beta^3 + 1} \tag{3.5}$$

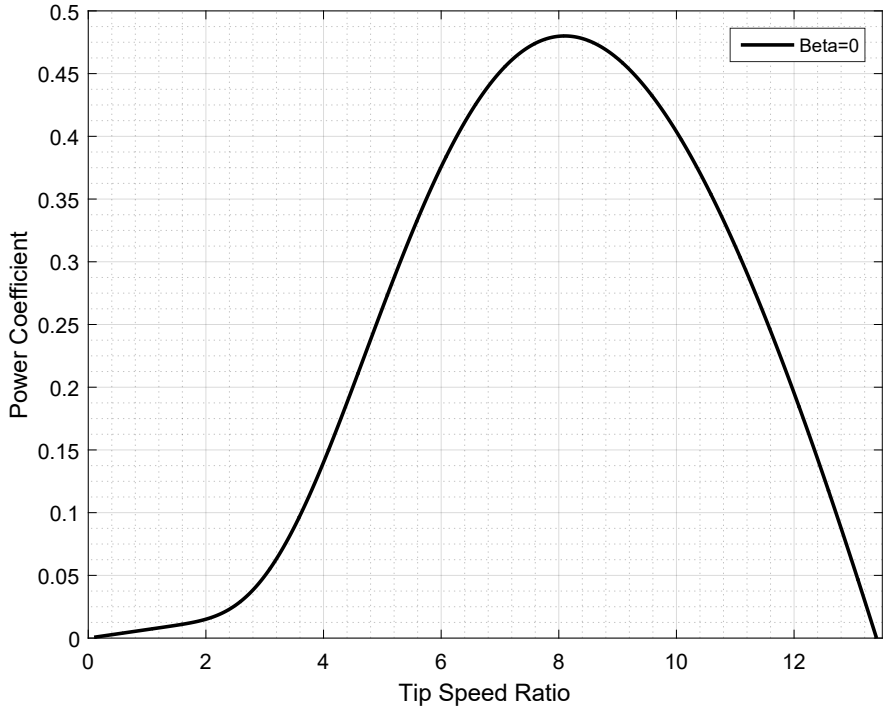

Figure 3.2: Power Coefficient Variation with Tip Speed Ratio under Zero Pitch Angle

Variation of power coefficient C_p is given in Fig. 3.2 for varying tip speed ratio. For the zero pitch angle, power coefficient has the maximum value of 0.48 for the tip speed ratio of 8.1. In order to ensure that the maximum of wind power is extracted, wind turbine should rotate a speed that gives the optimum tip speed ratio. This is ensured by the Maximum Power Point Tracking (MPPT) algorithms.

3.1.1.1 Maximum Power Point Tracking Algorithms

In the literature, different methods are presented in order to operate in the Maximum Power Point. Perturb&Obserb (P&O) is the most common MPPT method in the literature [40], [41]. The methods simply creates a perturbation in the generator speed. The change in the generator speed creates also change in the active power output. If

the power is increased with this perturbation, the generator speed is again perturbed in the same direction until a decrease in the active power is observed. This methods is the simplest method and does not require any calculation or wind speed measurement. However, the algorithm creates oscillations in the generator speed and active power. This method is also called as Hill-Climb Search (HCS) method in the literature.

Another MPPT algorithm is the wind speed measurement method [42], [43]. If the wind speed is estimated accurately, the optimal generator speed can be calculated. However, wind speed estimation is complicated and increases the cost. Another commonly used MPPT algorithm is the power-signal feedback (PSF) control [43], [40], [44]. This method requires maximum power curve of the wind turbine based on the experimental results. A look-up table is constructed with obtained wind turbine speed and active output power values. However, using generator speed and active power measurements is the main drawback of this algorithm. Finally, there are numerous number of much complex MPPT algorithms based on fuzzy-logic [45] or neural-network [46]. However, these MPPT algorithms are out of scope of this thesis. Therefore, optimal generator speed is provided in this study according to the wind speed.

3.1.1.2 Pitch Angle Control

According to Eq. (3.1), wind power increases with the cube of the wind speed. Hence, wind power increases dramatically for the high wind speeds. In order to decrease power, pitch angle i.e. blade angle is increased. Since the power coefficient, C_p is a function of the pitch angle, β, wind power can be curtailed with increased blade angle. Variation of power coefficient for two different pitch angle is shown in Fig. 3.3. Increasing pitch angle by 1.176° decreases power coefficient by 10%.

As long as wind power is below the rated power, the wind turbine is operated in MPPT speed. This is ensured by obtaining optimal tip speed ratio. This means that for zero pitch angle, MPPT speed is increased linearly with wind speed. Before reaching rated power, MPPT speed might reach maximum generator speed. In this case, wind turbine reference speed will be the maximum generator speed. However, turbine speed cannot be decreased down to reference speed when the torque limit is

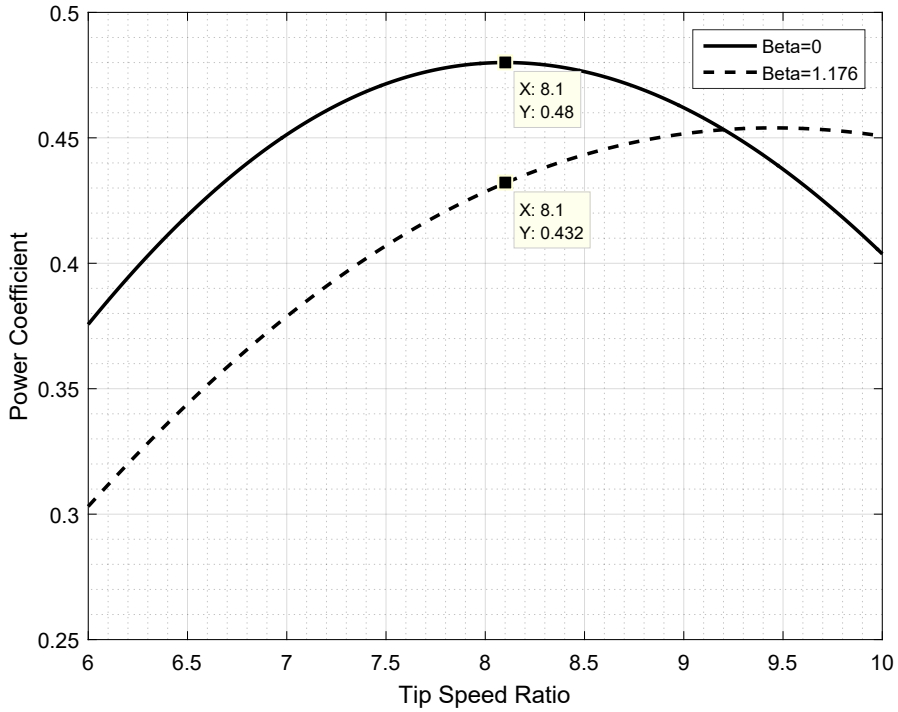

Figure 3.3: Power Coefficient Variation for Two Different Pitch Angle

reached. Hence, the pitch angle should be increased to regulate the turbine speed. Pitch angle controller is depicted in Fig. 3.4. Notice that the pitch angle is increased when the speed exceeds maximum generator speed. Otherwise, the pitch angle kept as zero.

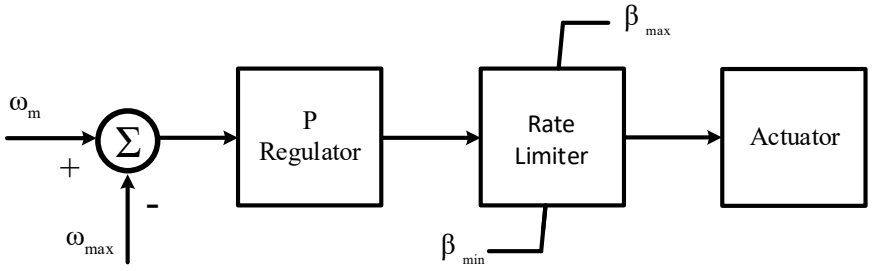

Figure 3.4: Pitch Angle Control Diagram

The responsibility of the pitch angle controller is the regulation of the blade angle but each blade in the wind turbine is a few tonnes. Therefore, the blade angle cannot be changed instantaneously and limited with rate limiter. The rate of change of pitch angle in this study is limited with $10°/s$ [38]. Besides, the pitch angle controller

takes action as soon as the maximum generator speed is exceeded. Therefore, wind turbine operation deviates from optimal tip speed ratio. This can also be observed from the variation of power coefficient, C_p with the wind speed for the wind turbine GE 2.75-103 used in this study. Variation of the C_p is shown in Fig. 3.5.

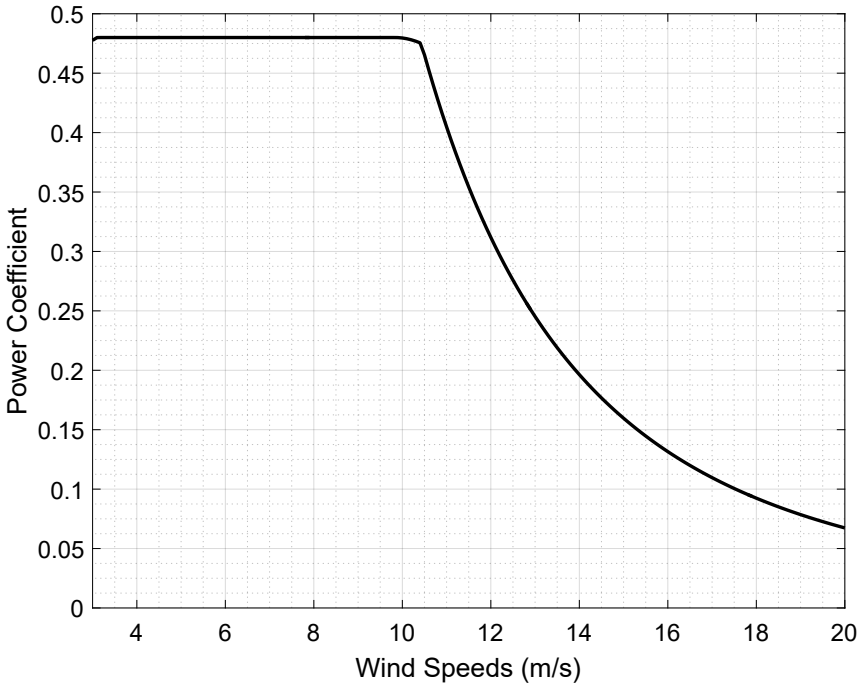

Figure 3.5: Power Coefficient Variation for GE 2.75-103

3.1.2 Gearbox

Variable speed PMSG wind turbines have a gearbox between turbine and generator except for direct-drive wind turbines. The gearbox increases angular speed and decreases the torque in the generator side. By decreasing the rated torque, generator size and cost can be reduced since the generator size is almost proportional to rated torque due to constant shear stress [47]. Moreover, turbine speed is increased to the allowable speed range of the generator which is generally much higher than that of wind turbines. Otherwise, generator should have high pole numbers.

A gearbox model is depicted in Fig. 3.6. They are mainly used for speed and torque conversion. It should be noted that the gearboxes are lossy systems. Therefore, the

output torque of the gearbox would be lower than the ratio of input torque to gearbox conversion ratio. Direct-drive systems are based on the elimination of the gearbox systems by direct connection between turbine and generator in order to increase efficiency and reliability [37]. In this study, 3 stage (1 planetary / 1 helical) gearbox is modelled with %97 efficiency [48].

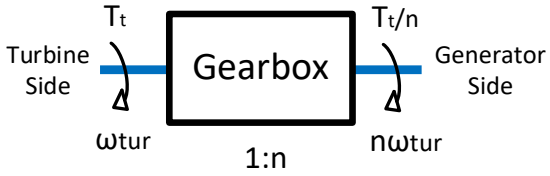

Figure 3.6: Gearbox Modelling

3.1.3 Permanent Magnet Synchronous Generator

PMSGs and electrically excited generators can be employed with full-scale power electronics. However, PMSGs are generally preferred over electrically excited synchronous generators due to their high efficiency. The absence of electrical excitation on the rotor decreases losses. Besides, slip ring is not needed in the generator which also increases the reliability of the PMSG wind turbines. Dynamical equations of the salient pole PMSG are projected on a reference frame which rotates synchronously with magnet flux and given in Eq. (3.6) and (3.7) where R_1 is stator resistance in Ω, L_{sd} and L_{sq} are d and q axis inductances in H, i_{ad} and i_{aq} are d and q axis currents in A, ω is the electrical angular frequency in rad/s, ψ_f is magnet flux linkage in Vs [38].

$$v_{1d} = R_1 i_{ad} + L_{sd}\frac{di_{ad}}{dt} - L_{sq}\omega i_{sq} \tag{3.6}$$

$$v_{1q} = R_1 i_{aq} + L_{sq}\frac{di_{aq}}{dt} + L_{sd}\omega i_{sd} + \omega\psi_f \tag{3.7}$$

Another important PMSG parameter is the power in dq frame. The power expression is given in Eq. (3.8). The electromechanical torque can be found by the relation between power and angular speed. The torque expression is also given in Eq. (3.9) where p is the number of pole pair.

$$P_{elm} = \frac{3}{2}\omega i_{aq}(\psi_f + i_{ad}(L_{sq} - L_{sd})) \tag{3.8}$$

$$T_e = \frac{P_{elm}}{w_m} = \frac{P_{elm}}{w/p_p} = \frac{3}{2} p_p i_{aq} (\psi_f + i_{ad}(L_{sq} - L_{sd})) \tag{3.9}$$

Given equations are defined for salient pole machines. If the clyndrical rotor machine is used, the torque equation reduces to the Equation 3.10.

$$T_e = \frac{3}{2} p_p i_{aq} \psi_f \tag{3.10}$$

3.1.4 Machine Side Converter

Variable speed wind turbines that are equipped with the back-to-back converters are able to decouple grid frequency and the turbine speed. This gives wind turbine degree of freedom for the rotational speed. In this way, turbine is able to capture the maximum available power from wind. Machine Side Converter (MSC) i.e. Generator Side Converter is the converter that is connected between generator and DC-bus. The three phase generator output AC voltage is converted to DC voltage. Conversion from AC to DC can be achieved by three-leg full bridge converters. This converter can be equipped with uncontrolled, semi-controlled and fully-controlled switches. Fully-controlled switches such as MOSFET,IGBT are commonly used in the industry and gives two control parameters to the user.

Voltages and currents are generally transformed into synchronously rotating reference frame or also called dq frame. Since the frame is rotating in synchronous speed, three-phase phasors are transformed to DC quantities. Therefore, its control becomes easier [49]. Proportional-integral (PI) controllers are associated with the dq control structure due to their satisfactory behaviour interaction to DC variables [50]. Hence, the control in the back-to-back converter is achieved with PI controllers in the dq frame.

The control diagram of the MSC is depicted in Fig. 3.7 according to the study in [51]. In dq frame, it is possible to control two parameters. One of these parameters is the d-axis current that is set zero in order to decrease the stator copper losses. The other parameter is the q-axis current that is proportional to the electromagnetic torque as it can be observed in the Eq. (3.10). However, q-axis current or torque is controlled in

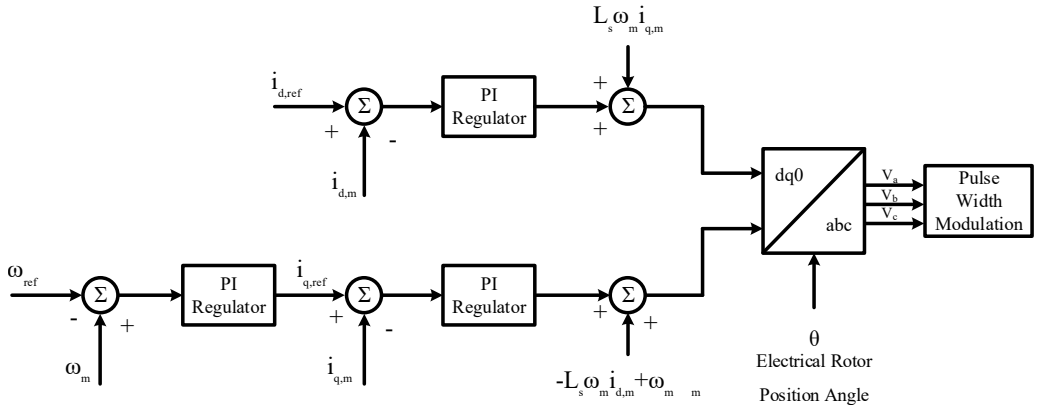

Figure 3.7: Machine Side Controller Diagram

order to regulate the turbine speed. Therefore, turbine speed is adjusted such that the turbine will capture maximum available power in the wind.

3.1.5 Grid Side Converter

Grid Side Converter (GSC) or Line Side Converter (LSC) is the converter that is connected between DC-link capacitor and grid. GSC works as an inverter that injects current synchronous to grid. Currents and voltages are transformed into synchronously rotating frame that is aligned with the grid voltage. Therefore, d-axis current determines the amount of current which is in phase with the grid voltage meanwhile q-axis current determines amount of current that is out of phase with the grid voltage. In other words, injecting d-axis current injects active power to grid meantime q-axis current injects reactive power to grid.

The responsibility of the GSC is regulating DC voltage and the reactive power injected to the grid. The control diagram of the GSC is given in Fig. 3.8. As seen from the figure, DC-bus voltage is regulated by controlling the d axis current. If the DC-bus voltage increases above the reference value, d-axis current reference is increased. As a result, active power increases. Increased active power also decreases the DC-bus voltage level. Reference value of the q-axis current is set to zero in normal operation, consequently unity power factor. For Low Voltage Ride-Through studies, q-axis current is determined according to the reactive power value requirement. [52]

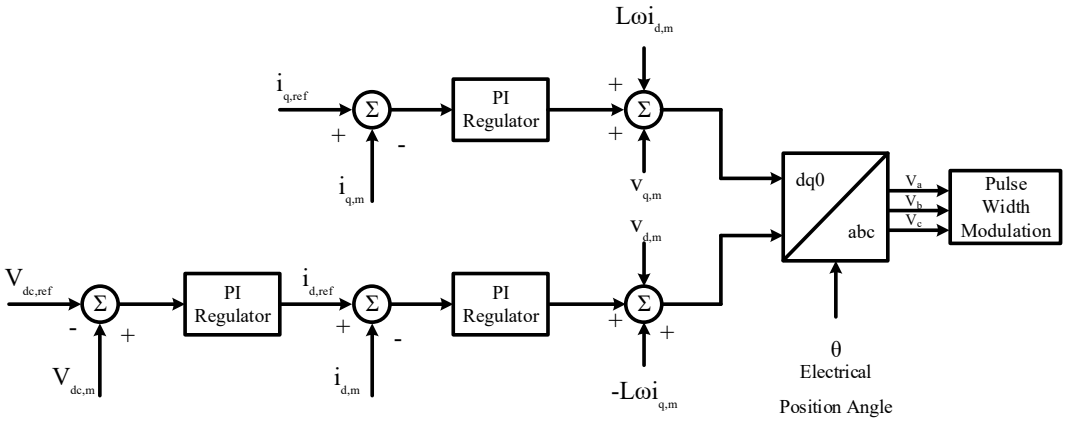

Figure 3.8: Grid Side Controller Diagram

GSC is connected to grid through a filter. Therefore, the output voltage of the converter is not equal to the that of grid. The relation between converter voltage, grid voltage and current is derived through Eq. (3.11) to (3.17) where v_c is the converter voltage, v_g is the grid voltage and i_g is the grid current measured in the grid side. As it is observed in Eq (3.16) and (3.17), converter side voltage includes same axis grid voltage and a term proportional to cross axis current which is called cross-coupled term. Therefore, the outputs of the inner PI regulators are compensated and forwarded to Pulse Width Modulation after transformation to three-phase voltages.

$$\overline{v_c} = v_{dc} + jv_{qc} \tag{3.11}$$

$$\overline{v_g} = v_{dg} + jv_{qg} \tag{3.12}$$

$$\overline{i_g} = i_{dg} + ji_{qg} \tag{3.13}$$

$$\overline{v_c} = \overline{v_g} + \overline{i_g} j\omega L \tag{3.14}$$

$$v_{dc} + jv_{qc} = v_{dg} + jv_{qg} + j\omega L(i_{dg} + ji_{qg}) \tag{3.15}$$

$$v_{dc} = v_{dg} - \omega L i_{qg} \tag{3.16}$$

$$v_{qc} = v_{qg} + \omega L i_{dg} \tag{3.17}$$

The PI regulators of the wind turbine model is tuned with trial error method. In this study, the modelled wind turbine is connected to grid with an L filter even though the actual turbine is connected to grid with an LCL filter. However, the actual system would operate better than the modelled case since the the LCL filter has superior performance than L filters [53]. Nonetheless, L filter has provided sufficient performance for the successful operation of the wind turbine in this study regardless from the power quality standards in the output current. The active power of the wind turbine under varying wind speed is given in the Fig. 3.9.

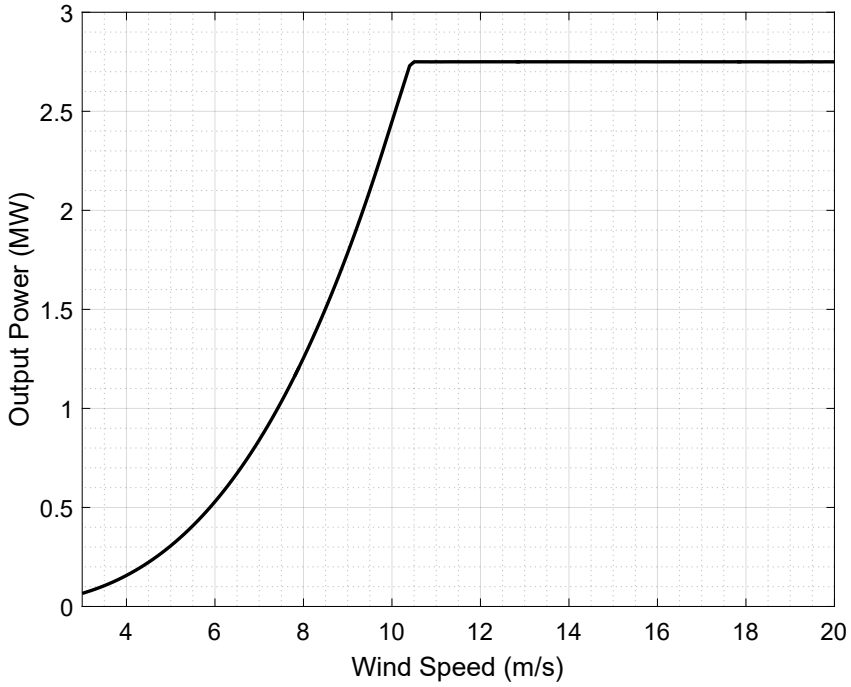

Figure 3.9: Variation of the Active Power of the Wind Turbine

3.2 Synthetic Inertia Implementation

As explained Section 2.2, synchronous generators change their speed according to the balance between input mechanical and electromechanical powers. Furthermore, if the frequency changes, the electromechanical power of the generators also change. Nonetheless, the renewable energy systems which are connected to grid with a power electronics interface are unresponsive to the deviations in the grid frequency.

The definition of the synthetic inertia is the controlled contribution of electrical torque that is proportional to RoCoF in the unit connection terminal [54]. Synthetic inertia (also called as 'virtual inertia') is the method that emulates the synchronous generator in the renewable energy systems. In this method, the active power output of the wind turbines are adjusted according to the Eq. (3.18) where H_{syn} is the synthetic inertia constant in seconds and ω_t is the terminal angular frequency in pu. The increase in the active power is proportional to RoCoF as well as the emulated inertia constant. The emulated inertia constant can be different from the inertia constant of the renewable energy system. For instance, the solar PV systems does not have inertia. Even in these systems, an inertia constant can be emulated as long as the system includes stored energy. In the wind turbines, the additional energy can be yielded from the kinetic energy in the turbine inertia. For solar PV systems, energy storage systems or the store energy in the DC-link capacitor can be utilized.

$$\Delta P_e = -2H_{syn}\frac{d\omega_t}{dt}\omega_t \tag{3.18}$$

In order to implement synthetic inertia in the system, a relation between frequency and active power of the wind turbine should be constructed. Wind turbine in this study is variable speed wind turbine with full scale power electronics. The speed of the turbine is controlled by MSC such that active power is adjusted. Inertial support modification is depicted in Fig. 3.10. The new value of the active power is determined according to the swing equation. However, the wind turbine in this study is operated with a reference speed rather than a reference power. Therefore, the assigned power value should be used in order to yield the q-axis current reference value. Reference q-axis current is derived between the Eq. (3.19) to Eq. (3.22).

$$P_{new} = (1 + \Delta P)P_{pre} \tag{3.19}$$

$$T_{new}\omega_m = (1 + \Delta P)T_{pre}\omega_{pre} \tag{3.20}$$

$$\frac{3}{2}p_p\psi_f i_{q,new}\omega_m = (1 + \Delta P)\frac{3}{2}p_p\psi_f i_{q,pre}\omega_{pre} \tag{3.21}$$

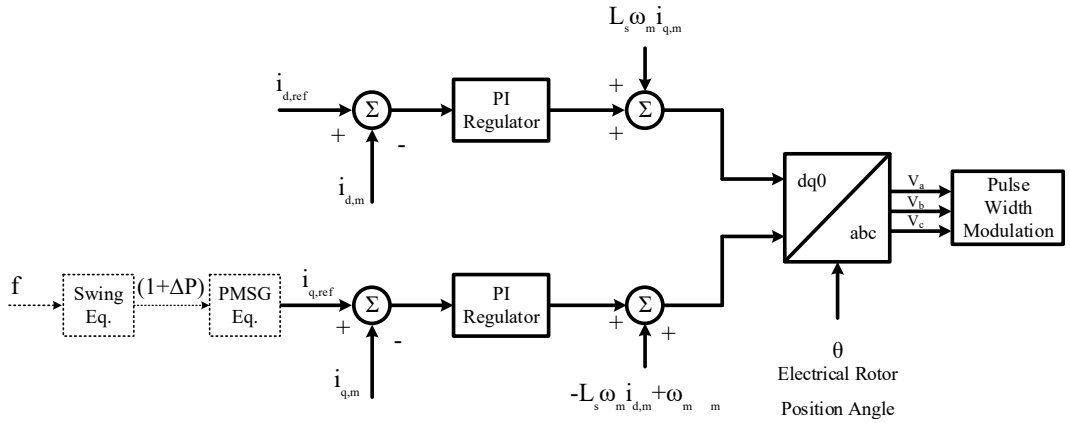

Figure 3.10: Modified MSC for Inertial Support

$$i_{q,ref} = i_{q,new} = (1 + \Delta P)\frac{i_{q,pre}\omega_{pre}}{\omega_m} \tag{3.22}$$

3.2.1 Synthetic Inertia Activation Schemes

Another issue about inertial support is the time instant to trigger synthetic inertia. In the literature, continuous operation, under-frequency trigger and maximum-frequency gradient are discussed [55]. It is obvious that continuous operation would create oscillations in active power output due to the continuous deviations in grid frequency. This is an unrealistic operation and is used for comparison purposes.

Second activation method is the under-frequency trigger which is the activation when the frequency decreases below a threshold value. It can be used for capturing the time instant for the inertial support. However, power grid might be in a stable point even if the frequency is 49.8Hz. Therefore, this method would be unsuccessful depending on the disturbance event.

Third activation scheme is the maximum-frequency gradient trigger. It uses a controller that is very similar to RoCoF relays and tracks the frequency gradient. Once the frequency gradient is below a threshold value, the synthetic inertia is activated. Since the severity of frequency disturbance event is related to the RoCoF, this activation scheme is the most remarkable scheme [55].

The activation of the inertial support by only frequency-gradient (RoCoF) might be

misleading. For instance, a negative RoCoF value when the frequency is above the nominal value is not a frequency disturbance. Therefore, the inertial support should not be activated unless the frequency is below a threshold. Thus, in this study, maximum-frequency gradient is used in coordination with the under-frequency trigger. The support is activated with a RoCoF threshold value of 0.1Hz/s and frequency dead-band of 10mHz. In this way, frequency regulating events inside the 49.99 and 50.01Hz band are not captured as frequency disturbance.

3.2.2 Source of the Inertial Support

The renewable energy systems cannot determine the amount of power in contrast the conventional systems. A thermal power plant, for instance, adjusts its power output as desired. However, the source of power in renewable energy is intermittent due to nature of the power source. This is why a spare energy is required in order to change the power output.

$$E_{electrostatic} = \frac{1}{2} C_{DC} V_{DC}^2 \tag{3.23}$$

Energy stored in DC bus capacitor is the only stored energy in PV systems. The amount of energy is given in Eq. (3.23) and negligible for inertial support studies. In the wind energy systems, there exists huge amount of kinetic energy in wind turbine generator and blades in addition to electrostatic energy. The kinetic energy expression is given in Eq. (3.25). It should be noted that J_{total} is the equivalent inertia in the generator side as given in Eq. (3.24),n is the gearbox conversion ratio and ω_m is the speed of the generator.

$$J_{total} = \frac{J_{tur}}{n^2} + J_{gen} \tag{3.24}$$

$$E_{kinetic} = \frac{1}{2} J_{total} \omega_m^2 \tag{3.25}$$

Note that the amount of kinetic energy is dependent on the generator speed. Therefore, the stored energy in wind turbine change according to the generator speed. Moreover, it can also be concluded that the energy is dependent on the wind speed. However, the generator speed is kept constant if the wind speed increases above the rated wind speed.

To illustrate the situation better, the electrostatic energy stored in DC bus and kinetic energy in turbine equivalent inertia are compared for GE2.75-103 wind turbine. The wind turbine has a DC bus capacitance of $27mF$ and $1200V$ DC link voltage. The corresponding electrostatic energy is calculated in Eq. (3.26). The generator speed of the corresponding generator is between $550rpm$ and $1735rpm$. The total turbine inertia is $1058.2kgm^2$ in the generator side. The minimum and maximum kinetic energy values are calculated in Eq. (3.27) and (3.28).

$$E_{DC-Link} = \frac{1}{2}27(10^{-3})1200^2 = 19.44kJ \tag{3.26}$$

$$E_{kinetic,min} = \frac{1}{2}(1058.2)57.6^2 = 1755.17kJ \tag{3.27}$$

$$E_{kinetic,max} = \frac{1}{2}(1058.2)181.7^2 = 17466.02kJ \tag{3.28}$$

It is obvious that the stored kinetic energy in the wind turbine is 90 times of the energy stored in DC bus capacitor even in the minimum generator speed. Therefore, utilization of the kinetic energy for inertial support studies is more efficient than using the stored energy in the capacitor.

Parameters	Minimum	Maximum
Generator Speed (rad/s)	57.6	181.7
Stored Kinetic Energy (kJ)	1755	17466
Inertia Constant (s)	0.58	5.75

Table 3.1: Dynamic Parameters of the Wind Turbine

Dynamical parameters of the wind turbine are listed in the Table 3.1. The stored energy in the turbine equivalent inertia varies with the square of the generator speed. Therefore, the minimum stored energy is one tenth of the maximum case. As a result of this, the inertia constant of the wind turbine is dependent on the wind speed and

varies between 0.58s and 5.75s. Notice that the inertia constants to be emulated by wind turbine in this thesis are not restricted to these inertia constant. Wind turbines can emulate higher inertia constants as long as they can increase the output power to desired levels.

3.3 Conclusion

In this chapter, the detailed modelling for PMSG wind turbine is presented. The MSC which is responsible for adjusting the turbine speed for MPPT operation is modified such that the wind turbine provides inertial support. The additional active power is obtained with the kinetic energy extraction from the turbine inertia.

The requirement of the inertial support provision is the back-to-back converter that enables the active power and speed control. Therefore, the method described in this chapter is not specific to PMSG wind turbines but the ones with full-scale power electronics.

CHAPTER 4

INVESTIGATION OF INERTIAL SUPPORT PRACTICAL LIMITS

The wind turbines are expected to participate frequency regulating mechanisms in the near future. However, their full capacity for fast frequency response is unknown. This chapter focuses the inertial support practical limits to explore the wind turbine potential under different wind speed scenarios.

4.1 Inertial Support Limits

The source of the power in a wind turbine is the aerodynamic wind power, P_{wind} which is constant for a constant wind speed, pitch angle and generator speed. In the steady state, this power is transferred through MSC as P_{gen}. If there is a difference between P_{wind} and P_{gen}, the difference is either stored in or extracted from the turbine and generator inertia as in the form of kinetic energy. Grid power, P_{grid} is received from MSC and injected grid. The difference between P_{gen} and P_{grid} is stored in or extracted from DC-bus capacitance. The active power flow diagram is depicted in Fig. 4.1.

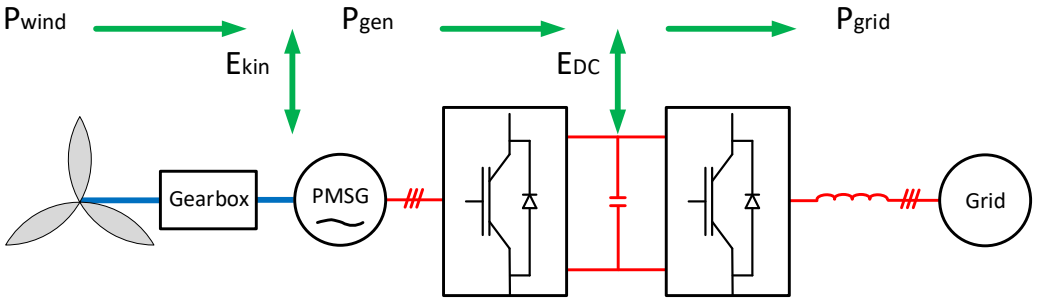

Figure 4.1: Active Power Flow Diagram

As mentioned in Chapter 3, stored energy exists in turbine and generator inertia and DC-bus capacitance. However, it is also stated that the E_{kin} is much larger than E_{DC} even in the lowest generator speed. Therefore, the source of additional power in the inertial support studies is the kinetic energy stored in the equivalent turbine inertia. Besides, the DC-bus voltage cannot be decreased below a threshold value that is dependent on the grid phase-to-neutral voltage. Therefore, the energy stored in DC-link capacitor is not utilized in this study.

Wind turbine active power can be increased by increasing the generator power P_{gen} as long as that power is successfully injected to grid . This can be achieved by adjusting the generator torque since the active power is proportional to electromagnetic torque. However, the active power is also dependent on the generator rotational speed as in Eq. (4.1). The active power can be increased by increasing the turbine torque but the increase is limited by the generator speed. Therefore, the active power increase is also dependent on the wind speed which determines MPPT speed in the steady state.

$$P_{gen} = T_e \omega_m \tag{4.1}$$

It is should be noted that the source of the additional power is the kinetic energy stored in the turbine equivalent inertia. Therefore, as soon as the power is increased, the turbine and generator speeds start decreasing. According to Eq. (4.1), the electromagnetic torque should be increased steadily to keep the generator power constant. As a result, the support time duration, the increase in the active power and the initial generator speed will determine the final generator speed as in the Eq. (4.2).

$$\int_{t_i}^{t_f} P_{wind} - \int_{t_i}^{t_f} P_{gen} = \Delta E_{kin} = \frac{1}{2} J_{total} (\omega_f^2 - \omega_i^2) \tag{4.2}$$

As seen from the Eq. (4.1), the generator power is the multiplication of generator torque and speed. In the high speeds, the generator speed ω_m, cannot be controlled with only the generator torque but also with the pitch angle. In this way, the rated power is not exceeded as in the Eq. (4.3) by keeping turbine at the maximum generator speed, ω_{max} and the maximum torque T_{P-lim} that is the torque limiting the turbine output power to rated active power. However, general practice is employing higher power rating converter than generator active power rating in the variable speed wind turbines [4]. Therefore, higher limit torque, T_{S-lim} can be used in such wind

turbine applications by considering the apparent power of the back-to-back converters. Therefore, the maximum power for a wind speed can be defined as in Eq. (4.4).

$$P_{rated} = T_{P-lim}\omega_{max} \tag{4.3}$$

$$P_{max} = T_{S-lim}\omega_{max} \tag{4.4}$$

It is obvious that the maximum available active power is dependent on the generator speed, hence, the wind speed for the corresponding operation time. This is why the amount of the active power increase also depends on the wind speed. By considering the MPPT speed operation in GE 2.75-103 model variable speed wind turbine, the maximum increase in the active power is shown in Fig. 4.2. The wind turbine can increase its active power by the lowest amount when the wind speed is high. Since the turbine output power is already close to converter maximum power rating, the increase in the active power is much lower than that of low wind speed operations. It is observed that the wind turbine output power can be increased by 1.3MW(0.43pu) when the wind speed is between 5m/s and 8m/s.

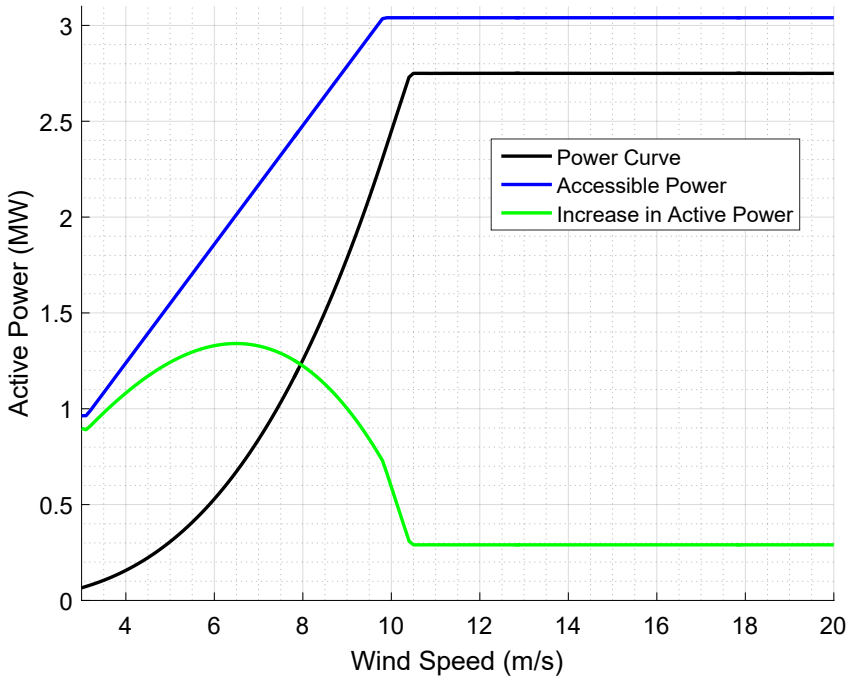

Figure 4.2: Accessible Active Power Output for Varying Wind Speeds

It is already stated that power system frequency is a function of input mechanical power of conventional synchronous generators and the output active powers. Therefore, frequency disturbances occur due to the imbalance between these. Since the aim of providing inertial support in the form of fast increased active power is to arrest the frequency decline, the increase in the output power is much more important than the total active output power.

4.2 Wind Turbine Properties

The wind turbine properties used in this study belong to GE2.75-103 model. Fig. 4.3 shows the wind farm in Balıkesir composed of corresponding model wind turbines. The properties of the GE2.75-103 is listed in Table 4.1.

Figure 4.3: GE2.75-103 Wind Turbine in Site

Property	Value	Unit
Turbine Type	GE2.75-103	-
Rated Turbine Power	2.75	MW
Converter Power Rating	3.04	MVA
Rotor Diameter	103	m
Blade Inertia	12600000	kgm^2
Generator Speed Range	550-1735	rpm
Rotor Speed Range	4.7-14.8	rpm
Cut-in Wind Speed	3	m/s
Cut-off Wind Speed	25	m/s
Air Density	1.225	kg/m^3
Gearbox Ratio	117.4	-
Generator Rated Voltage	690	V
Generator Type	PM Synchronous	-
Generator Inertia	240	kgm^2
Generator Pole	4	-
Generator Flux Linkage	2.5	Vs
DC-Link Capacitance	27	mF
DC-Link Voltage	1200	V

Table 4.1: GE2.75-103 Properties

4.3 Probabilistic Approach for Fast Inertial Support

In the Section 4.1, the inertial support limits are investigated for different wind speeds. It is stated that the wind turbines can increase their active power outputs by highest amounts in the low and medium wind speeds. In order to increase the meaningfulness of such support, probability of different wind speeds is studied. Wind speed measurements used in this thesis are taken from a real wind farm with GE 2.75-103 model wind turbines between 01/01/2017 and 21/08/2017. The variation of the wind speed in the side is depicted in Fig. 4.4.

Probability density function (PDF) of the measurements is given in Fig. 4.5. The

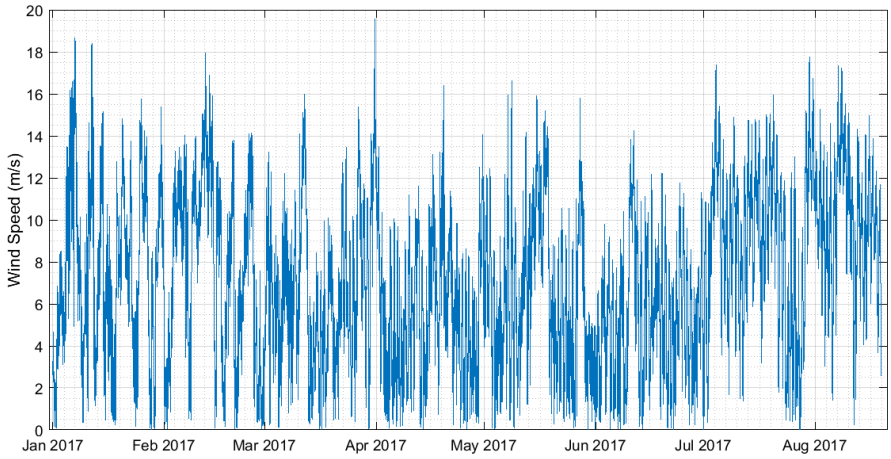

Figure 4.4: Variation of the Wind Speed in the Site

wind speed measurements have a mean of 7.13 with a standard deviation of 3.85.

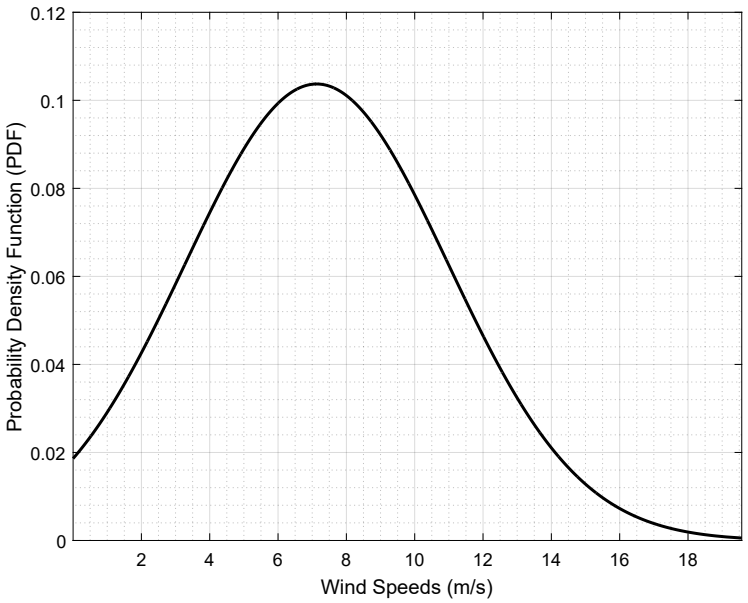

Figure 4.5: Probability Density Function of Measured Wind Speeds

For a defined wind speed, the active power increase can be calculated by considering the Section 4.1. However, likelihood of such an increase can be calculated by integrating PDF over desired the wind speed range.

It is obvious that the turbine can increase its output by an amount between 10% and

48% depending on the wind speed. However, the average inertial support from a wind turbine is another important property for testing the reliability of the support. By utilizing the wind speed measurements and the possible increase in the active output power, it is possible to define availability of the wind turbine for a possible inertial support. In other words, the increase in the active power can be united with the probability of the corresponding speed. In this way, the contribution from different wind speeds is obtained. The net power contribution for varying wind speed is given in the Fig. 4.6.

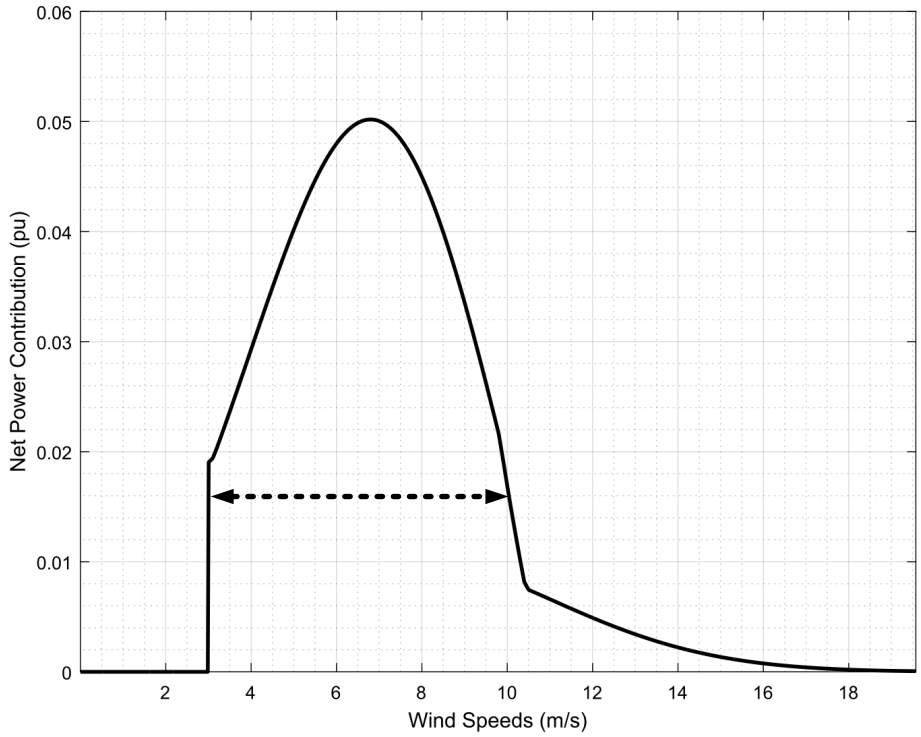

Figure 4.6: Distribution of Fast Inertial Support

Since Fig. 4.6 is basically product of the pdf given in Fig. 4.5 and the increase in the active power given in Fig. 4.2, the area under the graph gives average contribution from a wind turbine by considering the probability of the each wind speed measurement. Therefore, it can be concluded that the average contribution of wind turbine studied in this study is 0.3pu. This contribution is found by the area under the Fig. 4.2.

Moreover, the net contribution when the wind speed is below 3m/s is zero since the turbine is in the cut-off. The probability of the cut-off according to wind speed measurements is found out as %14.16. The main contribution concentrates inside the wind speed range between 3m/s and 10m/s that is shown with a dashed arrow inside Fig. 4.2. Due to the fact that this wind speed range has both higher probability and higher increase capability, the main contribution is provided inside this range. Meanwhile, the higher speed range has relatively lower contribution due to its lower probability and lower capability.

4.4 Fast Inertial Support Under Different Wind Speeds

Active power of the wind turbines is determined by parameters such as wind speed, pitch angle and turbine speed. Therefore, combination of these parameters have importance for a possible fast inertial support. In other words, wind turbine under high wind scenario has different potential than that under low wind scenario. Likewise, the resultant states of wind turbines for inertial support would be much different. In this section, the effect of wind speeds will be investigated for fast inertial support. Active power of wind turbines will be increased by different percentages in the fastest way independent of the grid frequency. Turbine internal parameters such as the change in generator speed, turbine and generator torques and pitch angle, if any, will be observed.

The rotational speed for varying wind speed is given in the Fig. 4.7. The minimum and maximum generator speeds exist between the 3m/s and 10m/s wind speeds. The Eq. (4.5) can be used to find out the rotational energy according to the wind speed.

$$E_{kinetic} = \frac{1}{2} J_{total} \omega_m^2 \tag{4.5}$$

The rotational energy is shown in the Fig. 4.8. The wind turbine stores almost 18MJ kinetic energy when the wind speed is above 10m/s. However, it stores 0.9MJ energy in the minimum generator speed. This energy can be extracted for the inertial support. However, a part of this energy is reserved for successful operation of the system such that the turbine speed deviation is limited as 30% [56]. The available energy that

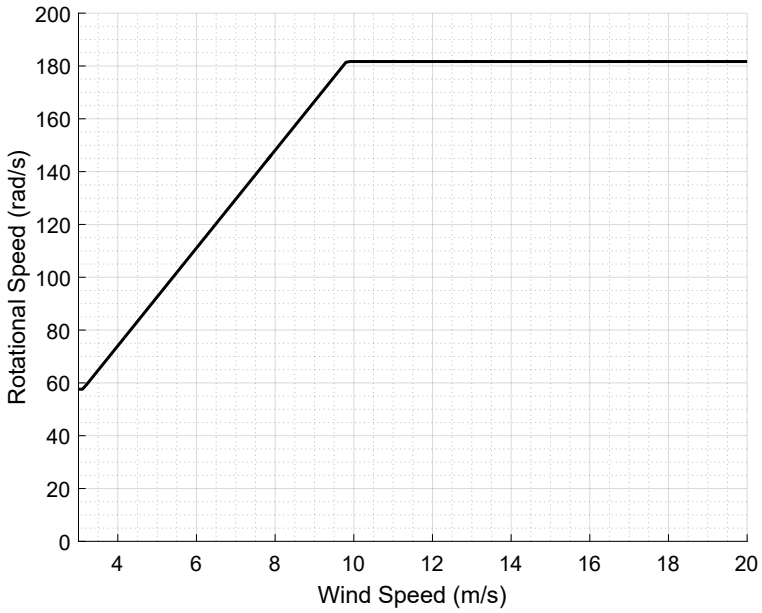

Figure 4.7: Variation of the Rotational Speed

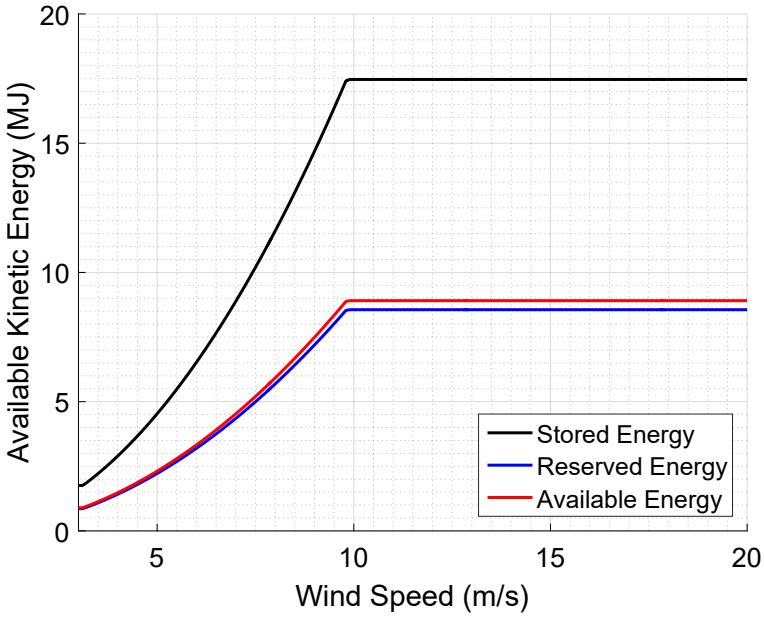

Figure 4.8: Variation of the Rotational Energy

can be used in the inertial support is shown in Fig. 4.8 as the difference between the stored energy and reserved energy.

Even though 9MJ rotational energy is available for inertial support in the wind speeds

above 10m/s, the turbine cannot increase its output power more than 0.1pu(275kW). Therefore, the rotational energy itself is not be meaningful without the converter capability. By considering the turbine capability for inertial support, the maximum support duration is found for the maximum power capability in the Fig. 4.9. The support duration is limited with 1 second in the lowest wind speed 3m/s meanwhile the support can be sustained permanently in the wind speeds above 10.8m/s.

In the following sections, wind turbine inertial supports will be investigated by considering the high, medium and low wind speed scenarios. In the each scenario, the wind turbine power will be increased to its maximum value according to the converter capability. The duration of the support is selected as 1 second since support duration of 1 second is achievable for all wind speeds as given in Fig. 4.9. Moreover, the wind turbine active power is increased by 10% for longer time durations (5, 10 and 20 seconds). The turbine internal dynamics will be investigated under in the limit and moderate cases of each wind speed scenario.

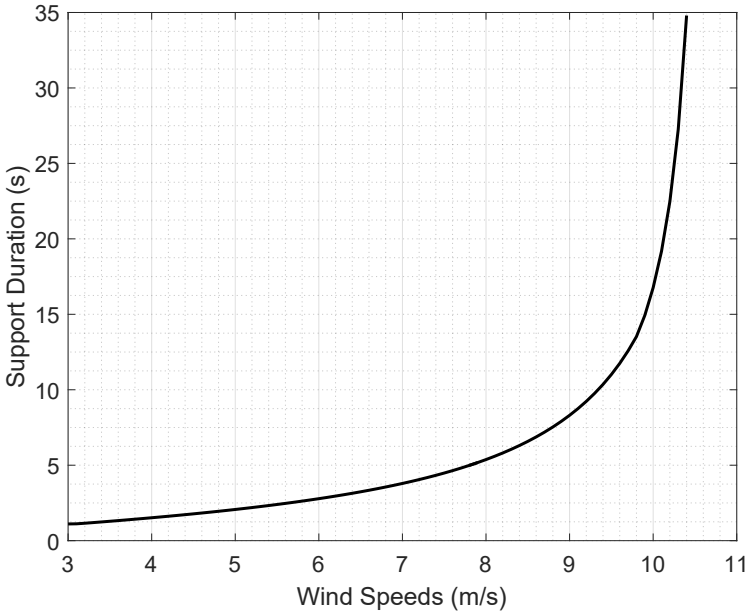

Figure 4.9: Maximum Support Duration of Inertial Support in the Limit Case

4.4.1 High Wind Scenario

In this section, wind turbine operation with 11.4m/s wind speed is investigated. The high wind scenario is much different than the low and medium wind speed scenarios. Firstly, the wind turbine injects its maximum power,P_{rated} to grid. Secondly, the generator reference speed is the maximum allowable speed, ω_{max} which implies that wind turbine operation is away from MPPT operation. In order to keep the generator in the maximum available speed, the pitch angle is used. The reason for using pitch angle is that the generator torque is limited by T_{P-lim}. Therefore, the wind turbine decreases turbine power and torque by increasing pitch angle.

Wind turbine in the high wind speed scenario has 10% capacity for active power increase. Therefore, it will increase its output power 10% both in the limit case (maximum achievable power with short time duration) and the moderate case (small increase in the active power with relatively longer durations).

4.4.1.1 Fast Inertial Support Limit in High Wind Scenario

Wind turbines are able to provide inertial support in high wind speed as long as converter power rating is higher than the wind turbine generator power rating. The wind turbine investigated throughout the study has a converter rating of 3.04MVA meanwhile turbine power rating of 2.75MW. Therefore, active power output can be increased up to 3.04MW during support interval as long as the converter and generator handle excess losses due to overloading. Otherwise, wind turbine cannot provide inertial support for high wind speeds. In the low and medium wind scenarios, the active power can be increased much higher than 10% in the limit case. However, the limit and moderate fast inertial support cases are the same for high wind speed scenario and limited by 10%.

In the limit cases, the active powers are increased to maximum achievable value and support is sustained for 1 second. However, this time duration is quite short for the high speed scenario since the speed is regulated with the help of pitch angle control. Therefore, the support duration in the high wind speed scenario is selected as 5 seconds. The generator power and torque are shown in Fig. 4.10. The generator

torque is increased from 1pu to 1.1pu. The increase in the torque rises the power to the maximum allowed power rating.

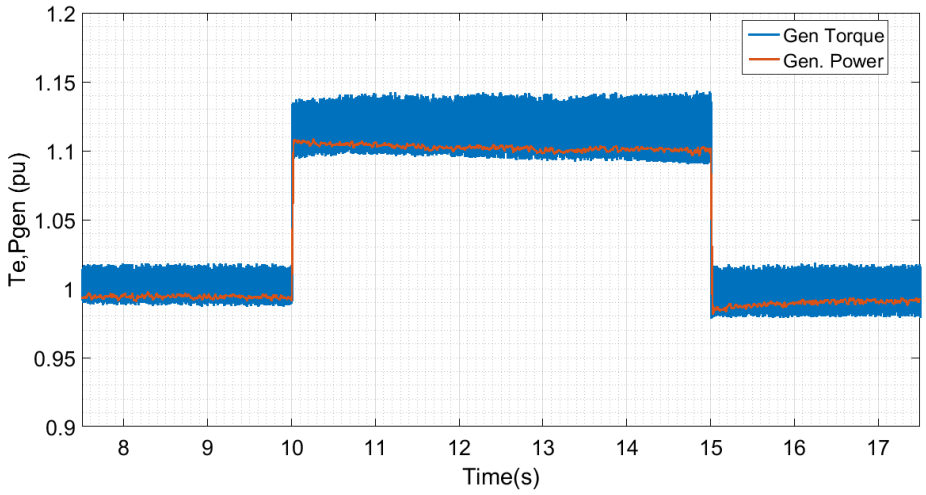

Figure 4.10: Fast Inertial Support Active Power Limit for High Wind Scenario

Turbine and generator powers, generator speed angle is shown in Fig. 4.11. The turbine power in this case rises with the inertial support that is different than low and medium wind scenarios. Moreover, the speed starts decreasing with the support. However, as the generator speed declines below the maximum generator speed, pitch angle of the turbine blades decreases which arrests the decrease in the generator speed. Furthermore, since the speed is below the maximum generator speed during support period, the pitch angle controller decreases the pitch angle causing an increase in the turbine torque. Therefore, the turbine torque goes slightly above 1.1pu and results in a small acceleration in the generator speed.

The variation of the pitch angle and the rate of change of pitch angle is shown in Fig. 4.12. The pitch angle is decreased from 1.4 to 0.8 that avoids the speed decrease in the generator. Therefore, the fast inertial support in the high speed scenario does not require speed recovery since the speed is close to the pre-support speed. The pitch rate in the beginning of inertial support reaches to $0.8°/s$ that is below the maximum allowable pitch rate of $5 - 10°/s$ [38].

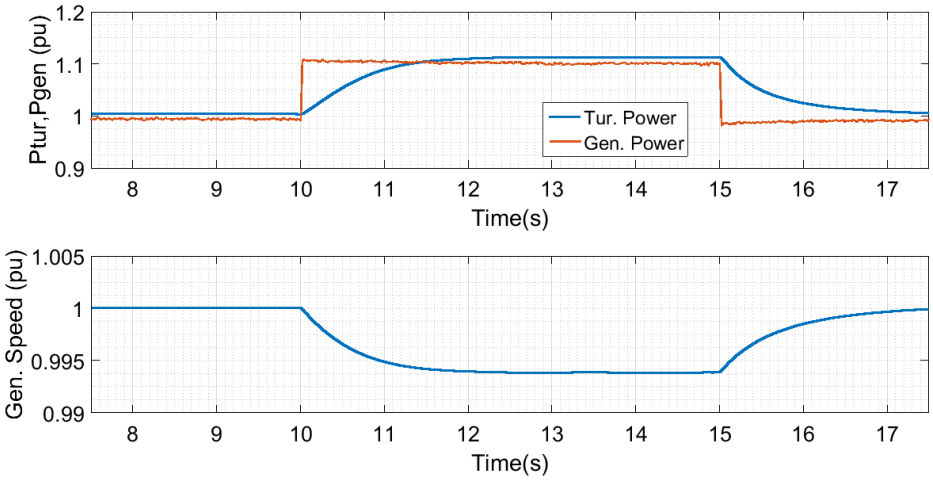

Figure 4.11: Turbine and Generator Powers and Generator Speed for High Wind Limit Scenario

4.4.1.2 Moderate Inertial Support Limit in High Wind Scenario

In this part, the active power of the wind turbine is increased again by 10% with three different time intervals. The active powers are shown in Fig. 4.13.

An interesting observation in high wind scenario is that there is no speed recovery process. As soon as the speed is decreased, the pitch controller decreases the blade angle which causes an increase in turbine torque. Therefore, in this case, turbine power decreases back to normal rather than a lower power value as in the other scenarios. In the high wind scenario, the generator torque hits the limit defined for normal operating conditions. This is why generator speed is regulated with the help of blade angle. Therefore, pitch angle is also important in this section.

Generator speed, turbine and generator torques as well as pitch angle for 20 seconds support case are shown in Fig. 4.14. Generator speed starts decreasing when the generator torque is increased. However, the pitch controller decreases the blade angle since the generator speed is below the maximum speed. Therefore, the generator speed rises when the pitch angle is decreased. Note that pitch servo acts slower than the generator torque increase time. This is why the generator speed decreases until the pitch angle is decreased. Generator speed might not be disturbed if the pitch

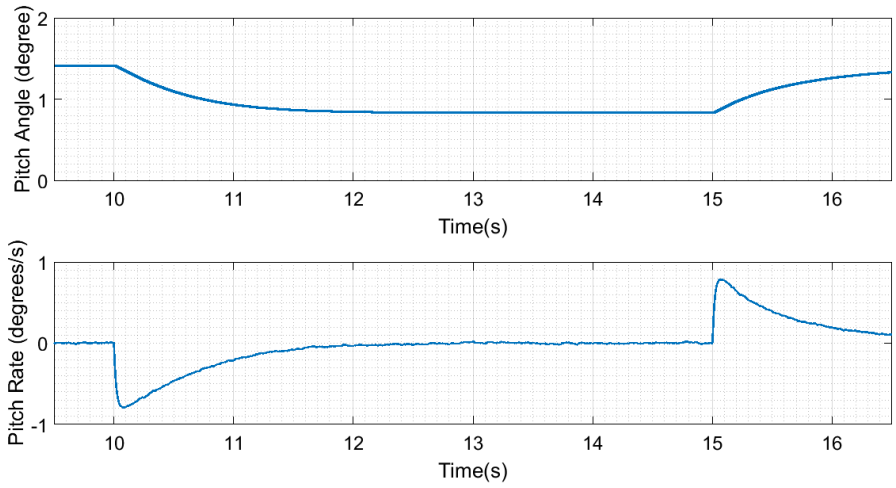

Figure 4.12: Pitch Angle and Rate of Change of Pitch Angle for High Wind Limit Scenario

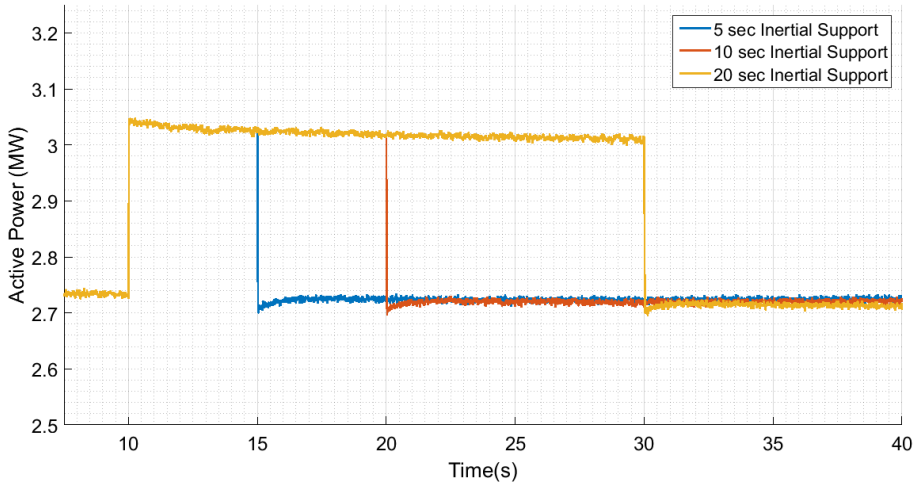

Figure 4.13: Active Power Output of the Wind Turbine for High Wind Scenario

controller is able act fast enough.

After the generator speed is arrested within 2 seconds by the pitch angle, generator speed starts rising towards the maximum generator speed. If the support time is increased, the generator speed will reach the maximum speed, and will stay constant with a new pitch angle. This means that the turbine is able to provide the support forever. However, the full capacity of the converter cannot be used permanently since it causes overloading of the converters in the wind turbine and excess heat losses.

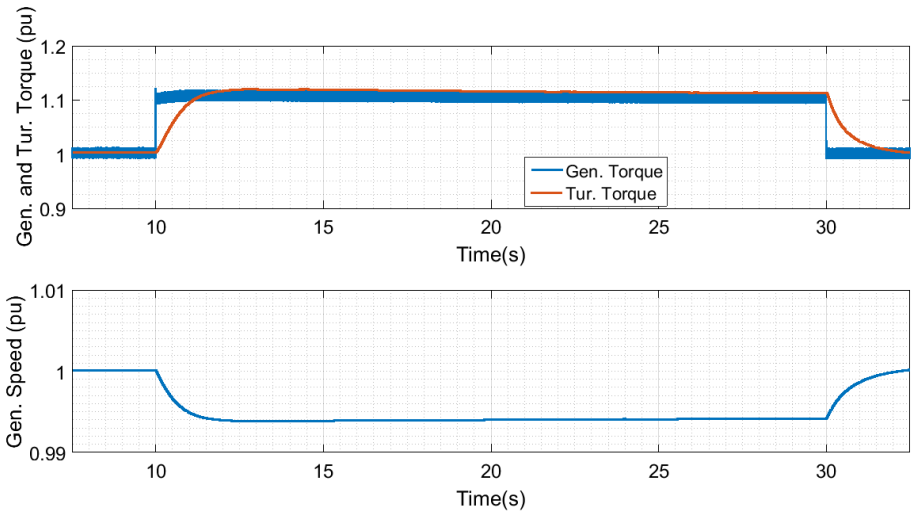

Figure 4.14: Generator and Turbine Torques and Generator Speeds for High Wind Scenario for 20 Seconds Support

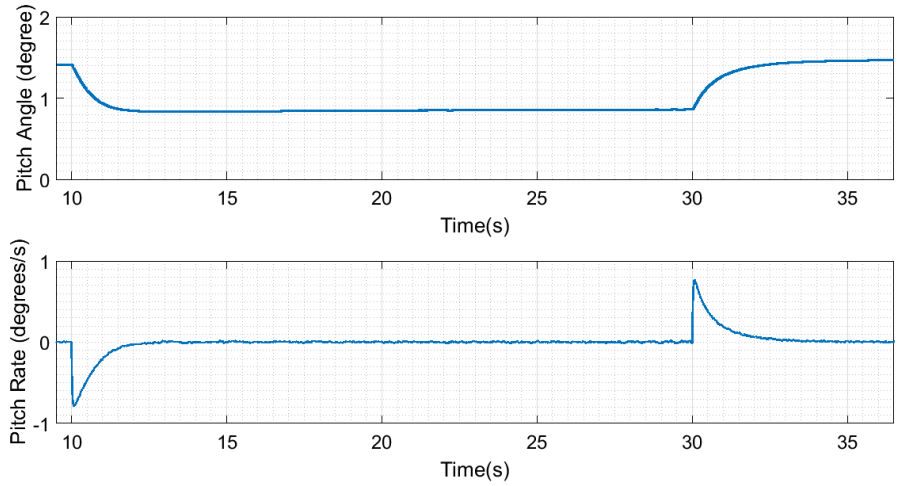

Figure 4.15: Pitch Angle and Rate of Change of Pitch Angle for High Wind Scenario for 20 Seconds Support

The pitch angle variation and the rate of change of pitch angle is given in Fig. 4.15. Rate of change of blade angle in the beginning of inertial support reaches to $0.8°/s$ as in the limit case.

4.4.2 Low Wind Scenario

The minimum speed of the wind turbine generator in this scenario is 550 rpm (4.7 rpm in the rotor). Wind speed that will capture the maximum power from wind in this generator speed is found out to be 3.12m/s. In this scenario, the kinetic energy stored in the turbine inertia is minimum as calculated in Eq. (3.27). This scenario investigates the case where the least amount of kinetic energy exists in the turbine equivalent inertia. By the fast inertial support provision, the wind turbine speed decreases below the minimum generator speed. However, the resultant minimum generator speed is dependent on the increase in the active power and also the support interval.

4.4.2.1 Fast Inertial Support Limit for the Low Wind Scenario

The electricity grid in the upcoming future might require sudden active power release from wind farms for short time durations to arrest steepest frequency declines. Therefore, it is important to observe the maximum achievable power for inertial support studies. The equation Eq. (4.4) implies that wind turbine in the low wind speed scenario cannot reach rated power since the generator speed is much lower than the maximum generator speed. However, the electromagnetic torque in steady state is much lower than the limit torque, T_{S-lim}. Therefore, the wind turbine in low speed scenario has the potential for increasing its active power by 0.32pu.

Fig. 4.16 shows the active power, output torque and the speed of the generator. The increase in the active power is obtained by ensuring the limit torque, T_{S-lim}. In this way, wind turbine can achieve a power value of 0.35pu in the limit case. However, since the generator speed is decreasing, the active power is also decreasing due to the fact that further increase in the generator torque is not possible.

The support duration is chosen as 1 second according to the available kinetic energy utilization. Even in this short duration, the generator speed declines by 25%. It should be noted that turbine might stall if the support duration is extended.

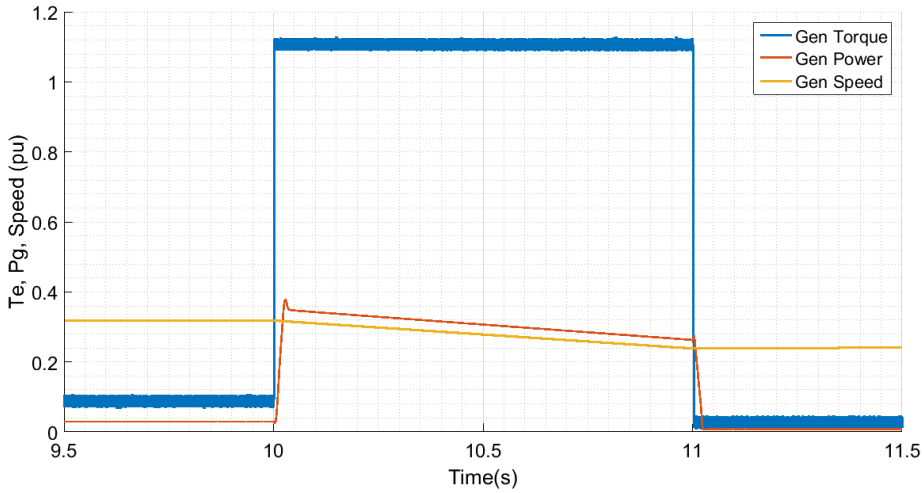

Figure 4.16: Fast Inertial Support Active Power Limit for Low Wind Scenario

4.4.2.2 Moderate Fast Inertial Support for the Low Wind Scenario

Wind turbines are able to increase its power by 0.32pu even in the low wind speed scenario. However, the time interval is kept as 1 second possible in order to be kept within the available kinetic energy limit. Nonetheless, the longer support periods can be achievable if the increase in the active power is decreased. Therefore, in this part, the active power of the wind turbine is increased by 10% for three different time intervals as 5, 10 and 20 seconds. The active power output of the wind turbine is given in Fig. 4.17. It is observed that turbine power decreases below the nominal value after the support period in order to recover the generator speed. Another observation is the fact that higher support time creates higher dip in the active power in the speed recovery period.

Generator speed decreases continuously until the support is ended. The generator speeds are shown in Fig. 4.18 for three support scenarios. The decrease in the generator speed is obtained with an increase in the generator torque. The turbine torque, generator torque and generator speed for 5 seconds support duration is given in Fig. 4.19. The generator torque is increased at t=10s for a time duration of 5 seconds. Turbine torque increases slightly with decreasing speed. However, the increase in the turbine torque is negligible when it is compared to the increase in generator torque. Therefore, the turbine torque can be considered to be constant for the support period

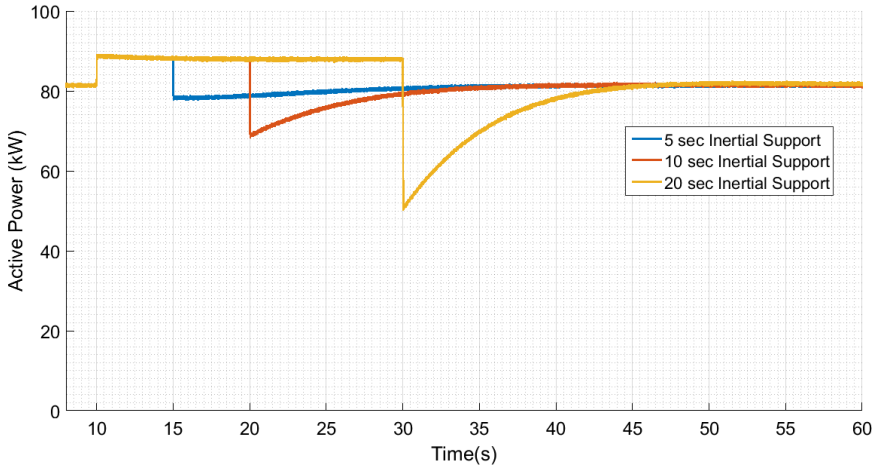

Figure 4.17: Active Power Output of the Wind Turbine for Low Wind Scenario

meanwhile the generator torque is increased. Wind speed in this scenario decreases 1.6%. Turbine and generator torque for 20 second case is also shown in Fig. 4.20 in which speed decreases by 4.8%.

4.4.3 Medium Wind Scenario

In the medium wind scenario, wind turbine is operated in 6m/s wind speed. This corresponds to the generator speed of 110.8rad/s (9rpm rotor speed). Wind turbine in the medium wind speed range can increase its power by 1.32MW for fast inertial support as stated in the Section 4.1. Even though the wind turbine has lower kinetic energy than that of high wind scenario, it can reach higher active power values due to its higher MPPT speed.

4.4.3.1 Fast Inertial Support Limit for the Medium Wind Scenario

It is already mentioned that wind turbines in the medium wind speed scenario can increase its power more than that of low wind speed scenario. The reason is the dependency of the active power on the generator speed. The active power limit in the medium wind speed scenario is given in Fig. 4.21. The wind turbine active power is increased by 1.32MW as expected in the Fig. 4.2.

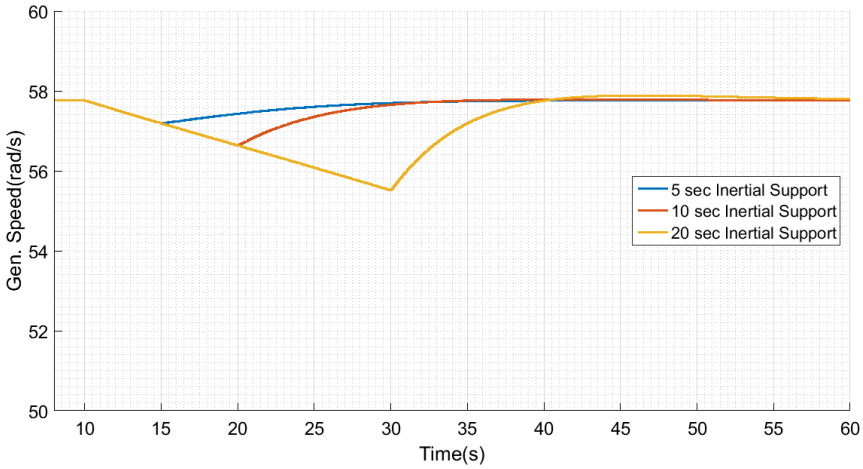

Figure 4.18: Generator Speeds of the Wind Turbine for Low Wind Scenario

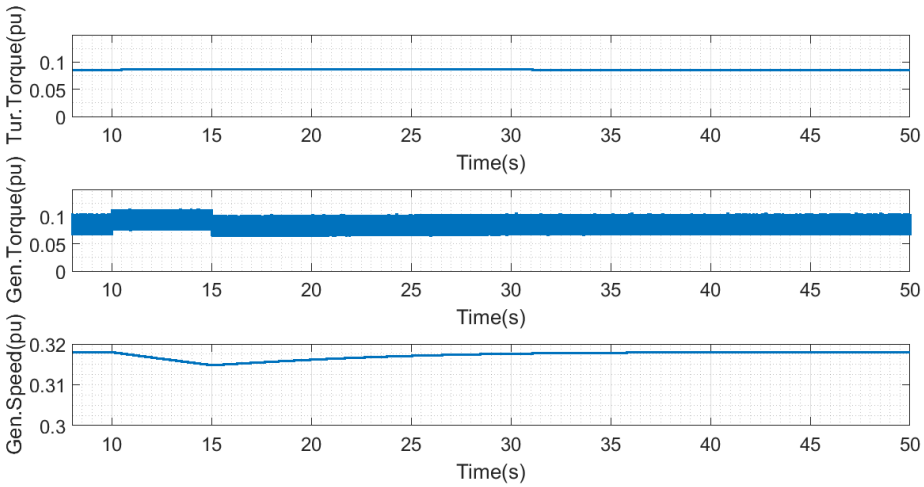

Figure 4.19: Turbine Torque, Generator Speed and Generator Torque for 5 Seconds Support Duration under Low Wind Speed

Generator speed decreases due to increased generator power while the turbine power is almost constant. Since the turbine leaves the MPP point, the turbine power declines. However, the change in the turbine power is small. Therefore, the turbine power is said to be constant for this interval.

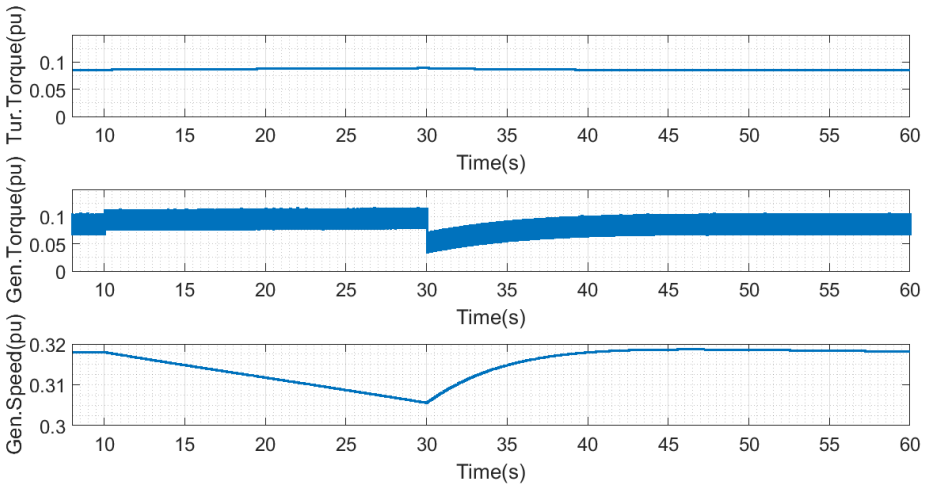

Figure 4.20: Turbine Torque, Generator Speed and Generator Torque for 20 Seconds Support Duration under Low Wind Speed

4.4.3.2 Moderate Fast Inertial Support for the Medium Wind Scenario

Fast inertial support with a duration of 1 second can be evolved to moderate inertial support with longer duration of support as 5, 10 and 20 seconds and small increase in active power. Therefore, the active power of the wind turbine is increased by 10% and it is shown in Fig. 4.22 for three different time intervals. The recovery period of shortest support case is much more smoother than the longer ones. When the support time is increased, active power of the wind turbine is almost halved that might cause also problems in frequency stability of the power systems.

In medium wind scenario, higher support time causes decreased active power after the support. The reason is the lower speed value obtained with higher support time. Generator torque is decreased much higher for this case in order to recover the speed. The generator speed, turbine and generator torques are shown in Fig. 4.23. After the support, MPPT algorithm takes action and regulates the speed correspondingly. Therefore, the generator torque jumped down to lower value to restore the MPPT speed. The negative jump in generator torque crates a negative jump in the active power of the wind turbine since the transferred power is the multiplication of generator torque and generator speed.

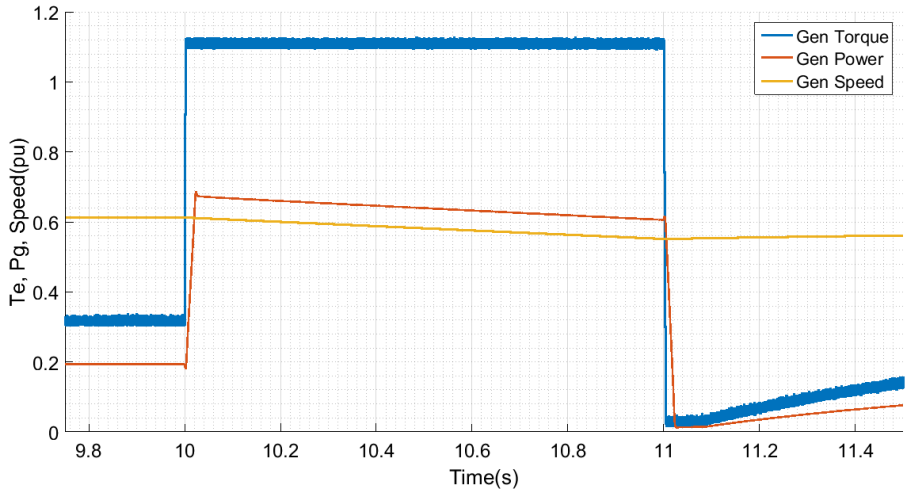

Figure 4.21: Fast Inertial Support Active Power Limit for Medium Wind Scenario

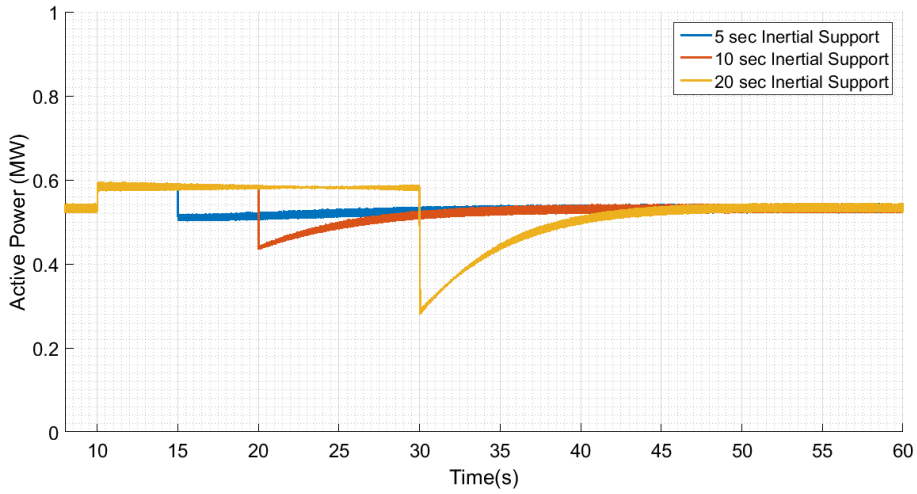

Figure 4.22: Active Power Output of the Wind Turbine for Medium Wind Scenario

4.5 Conclusion

In this section, the wind turbine practical limits are investigated for the inertial support provision. The capability of the wind turbine is revealed based on the different wind speed scenarios. The results has shown that the turbine is able to increase its active power by 0.45pu when the turbine operates in the medium wind speed range (6m/s and 8m/s). The turbine capability decreases down to 0.1pu additional power when the turbine operates in the high wind speed range which is above the 10m/s.

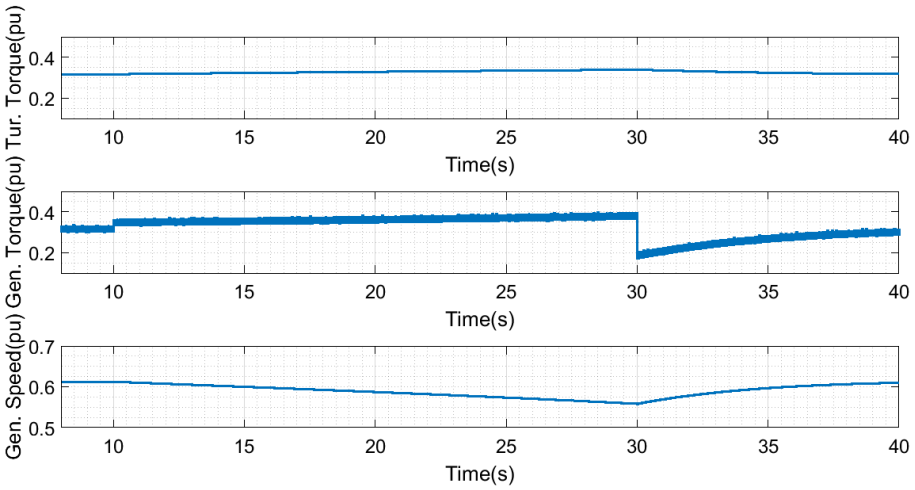

Figure 4.23: Generator Speed, Generator and Turbine Torques for Medium Wind Scenario for 20 Seconds Support

Another conclusion of this chapter is the fact that the studied wind turbine is appropriate for inertial support provision. The internal turbine parameters such as generator torque and active power are kept inside the operational limits inside the support duration. In the high wind speeds, the pitch angle controller first decreases the blade angle as the generator speed decreases. The blade angle is increased after support duration. During these transitions, rate of change of pitch angle is kept inside the operational limits. The maximum pitch angle rate is $0.8°/s$ that is much below the maximum pitch angle rate limit of $10°/s$ [38].

Finally, it is shown that the wind turbines can increase its active power up to 0.45pu during the 1 second support duration. Meanwhile, the support duration can be increased up to 30 seconds as the support power is decreased to 10%. The fast inertial support is provided to grid with an amount independent from the grid frequency. The active power can be increased 20ms after the support command. The fast injection of the active power decreases the initial RoCoF following a frequency disturbance. However, the grid frequency is subjected to a second dip as soon as the inertial support is ceased. This is another disadvantage of the fast inertial support and might cause another frequency disturbance in weak power systems.

The fast inertial support is independent of the grid frequency. However, the increase

in the active power can be a function of the frequency behaviour as in the case of synthetic inertia. In the Chapter 5, the inertial support proportional to RoCoF will be investigated.

CHAPTER 5

IMPLEMENTATION OF SYNTHETIC INERTIA IN A 9-BUS TEST SYSTEM

In the Chapter 4, it is shown that the wind turbine that is connected to grid with back-to-back converter is able to increase its power by almost 0.5pu. Active output power of the turbine can be increased suddenly by utilizing the kinetic energy in the turbine inertia. However, the increase in the fast inertial support is not a function of the grid frequency but a pre-defined period. Nonetheless, the concept of synthetic or virtual inertia suggests a frequency response from renewable energy systems depending on the RoCoF of the electricity grid. As explained at the end of Chapter 3, a renewable energy system can provide an additional power according to the Swing Equation.

In this chapter, the synthetic inertia implementation on a variable speed PMSG wind turbine is tested in P.M. Anderson 9 bus test case which is constructed in Matlab-Simulink environment. Frequency response of the test case is investigated against the sudden load connections in different scenarios. Moreover, the synthetic inertia concept is evaluated in terms of the Turkish electricity network.

5.1 P.M.Anderson 9 Bus Test Case

In order to understand frequency dynamics better, P.M. Anderson test case has been used in the study. P.M. Anderson 9-bus system is one of the test systems in the area of Power Systems to validate the proposed methodologies. It is composed of 9 buses, 3 loads, generators and transformers and 6 lines. IEEE also offers 14, 30 and 118 bus test systems. However, Matlab-Simulink environment restricts the number of buses due to computational burden. This why the 9-bus test system is selected for the syn-

thetic inertia implementation. The single line diagram of the test system is given in Fig. 5.1. The test case consists of three generators and three loads. Generators in the system are connected to 230 kV high voltage (HV) network with step-up transformers.

The biggest generator in the system is a hydro power plant with a power rating of 247.5 MVA. The remaining ones are steam generators. The power ratings of the generators are given in Table 5.1.The loads in the system are connected directly to the HV network. The active and reactive power ratings of the loads are listed in Table 5.2. Detailed system properties are given in Appendix A.

Generators	Power Rating (MVA)	Plant Type
Gen 1	247.5	Hydro
Gen 2	192	Steam
Gen 3	128	Steam

Table 5.1: Generator Properties of test System

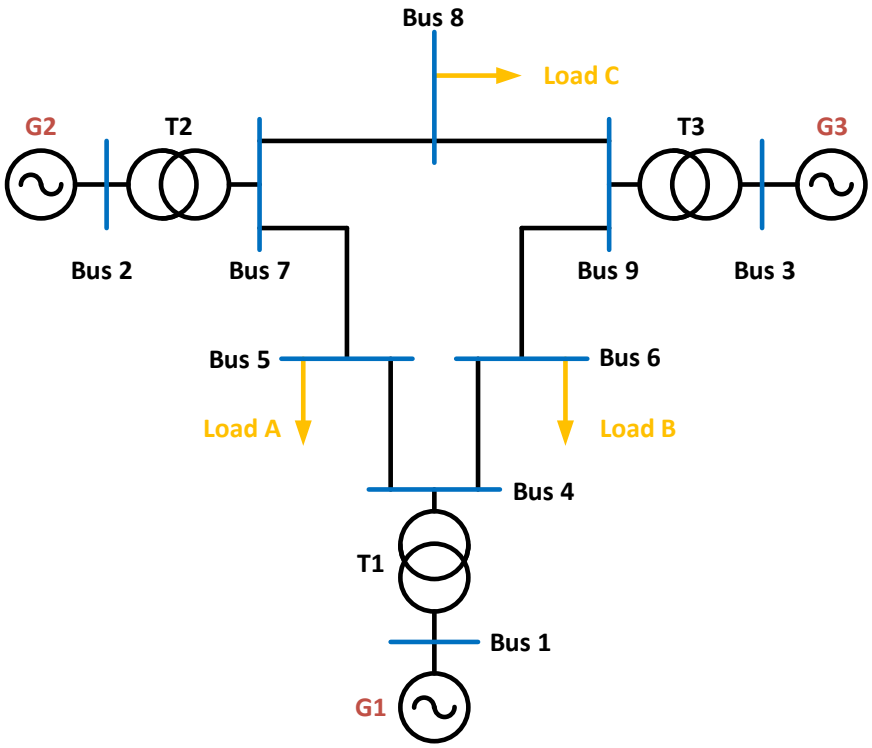

Figure 5.1: P.M.Anderson Test Case [10]

Generators	Active Power (MW)	Reactive Power (MVAr)
Load A	125	50
Load B	90	30
Load C	100	35

Table 5.2: Load Properties of Test System

5.1.1 Load Flow Analysis for Base Case

Successful grid operation requires a load flow analysis in order to ensure that bus voltages are within the allowed band and power flows are below the power carrying capabilities of the lines. In a load flow, bus voltages and phase angles are calculated. The buses which have a connection with a generator is called as 'PV' bus due to the fact that active power injected to system as well as bus voltage are known before the load flow. Meanwhile, the only load connected buses are called 'PQ' bus with the knowledge of the active and reactive power. For the load flow in the system, one of the buses is selected as slack bus, 'SL' bus with only the voltage is predetermined. The generation of the slack bus will be calculated after the load flow analysis due to the fact that transmission losses in the system are unknown before the analysis. Load flow results are tabulated in Table 5.3.

Bus #	Bus Type	Voltage(pu)	Angle(°)	Pg(MW)	Qg(MVAr)	Pl(MW)	Ql(MVAr)
1	SL	1.04	0	71.65	27.05	0	0
2	PV	1.025	9.28	163	6.65	0	0
3	PV	1.025	4.66	85	-10.86	0	0
4	PQ	1.0258	-2.22	0	0	0	0
5	PQ	0.9956	-3.99	0	0	125	50
6	PQ	1.0126	-3.69	0	0	90	30
7	PQ	1.0258	3.72	0	0	0	0
8	PQ	1.0159	0.73	0	0	100	35
9	PQ	1.0323	1.97	0	0	0	0

Table 5.3: Load Flow Results in Base Case

5.1.2 Base Case Frequency Response for Additional Load Connection

It is obvious that power system networks experience high RoCoF when either high amount of generation trips or high amount of load is connected to the system. These two main events can be used in the simulation to create frequency disturbances.

Total System Load	315 MW
Generator Droop Settings	5%
Stored Kinetic Energy	3.3 GJ
Effective Kinetic Energy	3.3 GJ
Gen 1 Inertia Constant	9.55 s
Gen 2 Inertia Constant	3.92 s
Gen 3 Inertia Constant	2.77 s

Table 5.4: System Dynamical Properties

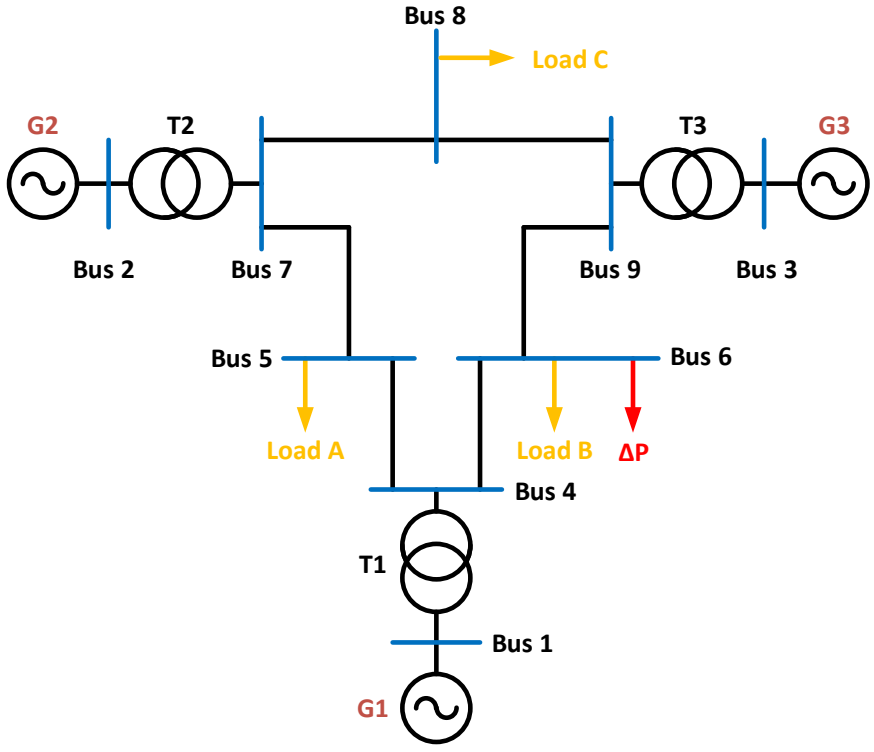

Figure 5.2: Location of the Additional Load

The dynamical properties of the system are listed in Table 5.4. The system load 315MW is supplied from three conventional generators that have inertia constants

ranging between 2-9 seconds. Three generators are equipped with governors with 5% droop settings. Furthermore, the system has 3.3GJ kinetic energy which are effectively supplied from the conventional synchronous generators.

Power generation references are determined based on the load flow of "powergui" toolbox. Machine initialization toolbox is also used to initiate the state of generators in the system. However, the system does not start with the steady state but reaches the steady state within a few seconds. Frequency of the network is disturbed with a load connection when t=10 seconds in order to observe the frequency stability of the system. For 10% load connection, a load of 31.5MW is connected to system from Bus 6. Location of the additional load is depicted in Fig. 5.2.

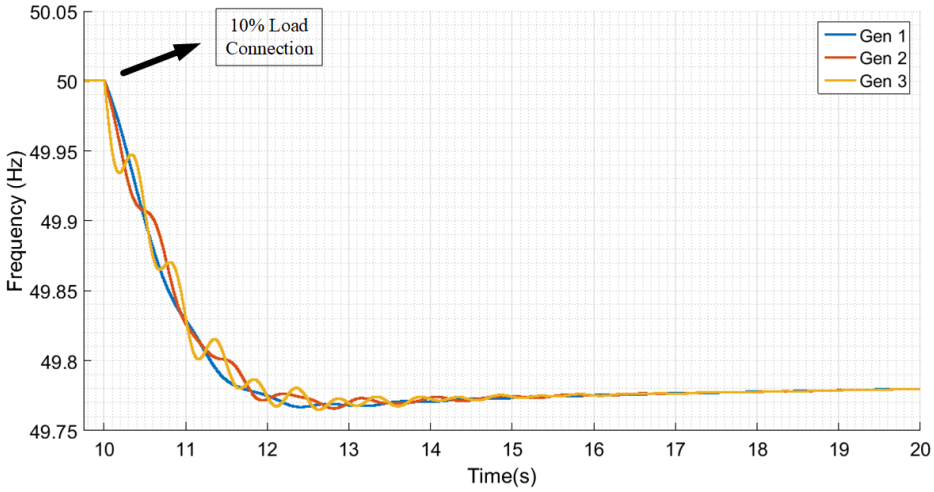

Figure 5.3: Generator Frequencies for Frequency Disturbance in Base Case

According to the 10% load connection to system, generator frequencies are shown in Fig. 5.3. As it can be seen from Fig. 5.3, rotor swings exists in the frequencies. However, the frequency of generator-1 is the most smooth one due to its huge inertia constant. Meanwhile, the generator-2 and generator-3 follow the frequency of generator-1 with rotor swings.

In the system, the frequencies of loads are almost the same throughout the network since the test system is small enough to assume a single frequency inside the network. This can also be observed in Fig. 5.4 which shows the frequency of the generator-1 as well as the load frequencies captured with PLL (Phase-Locked Loop) block.

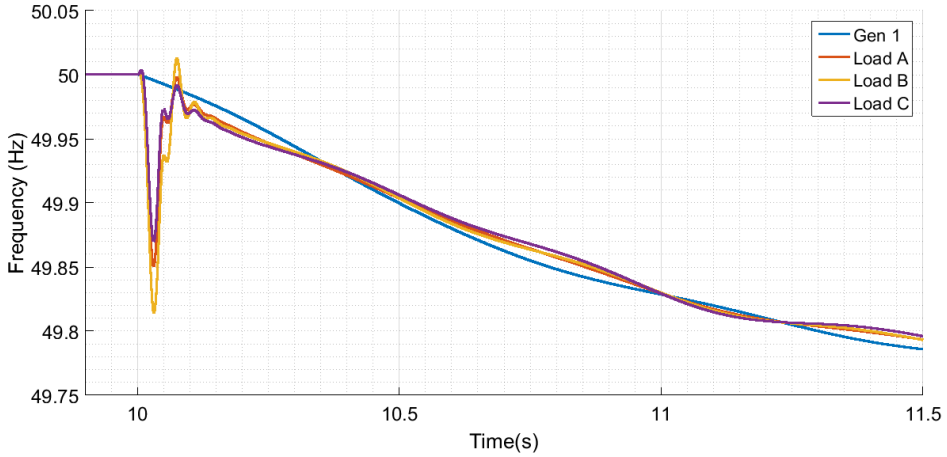

Figure 5.4: Frequencies in Generator 1 and Load Buses

Another observation is that the load frequencies are also close to the frequency of the generator-1. The only difference is the instant following the load connection. The sharp frequency decline delays the PLL loop to capture the frequency.

5.2 10% Renewable Generation Case

In order to observe the effect of the renewable energy penetration to the grid, the P.M. Anderson test case is modified such that a wind farm consists of 20 wind turbine is connected to the network. The wind farm has 55MW power rating that consists of 20 of 2.75MW GE2.75-103 model wind turbines. The share of the renewable energy is selected as 10% of the installed capacity. Moreover, the wind speed is selected as 9m/s that provides 10% active power generation of the system demand.

Since the transmission network of the test case is under-utilized, the location of the wind farm has no effect on the frequency disturbance. Hence bus 5 is selected as the location for wind farm connection. Modified system is depicted in the Fig. 5.5. In this case, generators 2 and 3 are still assigned to same power generation references. However, the reference generator (generator 1) production is found according to the load flow results. Since the wind turbine also injects power to the transmission network, generator-1 decreases its generation according to the base case.

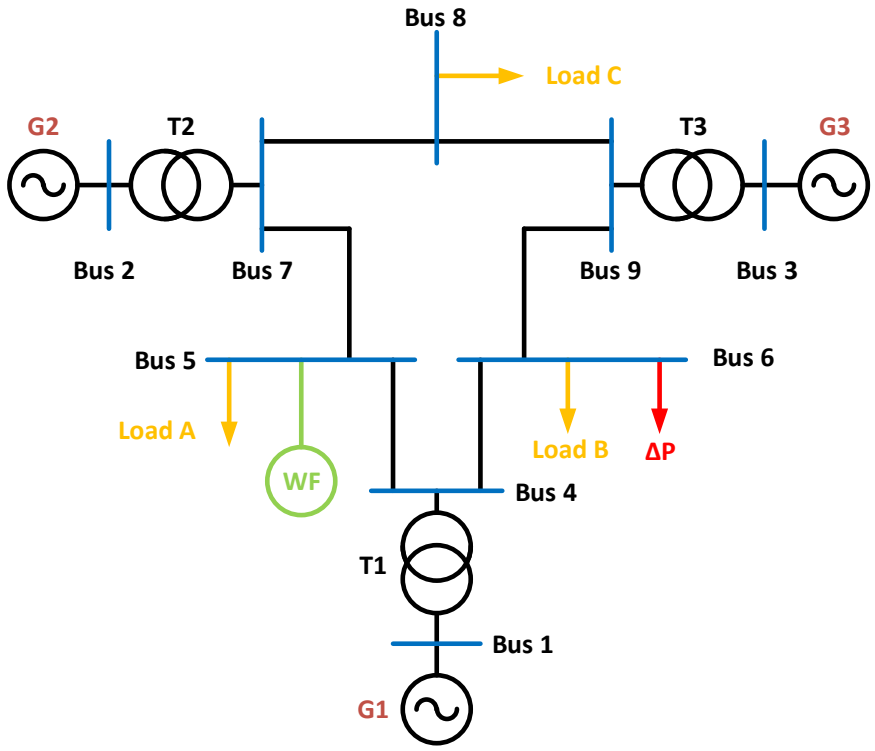

Figure 5.5: 10% Renewable Generation Case Single Line Diagram

5.2.1 Load Flow Analysis for 10% Renewable Generation Case

Load flow analysis for the modified case is listed in Table 5.5. The power injected from Bus 1 is decreased as expected. This can also be seen from the phase angle between buses 1 and 4 which decreased from $2.22°$ to $1.18°$. Total power generation from active power from conventional generation units are also decreased. Therefore, the modified system resembles the base case with low power demand. The wind farm production cannot be shown in the Bus-5 power generation section since the corresponding bus is a PQ bus. Therefore, the wind farm power is shown in the load side as negative injection to the system. Wind farm produces 35.7MW active power at unity power factor.

Bus #	Bus Type	Voltage(pu)	Angle(°)	Pg(MW)	Qg(MVAr)	Pl(MW)	Ql(MVAr)
1	SL	1.04	0	38.06	25.07	0	0
2	PV	1.025	11.33	163	6.65	0	0
3	PV	1.025	6.32	85	-10.86	0	0
4	PQ	1.0263	-1.18	0	0	0	0
5	PQ	0.9995	-1.54	0	0	125-(35.7)	50-(0)
6	PQ	1.0128	-2.43	0	0	90	30
7	PQ	1.0266	5.77	0	0	0	0
8	PQ	1.0164	2.62	0	0	100	35
9	PQ	1.0326	3.62	0	0	0	0

Table 5.5: Load Flow Results for Modified Case

5.2.2 10% Renewable Case Frequency Response for Additional Load Connection

10% Renewable Case is very similar to the Base Case except for a wind farm located in Bus 5. The wind farm consisting of 20 turbines also has stored kinetic energy depending on generator speed. Wind speed of 9m/s stores 293.7MJ kinetic energy in the wind farm. By considering this stored energy, dynamical properties of the system is updated in the Table 5.6. Nonetheless, the effective kinetic energy is unchanged in the system due to the fact that rotor frequency is decoupled from grid frequency in the existing wind turbine model.

Total System Load	315 MW
Generator Droop Settings	5%
Stored Kinetic Energy	3.6 GJ
Effective Kinetic Energy	3.3 GJ
Gen 1 Inertia Constant	9.55 s
Gen 2 Inertia Constant	3.92 s
Gen 3 Inertia Constant	2.77 s

Table 5.6: System Dynamical Properties with Wind Farm

The renewable energy system in this case can be considered as a negative load of

35.7MW. Therefore, base case with decreased load is under discussion in this subsection. 10% additional load (31.5MW) is connected to Bus 6 and the frequency response of the 10% Renewable Case is shown in Fig. 5.6a.

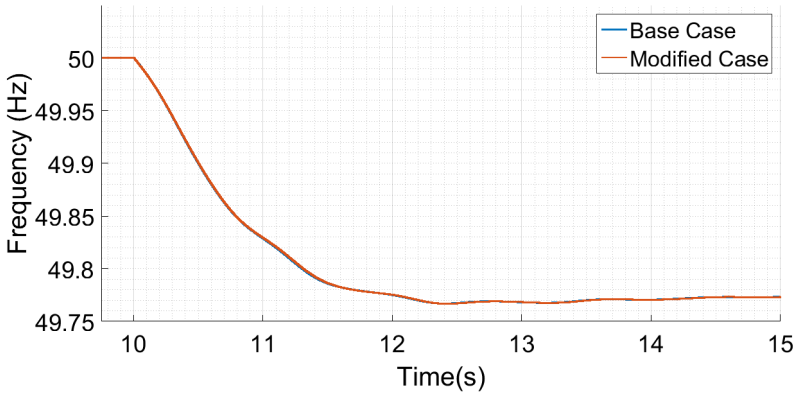

(a) Comparison of Frequencies

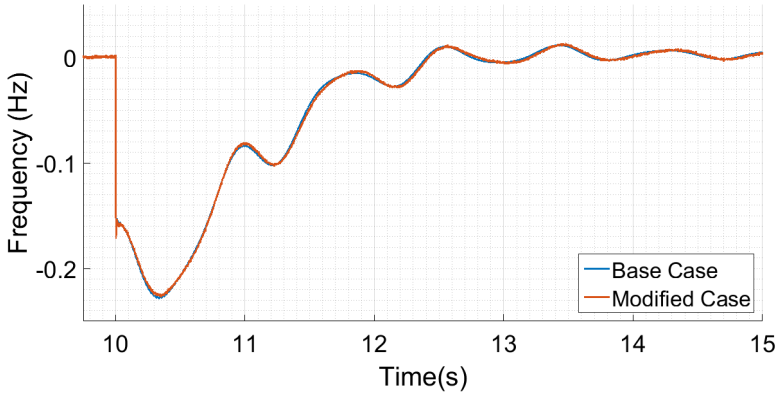

(b) Comparison of RoCoFs

Figure 5.6: Comparison of Base Case and 10% Renewable Generation Case

Almost the same frequency response is observed in the system, as both systems have the same amount of stored kinetic energy. Another reason is that there is no congestion in the system due to under-utilized of transmission network. The same frequency response can also be observed in the rate of change of frequencies in Fig. 5.6b. This concludes that renewable energy penetration does not change the frequency response of the system if the only change in the system is the inclusion of renewable energy system. In other words, renewable energy systems does not affect the frequency response of the grid unless the system is preferred over a conventional generation unit.

Notice that the renewable energy systems are intermittent energy sources. Nonetheless, the wind speed is assumed as constant in this study. Assuming constant wind speed is not a disadvantage since the inertial support is based on the kinetic energy of the wind turbine. The variation of the wind speed during the support period affects only the speed recovery process.

5.3 Reduced Inertia Case

As seen in the %10 Renewable Generation Case, the frequency response of the system does not change with renewable energy inclusion. However, it is inevitable that renewable energy systems will replace the conventional units in the future. The economic dispatch determines the power plant generation levels according to their energy prices. Since the thermal units have fuel costs compared to wind and solar systems, they might be shut down consequently. In order to investigate the effect of thermal decommissioning, the smallest generator, generator-3, is shut down. When the generator-3 is out of service, the effective inertia decreases by %10. The reduced inertia case diagram is shown in Fig. 5.7.

Total System Load	315 MW
Generator Droop Settings	5%
Stored Kinetic Energy	3.3 GJ
Effective Kinetic Energy	3.0 GJ
Gen 1 Inertia Constant	9.55 s
Gen 2 Inertia Constant	3.92 s

Table 5.7: Reduced Inertia Case Dynamical Properties

Since the generator-3 is out of service, the stored kinetic energy is decreased in the system. Dynamical properties of the reduced inertia case are updated and given in Table 5.7. Higher RoCoF value and lower frequency nadir are expected with the same additional load since the system dynamical properties are deteriorated with the removal of generator-3.

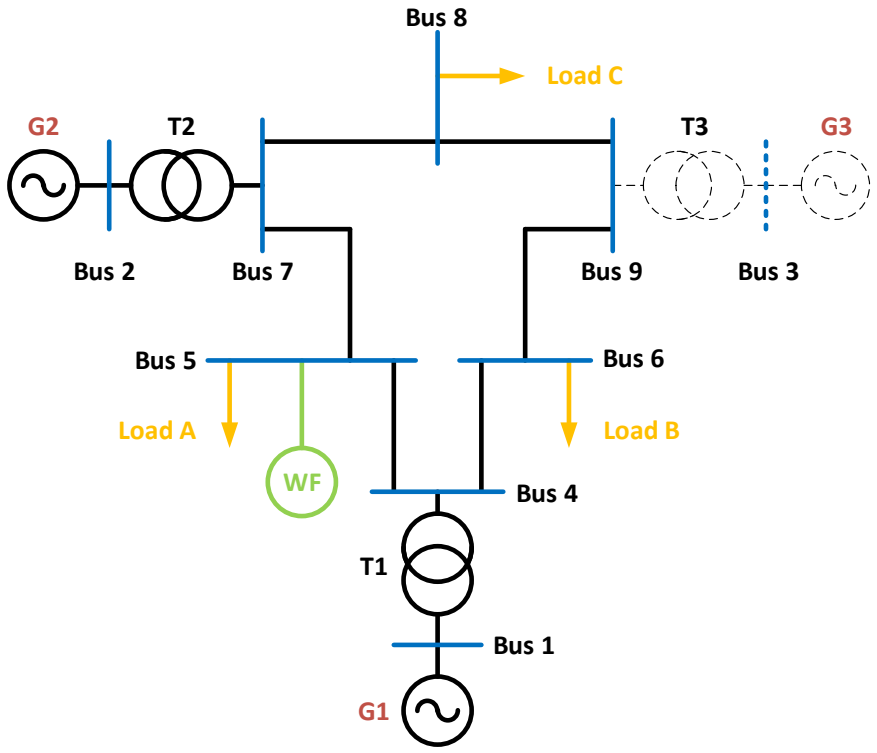

Figure 5.7: Reduced Inertia Case Single Line Diagram

5.3.1 Load Flow Analysis for Reduced Inertia Case

In this case, the same active power reference (163MW) is again assigned to generator-2. Besides, the wind farm generates active power, 35.7MW at unity power factor. Since the generator-3 is out of service, generator-1 loading is increased. Load flow analysis for reduced inertia case is given in Table 5.8.

Bus #	Bus Type	Voltage(pu)	Angle(°)	Pg(MW)	Qg(MVAr)	Pl(MW)	Ql(MVAr)
1	SL	1.04	0	121.76	16.26	0	0
2	PV	1.025	4.18	163	0.65	0	0
4	PQ	1.0332	-3.74	0	0	0	0
5	PQ	1.0083	-5.63	0	0	125-(35.7)	50-(0)
6	PQ	1.0224	-7.65	0	0	90	30
7	PQ	1.0294	-1.36	0	0	0	0
8	PQ	1.0207	-5.82	0	0	100	35

Table 5.8: Load Flow Results for Reduced Inertia Case

5.3.2 Reduced Inertia Case Frequency Response for Additional Load Connection

Decommissioned system is also subjected to the same frequency disturbance which is the additional load connection from Bus 6. System frequency response is observed and compared to Base Case and Modified Case in Fig. 5.8a. The frequency response of the system gets worse with the generator 3 decommissioned. It results that the frequency nadir is decreased from 49.77Hz to 49.65Hz due to the decrease in the stored kinetic energy in the system. The deteriorated frequency response can also be seen from the comparison of RoCoFs that is given in Fig. 5.8b.

5.4 %10 Renewable Generation Case with Synthetic Inertia

The frequency response of the %10 renewable generation case is investigated in Section 5.2 and the system frequency was almost the same with test system base case. However, the response of the system can be improved by provision of synthetic inertia. By utilizing the inertial support in the wind turbines, the effective kinetic inertia of the system can be increased. To achieve this purpose, the active powers of the wind turbines are increased according to the grid RoCoF.

$$2H_{max,med}\overline{f}_{max}\frac{d\overline{f}_{max}}{dt} = \Delta\overline{P}_{e,max} \tag{5.1}$$

$$2H_{max,med}\frac{0.25}{50} = \frac{1}{3.04} \tag{5.2}$$

$$H_{max,med} = 32.9s \tag{5.3}$$

Chapter 4 estimates the turbine capability for inertial support depending on the wind speed in the site. Since the wind speed is selected as 9m/s for all turbines in the farm, each wind turbine is able to increase its active power by 1MW according to the Section 4.1. According to the maximum increase 1MW in the active power and the worst case RoCoF 0.25H/s, maximum inertia constant which can be emulated in the wind speed 9m/s is calculated in Eq. (5.3). However, the increase in the high speed

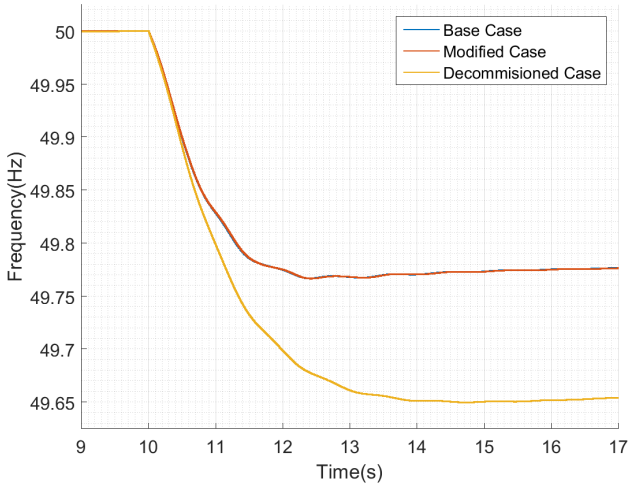

(a) Comparison of Frequencies

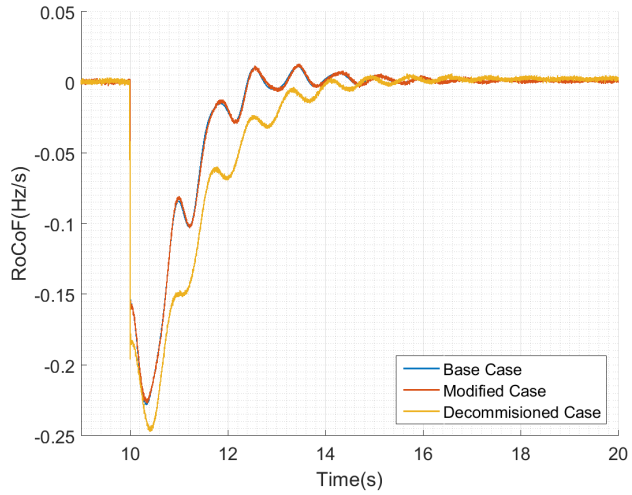

(b) Comparison of RoCoFs

Figure 5.8: Comparison of Base Case, %10 Renewable Case (Modified Case) and Reduced Inertia Case (Decommissioned Case)

limits the maximum inertia constant to 10s as derived in Eq. (5.4). As the RoCoF decreases, the inertia to be emulated can be increased above 10s. Hence, the wind turbines are equipped with synthetic inertia that emulates inertia constants of 5s, 10s and 15s. The active power generation of the wind turbines are shown in Fig. 5.9b. The inertial support is provided simultaneously in each wind turbine following the frequency disturbance. The increase in the active power is much lower than 1MW

which implies that the turbine is under utilized. The system response with inertial support provision is given in the Fig. 5.9a.

$$2H_{max,all}\frac{0.25}{50} = 0.1 \tag{5.4}$$

$$H_{max,all} = 10s \tag{5.5}$$

Since the modified case frequency response is almost the same with the base case, the synthetic inertia implementation is improved the system frequency response. In other words, the wind turbines are integrated to the system by emulating the synchronous generator behaviour. It should be noted that huge amount of kinetic energy up to 18 MJ exists in the wind turbine systems. That stored energy can be utilized with the synthetic inertia method in order to improve frequency dynamics of the system.

Emulation of synchronous generator behaviour is basically increasing the amount of active power depending on the RoCoF of the grid and the inertia constant to be emulated. Since the higher inertia constant requires higher active power increase, the inertia constants of 10s and 15s result in better frequency dynamics. The frequency nadir of the base case is slightly increased.

The effect of the synthetic inertia provision can also be observed in the system RoCoF values. Fig. 5.9c shows that the base case experiences RoCoF up to 0.23Hz/s during the first second of the frequency disturbance. While the remaining cases is subjected to lower RoCoF at first (0.18-0.21Hz/s), the base case RoCoF is the lowest following seconds. Another observation is that all cases converges to the same steady state frequency due to the fact that inertial support affects the transient rather than the steady state values. The steady state frequency is dependent on the capacity of conventional synchronous generators and their droop constants. This is why the reduced inertia case steady state frequency is lower than that of 10% renewable case. Due to the fact that the frequency nadir of the system is closed to the steady state frequency (the frequency where the decline in the frequency is arrested and stabilized), the improvement in the frequency nadir is small. The system frequency nadir would be improved

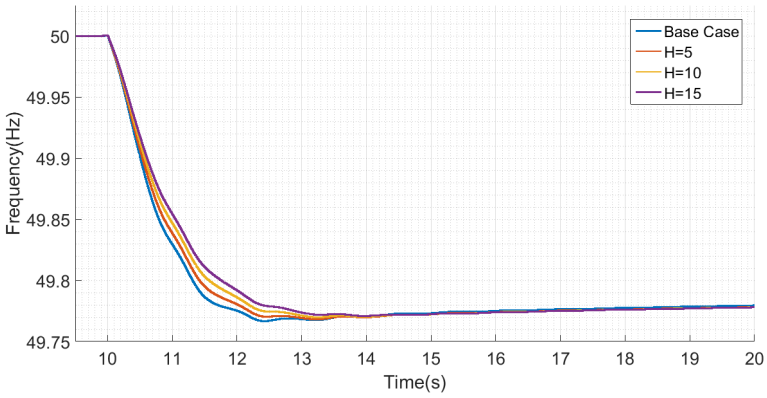

(a) Comparison of Frequencies

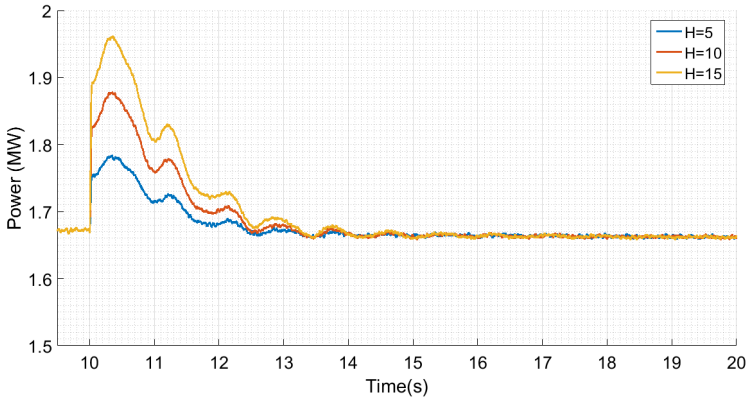

(b) Active Power Generations of the Wind Farms (wind speed=9m/s and n=1490rpm)

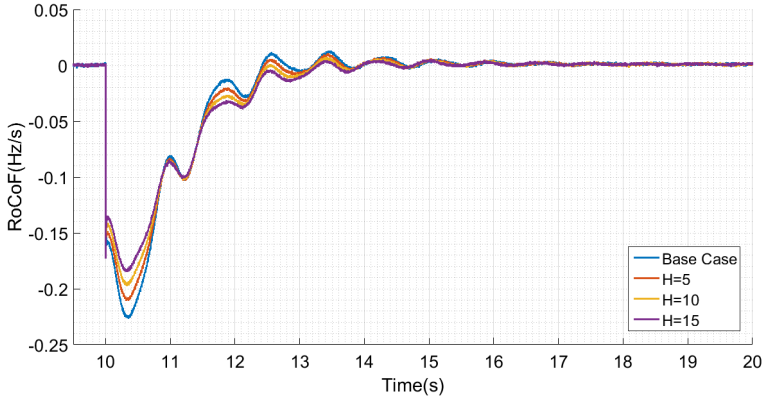

(c) Comparison of RoCoFs

Figure 5.9: Emulation of the Different Inertia Constants in the %10 Renewable Generation Case

significantly if the frequency nadir is significantly below the steady state frequency.

5.5 Reduced Inertia Case with Synthetic Inertia

Reduced Inertia case frequency response for 10% additional load connection is studied in the Section 5.3. The System frequency experiences high RoCoF up to 0.25Hz/s and frequency nadir, 49.65Hz because of the removal of the generator-3. In this section, synthetic inertia method is again implemented in the wind farm with different inertia constants 5s, 10s and 15s. The resultant frequency responses are shown in the Fig. 5.10a. As in the 10% renewable case, base case frequency response experiences steepest decline up to 0.25Hz/s meanwhile the maximum value of RoCoF decreases down to 0.19Hz/s.

The active power generations of the wind farm for the different inertia constants are given in Fig. 5.10b. It should be noted that the active power of the wind turbine is proportional with the RoCoF that is also given in Fig. 5.10c. Notice that inertia constant H=15s is also emulated. It is stated that conventional generator inertia constants lie between 2-9s [35]. Nonetheless, synchronous generators have constant kinetic energy in the nominal frequency. However, the kinetic energy stored in the turbine inertia fluctuates with the generator speed. Moreover, wind turbine is able to emulate different inertia constant as soon as it has the capacity to increase its power. Even with the inertia constant of 15s, the wind turbine is far away from its maximum allowable power for the wind speed 9m/s. However, the turbine inertia constant is limited with H=10s for the high wind speed operation. In this way, it is ensured that wind turbine is able to emulate the inertia constant H=10s independent of the wind speed. However, the turbine is under utilized for the low and medium wind speed ranges.

The comparison of the case properties is given in Table 5.9. The base case and 10% Renewable case maximum RoCoFs are the same as 0.23Hz/s meanwhile it increases up to 0.25Hz/s in the reduced inertia case. In the reduced inertia case, the network power frequency characteristic decreased due to the generator-3 outage. Therefore, the frequency stabilizes in a lower frequency, 49.65Hz. Finally, by emulating inertia

constant H=10s, the effective kinetic energy is increased above the stored kinetic energy. Consequently, the synthetic inertia implementation decreases the maximum RoCoF values down to 0.19Hz/s for 10% Renewable Generation case and 0.21Hz/s for Reduced Inertia Case.

	Without Synthetic Inertia Implementation			With Synthetic Inertia (H=10s)	
	Base Case	10% Renewable Generation Case	Reduced Inertia Case	10% Renewable Generation Case	Reduced Inertia Case
Stored Kinetic Energy	3.3	3.6	3.3	3.6	3.3
Effective Kinetic Energy (GJ)	3.3	3.3	3	3.9	3.6
Maximum RoCoF (Hz/s)	0.23	0.23	0.25	0.19	0.21
Network Power Frequency Characteristic (MW/Hz)	113.5	113.5	87.9	113.5	87.9
Frequency Nadir (Hz)	49.77	49.77	49.65	49.77	49.65

Table 5.9: Comparison of the Case Properties

5.6 Comparison of the Synthetic Inertia and Fast Inertial Support

In the Chapter 4, it is shown that the wind turbines have sufficient capacity in order to increase its active power. For medium and high wind speed cases, increase up to 48% can be achieved. This capacity in the wind turbine is utilized in Chapter 4 for the fast inertial support which is the fast release of active power from energy generating unit. The exaggerated inertial supports are studied to observe the turbine internal dynamics. Besides, the fast inertial support is studied for 10% increase in the active power in different support durations.

In this section, the fast inertial support will be compared with the inertial support that

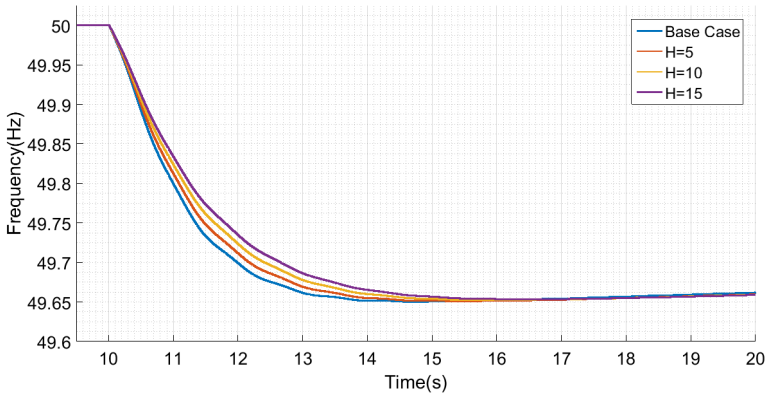

(a) Comparison of Frequencies

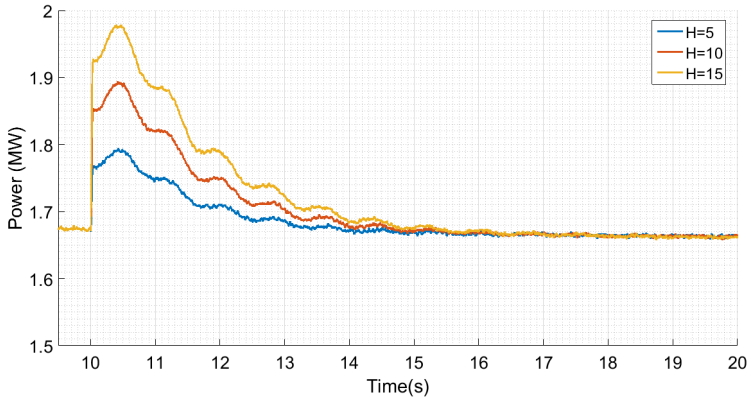

(b) Active Power Generations of the Wind Farms (wind speed=9m/s and n=1490rpm)

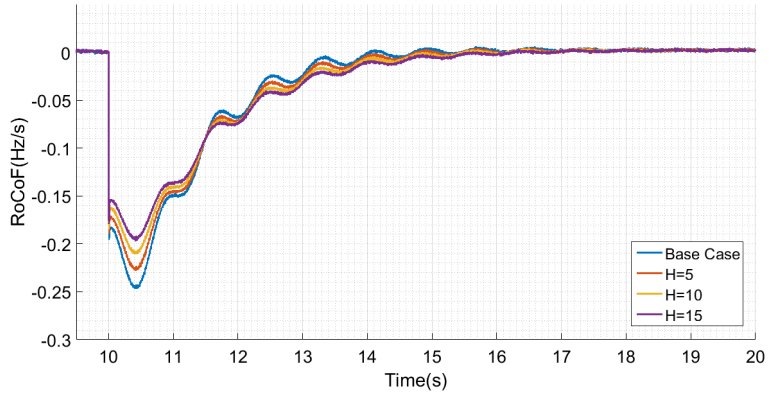

(c) Comparison of RoCoFs

Figure 5.10: Emulation of the Different Inertia Constants in the Reduced Inertia Case

is proportional to grid RoCoF. In other words, increasing active power by a defined percentage will be compared to a rise in the active power proportional to RoCoF. For this reason, the same frequency disturbance is tested on the reduced inertia case, the case where inertia constant of 10s is emulated and also the one with fast inertial support with 5% increased power by 5 seconds. The inertia constant is selected as 10s since it is applicable to whole wind speed range. The fast inertial support with 5% active power increase is selected such that the same amount energy (400kJ) will be extracted from wind turbine during the 5 seconds following the disturbance.

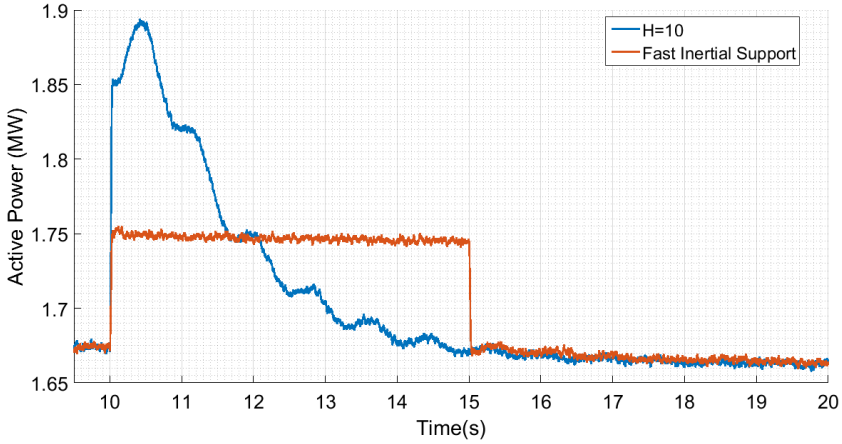

(a) Comparison of the Active Powers

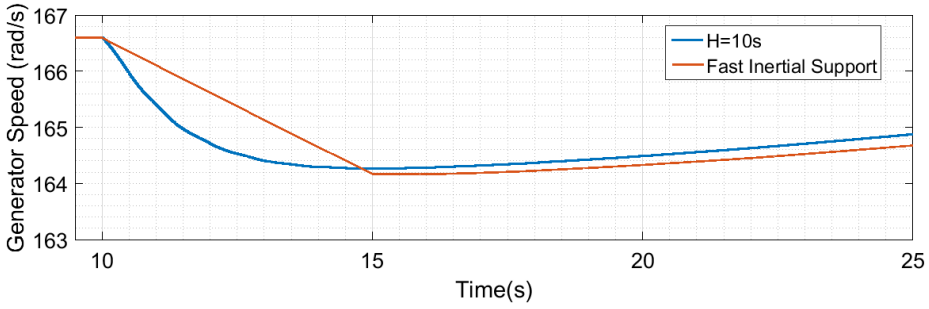

(b) Comparison of Generator Speeds

Figure 5.11: Comparison of Fast Inertial Support and Synthetic Inertia

Fig. 5.11a shows the variation of the active power. It should be underlined that the active power of the inertia emulated case is increased proportional to the RoCoF. Therefore, it declines as the RoCoF declines. Therefore, in the other half of the support time, it is below of the fast inertial support case. This phenomena can be

clearly observed in the frequency response. Nonetheless, the active power of the fast inertial support is the same during the support. The variation of the generator speed is depicted in Fig5.11b. When the same amount of power is extracted from turbine in the fast inertial support, the speed decreases linearly. However, the change in the speed is higher at the beginning of the support for synthetic inertia implementation due to high RoCoF. Nonetheless, the final speeds of supports are the same due to fact that the same amount of power is extracted for both cases. Notice that the pitch angle is zero for this operation since the generator speed is below the maximum generator speed, ω_{max}.

The frequency response of these three cases is shown in Fig. 5.12. It is obvious that the base case frequency response has the poorest transient frequency. Besides, the synthetic inertia implemented case has the best transient behaviour for the very first seconds. Nonetheless, the fast inertial support case first converges to higher steady state frequency until the end of the support period. However, as soon as the support ends, the sharp decrease in the active power results a second dip in the frequency. The decrease in the active power can be considered as a second load connection to system. Therefore, the frequency is exposed to a second decrease at the end of support period in fast inertial support implementation. In contrary, the synthetic inertia case active power is decreased down to lower values as the RoCoF is positive. Than means that the recovery process is already started inside the support. Hence, the secondary dip is not observed in this case.

Finally, it should be noted that the energy extracted from wind turbine during support duration are the same for both methods as 400kJ. However, synthetic inertia support utilizes that energy better by distributing the energy according to the RoCoF. The maximum value of the RoCOF in the Reduced Inertia case is 0.25Hz/s. The fast inertial support decreases the RoCoF value down to 0.23Hz/s. Nonetheless, maximum value of the RoCoF decreases to 0.21Hz/s with the synthetic inertia implementation thanks to the active power increase according to the RoCoF. The maximum value of the RoCoF is crucial especially for the RoCoF relays. Even though the frequency nadir in the system is not increased significantly, the limitation of the RoCoF value is important for the successful operation of the system. If one more outage due to the RoCoF protection of the generator occurs in the system, the cascading generator trip

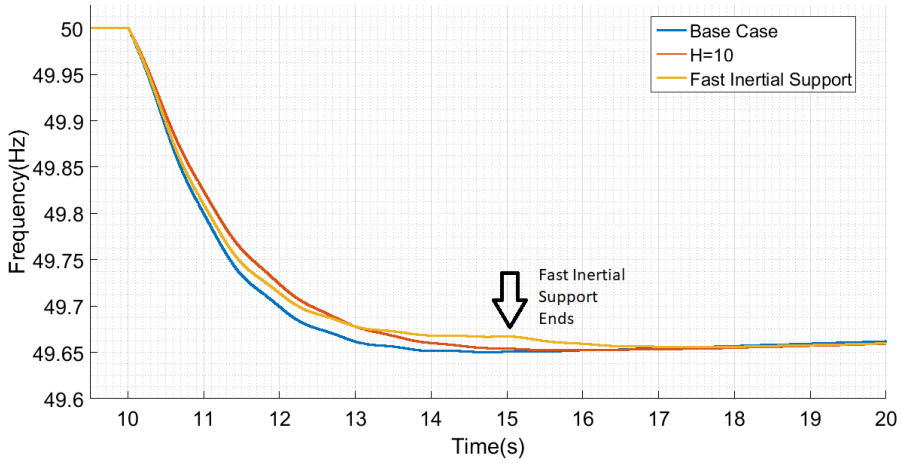

Figure 5.12: Comparison of the Frequency Responses for the Base, Fast Inertial Support and Synthetic Inertia Cases

might end up with the system blackout. Therefore, the synthetic inertia implementation is important for weak power systems with high wind penetration.

5.7 Effect of the Synthetic Inertia to Turkish Electricty System

The installed wind energy capacity of the Turkey has reached 7012MW on the July 2018 [57]. In the Turkish market, 97% of the installed wind turbines belongs to Nordex, Enercon, Vestas, GE, Siemens and Gamesa. The wind turbine topology used by Nordex is DFIG which is connected to grid by partial scale power converter (PSPC) meanwhile the models of Enercon are connected to grid by full-scale power converter (FSPC). Besides, Vestas and GE uses both DFIG or PMSG topologies. By considering the wind turbine models inside the wind farms in Turkey, the share of the wind turbines that are connected to grid with FSPC is found as 54%. The share of the wind turbines with FSPC can be used to estimate the energy produced by this category.

The aggregated inertia constant of the electricity network depends on the generation variety. In other words, the grid aggregated inertia changes according to the share of the conventional generators and the share of renewable energy in the total energy production. Therefore, it is a function of the stored kinetic energy and the total gener-

ated power. The variation of the power generation between 01 Jan. 2018 and 31 Dec. 2018 is given in the Fig. 5.13 according to the data shared by TEİAŞ Transparency Platform [9]. The highest generation occurred on 03 Aug. 2018 as 45923MW meanwhile the lowest generation occurred on 16 Jun. 2018 which is one of the Ramadan Feast days.

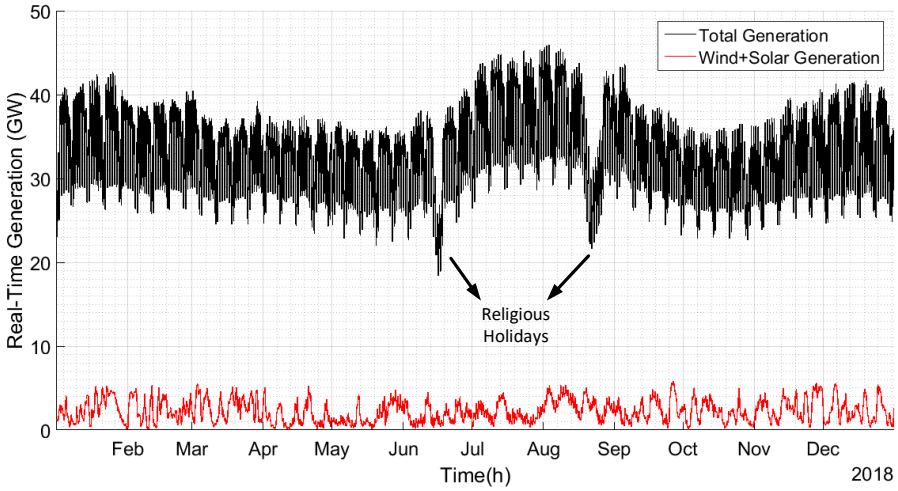

Figure 5.13: Variation of the Total and Solar+Wind Energy Production between 01 Jan. 2018 and 31 Dec. 2018 (hourly basis) [9]

The inertia constants of conventional synchronous generator vary between 2-9s [35] as stated in the previous chapters. As the variety of the generating units changes, the aggregated grid inertia constant also changes. However, in order to observe the effect of the renewable energy on the grid inertia constant, the inertia constant of the generating units can be assumed as constant as H=5s. The stored kinetic energy in the electricity network is estimated by assuming inertia constant H=5s for conventional generators and zero inertia constant for wind and solar energy generation. Due to the absence of the inertial contribution from wind and solar energy systems, the aggregated inertia constant goes below 5s. The aggregated inertia constant deviates from 5s with the increase in the wind and solar generation. The variation of the aggregated inertia constant is depicted in Fig. 5.14. The minimum and maximum of aggregated inertia is 3.97s and 4.99s respectively.

The grid aggregated inertia can be increased by the synthetic implementation in the wind turbines with FSPC. In order to estimate the system inertia with the synthetic

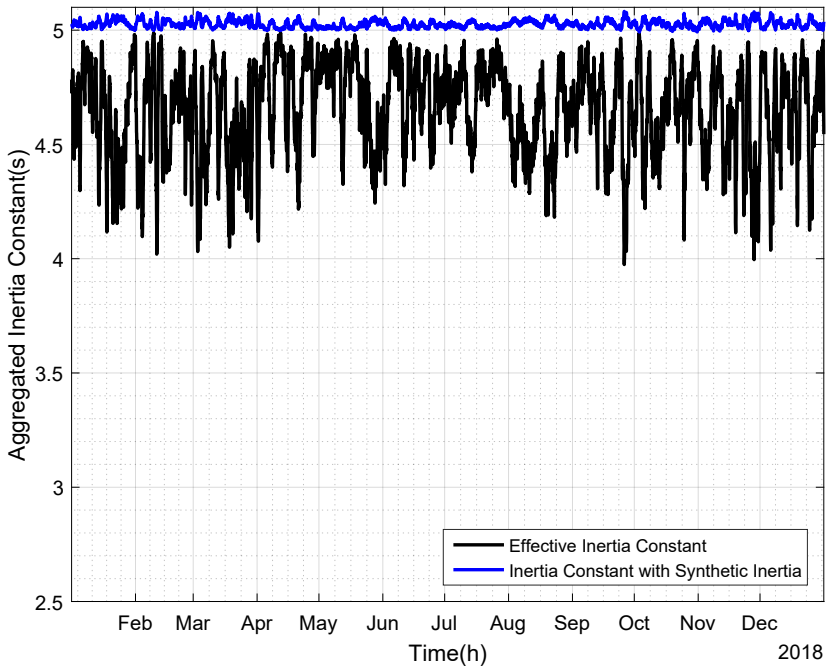

Figure 5.14: Variation of the Aggregated Inertia Constant between 01 Jan 2018 and 31 Dec. 2018 (hourly basis)

inertia implementation, all wind turbines with back-to-back converter are assumed to be able to provide inertial support with the inertia constant H=10s. Moreover, it is assumed that the generated wind power is distributed homogeneously inside each wind farm. In this way, the generation from FSPC wind turbines can be assumed as 54% of total wind generation. According to these assumptions, grid aggregated inertia constant is calculated and presented in Fig. 5.14. In this case, the minimum and maximum values of the inertia constant is found out to be 4.99s and 5.08s.

The network details of the inertia constant extremes are listed in Table. 5.10. The existing system inertia constant deviates according to the share of the generation. The inertia constant decreases down to 3.97s that is the worst case scenario in the system. The reason of the decrease is the high wind generation profile. Nonetheless, best improvement in the aggregated inertia constant is achieved with the same scenario. This means that the existing wind turbines with FSPC are able to compensate the deterioration caused by other wind turbine technologies (DFIG and other).

Existing System			Inertial Support Implementation (H=10s)		
	Minimum Inertia H=3.97s	Maximum Inertia H=4.99s		Minimum Inertia H=4.99s	Maximum Inertia H=5.08s
Date	26/09/2018 03:00	12/04/2018 09:00	Date	03/10/2018 10:00	26/09/2018 03:00
Total Generation (MW)	27495.5	34828.4	Total Generation (MW)	33552.0	27495.5
Wind (FSPC) (MW)	3045.4	37.9	Generation (MW)	26.7	3045.4
Wind (Other) (MW)	2594.2	32.3	Wind (Other) (MW)	22.8	2594.2
Solar (MW)	0.0	11.7	Solar (MW)	56.4	0.0
Other (MW)	21772.9	34639.5	Other (MW)	33446.1	21772.9

Table 5.10: Contribution of the Synthetic Inertia Implementation to System Aggregated Inertia based on 2018 Generation Data

5.8 Conclusion

In this chapter, it is shown that the wind turbine is able to emulate high inertia constants up to 32.9s. In the low and medium speed range, the turbine converter has capacity to increase the power by significant amounts such as 1.3MW. Nonetheless, the turbine converter is not available for the increase in the active power especially in high wind speeds. Therefore, the inertia constant that can be emulated inside the whole wind speed range is found out to be 10s.

The provision of inertial support that is proportional to grid RoCoF is more advantageous than that of fast inertial support. First of all, the grid frequency is not subjected to a second frequency dip since the support power goes below the pre-disturbance power according to the RoCoF. In contrary, the step decrease at the end of support duration creates another frequency disturbance in the fast inertial support. Therefore, synthetic inertia implementation is more appropriate for weak power systems compared to fast inertia support since it deteriorates the stability of the weak power

systems. Another advantage of the synthetic inertia implementation is the provision of additional power that is proportional to grid RoCoF. In this way, the turbine contributes the grid stability depending on the requirement of the power grid. Therefore, the synthetic inertia implementation is better shaped fast inertial support.

Wind turbines can contribute to the grid frequency stability by emulating inertia constants. A variety of inertia constants can be emulated by wind turbine inside the low and medium speed ranges. However, the high wind speed scenario limits the active power increase and the inertia constant to be emulated. Therefore, inertia constant H=10s is appropriate for the whole wind speed range.

By using the inertia constant H=10s, the effect of the synthetic inertia on the Turkish electricity network is observed. It is shown that the implementation on the wind turbines with FSPC can compensate the degradation in the effective inertia constant of the grid.

CHAPTER 6

EVALUATION OF FAST INERTIAL RESPONSE AND SYNTHETIC INERTIA IMPLEMENTATION

Increase in the share of renewable energy in the installed capacity brought operational problems. Due to the fact that PV systems do not have rotational mass at all or wind turbines with full-scale or partial scale power electronics do not effectively contribute the grid aggregated inertia, the power system with increasing renewable energy penetration will be exposed to high RoCoF for the frequency disturbances. This implies that system will encounter unacceptable RoCoF values (around the RoCoF protection settings of the generating units) in the normal operation as long as the renewable penetration continues. Therefore, the upcoming future power system will require auxiliary services such as synthetic or virtual inertial support from all generation technologies that includes power electronics.

Renewable energy systems produces power according to the type of its power source. The input power is constant for an instant since the source (solar radiation, wind speed etc.) is constant. Therefore, the operation of renewable systems is different from the conventional power plants in which input power can be increased steadily by the operator. Nonetheless, an additional energy source is required in the renewable systems in order to increase active power as desired. For this purpose, kinetic energy in wind turbine blades and generator can be utilized. In this way, the wind turbines are able to increase their active output power by extracting the kinetic energy stored in the turbine equivalent inertia. However, the amount of active power increase can be either non-dynamic as in the case of Chapter 4 or dynamic (proportional to RoCoF) as in the case of Chapter 5.

6.1 Fast Inertial Support

Wind energy systems with full-scale power electronics can adjust its active power by controlling its output torque. Therefore, the active power can be quickly raised by extracting the stored energy in turbine inertia. However, the maximum value of the active power depends on the operating conditions. Since the generator active power is also dependent on its speed, turbine power cannot be increased up to rated power but to half of the rated power in wind speeds lower than 5m/s. In wind speeds above 10m/s, the active power before the support is already close to its rated value. Therefore, the increase in the active power is limited as 10% (as long as converter rating has the capacity) in high wind scenarios.

In this study, the wind turbine can increase its active output power by 1.2MW in the wind speeds between 5m/s and 8m/s for fast inertial response. The highest active power release is found in the wind speed 6.5m/s as 1.3MW. Besides, wind turbines can contribute better in low wind scenarios than that of high wind speed for short time intervals. However, when the active power increase is limited with 10%,

It should be noted that the frequency disturbance occurs due to the unbalance between input mechanical power and output powers of the generators. Hence, the additional amount of active power that is provided from renewable energy sources in such instants is favourable. This is why the amount of increase in the active power is more important than the final active power amount. Therefore, knowledge of active power limits reveals the potential of wind turbines with FSPC in order to contribute the frequency stability of the power systems.

Fast inertial response can be provided within different time durations up to 30 seconds. Since the larger amount of support might result in higher speed deviations, the support time might be decreased. In contrary, higher support durations can be achieved with lower amount of fast inertial response.

Fast inertial response in this study is not a direct function of the RoCoF. In other words, the support power is independent from RoCoF or frequency deviation. However, the activation of the support is based on a RoCoF threshold of 0.1Hz/s with the frequency dead-band 10mHz. A RoCoF indexing can be developed to obtain different

support power values. In this case, the indexing scheme requires a RoCoF threshold and different RoCoF intervals. The highest RoCoF interval corresponds to the most severe frequency disturbances case and requires the highest amount of fast inertial support release with highest available support time. Meanwhile, the lowest RoCoF interval would be assigned to lowest inertial support release with time duration in order not to result higher speed deviation. It should be noted that the higher energy extraction might even result in the stall of the turbine. Nonetheless, critical instant following the disturbance is much more important than the turbine speed recovery. Hence, grid operators might choose to extract the available active power in the expense of turbine stall according to the optimized decision.

6.2 Synthetic Inertia Implementation

Even though wind turbine power can be increased as desired inside the 0.1pu and 0.45pu range by using fast inertial support, the fastest release of the power independent of the frequency is not the best solution especially for weak power grids. Although additional amount of power is released in the disturbances, the restoration of the energy to the turbine causes might create a second frequency decrease in the grid. Therefore, the increase amount should be in coordination with the grid frequency behaviour. This is why dynamic frequency response is obtained with the synthetic inertia implementation in the Chapter 5.

By adjusting active power according to the RoCoF of the grid, the active power is increased or decreased depending on the grid status. If the frequency decreases, additional amount of active power proportional to RoCoF will be injected to grid. The advantage of the dynamic frequency response is the fact that the active power is decreased below the pre-disturbance power value as grid RoCoF is positive. This implies that the restoration of the turbine speed begins with positive RoCoF avoiding a second drop in the frequency.

In order to observe the effects of synthetic inertia implementation, a dynamical 9-bus test system is constructed in Matlab-Simulink environment. The test system is composed of the conventional generators and subjected to a frequency disturbance

with a load connection. In order to see the effects of the renewable energy penetration, a wind farm with 20 turbines is connected to system. In the 10% Renewable Case, the system frequency behaviour is not affected from the renewable penetration. The maximum RoCoF of 0.23Hz/s is observed in the system. The maximum RoCoF decreased down to 0.25Hz/s in the Reduced Inertia Case. The frequency behaviours are improved by the synthetic inertia by lowering the RoCoF values down to 0.19Hz/s in 10% Renewable Case and 0.21Hz/s in the Reduced Inertia Case.

The most important feature of the synthetic inertia implementation is the RoCoF dependency. The inertial support in this method does decrease the active power as soon as RoCoF turns positive meaning that turbine speed recovery can be started. Thus, the speed recovery of the synthetic inertia method begins with the frequency nadir is reached.

The synthetic inertia implementation is used for improving the transient behaviour of the frequency. In the literature, variety of inertia constants are emulated in variable speed wind turbines between the inertia constant up to 10 seconds [31], [58]. Nonetheless, Chapter 4 demonstrates that the wind turbines are able to increase its active power temporarily by 0.45pu. Therefore, in this study inertia constants more than 10 seconds are also tested. Nonetheless, the inertia constants more than 10s is not possible in the high wind speed range. Nonetheless, inertia constant of 10s is applicable for whole speed range. Inertia constants above 10s can also be achievable as long as the converter rating is available. In the worst case scenario, output power saturates to the limit for a part of the support duration. However, as the RoCoF decreases, output power can follow the commanded output power.

Synthetic inertia implementation in the Turkish electricity network is also evaluated based on the hourly generation data from 2018. The effect of the varying generation profile is calculated by considering wind and solar energy. It is proven that the decrease in the aggregated inertia constant of the grid can be compensated with the help of synthetic inertia implementation to wind turbines with FSPC. In fact, the wind turbines with FSPC are able to compensate not only the decrease due to their existing structure but also the decrease due to other wind turbines (DFIG and Type I-II) and PV systems. This is why the synthetic inertia should be implemented in all of the

wind turbines with full-scale power converter.

6.3 Economical Motivations for Energy Providers

As explained in Section 2.5.4, renewable energy systems in Turkey and most of the EU countries sell electricity with feed-in tariff. It basically means that all the generated energy will be bought for sure without trading inside the market. Even though the problems are arising with renewable energy systems, the energy providers would not be a volunteer for ancillary services unless the regulations impose sanctions or additional payment is provided. Hence, the system operator should prepare more advantageous paying mechanisms in order to persuade energy providers to implement grid supporting methods.

The system operators has already started preparing new frequency regulations. One of the examples is the Firm Frequency Response (FFR) by National Grid [59]. FFR is basically frequency support method that is activated with the frequency thresholds. As the frequency falls below a pre-determined value, the response is needed from energy providers (either from synchronous generator or energy storage units). These energy providers are taken into operation according to tenders. The response is either non-dynamic (independent from the frequency shift) or dynamic (pre-determined percentage increase according to frequency). Moreover, the support power should be sustained up to 30 seconds dynamic response and up to 30 minutes for non-dynamic response for the primary [60]. This is why the response is provided by synchronous generators and energy storage systems in which active power output can be adjusted as desired. It should be noted that this mechanism is not appropriate for the renewable energy systems where the output power can be increased up to 30 seconds by utilizing the stored energy in the inertia or DC-link capacitor.

Another frequency regulating mechanism is applied in USA according to the FERC 755 regulation [61]. The frequency regulation includes different metrics for payment such as capacity, performance and mileage. Based on this regulation, energy price for the high performance frequency regulation resources is increased over three times of the old price of the PJM which is a regional transmission company [62]. Since one of

the metrics effecting the payment is performance, the regulation is advantageous for energy storage systems that can adjust its active power quickly thanks to their power electronics interface.

When the wind turbine is used for inertial support mechanisms, additional power up to 0.45pu can be achieved for 3s or 0.1pu power with unlimited duration (as long as converter can handle). The longer time durations might cause problems for power converter such as heating. Even though the turbine injects significant amount of power to grid, the additional amount of energy (4000KWs) is negligible compared to daily energy production. Therefore, the payment to energy provider for the additional amount of energy would not be beneficial.

In order to investigate the economical side of the frequency regulating mechanisms in the renewable energy systems, a frequency support case is evaluated with two hypothetical payment methods. One of the methods takes into account of the additional energy supplied during the frequency disturbance. Other payment method considers the availability of the wind turbine. Table 6.1 shows the average energy generation according to the measurements from site as well as the hypothetical profits from inertial support based on either additional energy or incentive. It is obvious that the wind turbine in this study earns average 1679$ each day. If the additional active power is sold with a 248.2$/MWh price (3.4XFeed-In Tariff), 2.76$ additional profit is yielded by assuming 10 daily support. This corresponds to 0.16% of the daily profit and it is insignificant to energy provider.

Second payment method is based on the availability of the wind turbine for the frequency regulation mechanisms. Notice that renewable energy systems get additional payment from the local content bonus. A similar incentive can be assigned to wind turbines for their availability for grid supporting mechanisms. For this purpose, the lowest local content bonus amount which is additional 0.6cent/kWh for local turbine tower is used for this study. Therefore, the turbines providing synthetic inertia support is paid with 79$/MWh. In this way, 138$ additional profit can be obtained regardless of the number of support or the additional energy. In this case, the energy provider can increase the average income by 8.2%. Therefore, assigning incentives for the grid supporting services might be attractive for the energy providers. Moreover, sys-

Base Case Profit		
Daily Generated Energy Production	23	MWh
Feed-In Tariff	73	$/MWh
Daily Generation	1679	$
Profit by Additional Energy		
Energy From Single Support	4000	kWs
Supported Energy Price (3.4xFeed-In Tariff)	248.2	$/MWh
Additional Profit for Single Support	0.276	$
Number of Support (Daily)	10	
Additional Profit	2.76	$
Profit with Incentive		
Generated Energy	23	MWh
Supported Feed-In Tariff	79	$/MWh
Additional Profit	138	$

Table 6.1: Comparison of the Frequency Support Pricing Methods

tem operators of the weak power grids might lean towards the inertial support by wind turbine operators even at the expense of the additional incentives to the energy providers.

The effect of the wind and solar energy is investigated at the end of Chapter 5. It is shown that grid aggregated inertia constant depends on the wind and solar production. The variation of the kinetic energy stored in the grid is given in Fig. 6.1. The average stored energy in the grid can be increased by 8% with the synthetic inertia implementation. Notice that the difference between the existing stored energy and the one with synthetic inertia implementation is dependent on the share of wind and solar systems. Therefore, the difference between these energies will increase with the increasing renewable penetration. Therefore, the system operator should prepare frequency regulating regulations for the renewable energy systems. Moreover, a convincing solution should be constructed to avoid upcoming frequency stability problems.

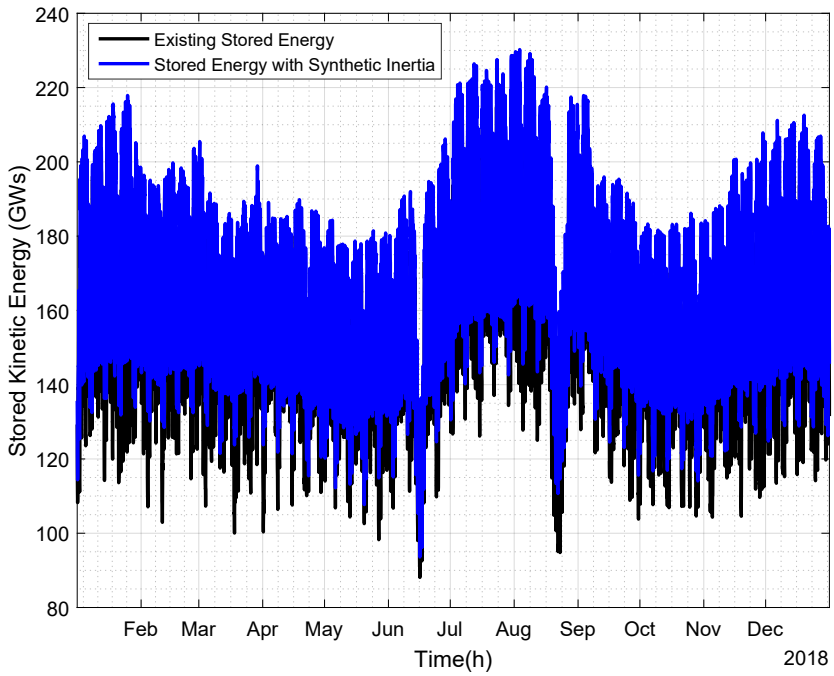

Figure 6.1: Variation of the Stored Kinetic Energy between 01 Jan. 2018 and 31 Dec. 2018 (hourly basis)

6.4 Future Work

The following issues can be further studied in detail:

- Fast inertial support implementation has huge potential to increase the active power. However, as soon as the support ends, the decrease in the active power resembles a second load connection to system especially in the weak power systems. Therefore, the system is exposed to a secondary decrease in the frequency. This is why the amount of additional power should be adjusted according to the grid frequency. Hence, a support index can be developed to reshape the fast inertial support.
- The increase percentage of fast inertial support is not a function of the grid parameters. The index to be constructed should also determine the increase percentage based on the pre-determined values.
- The effects of the fast inertial support on the DC-link voltage might be bet-

ter investigated with more realistic modelling. The effectiveness of the new modelling might be tested in the wind turbine emulators.

- When the support is required in the high wind speeds, support power might hit the maximum allowed converter powers. The extra heat and mechanical stresses might also be tested in wind turbine emulators.
- Storage technologies would increase the support time and amount. Economical motivations can be united with storage technologies.

REFERENCES

[1] "Enerji Kaynaklarının Elektrik Enerjisi Üretimi Amaçlı Kullanımına İlişkin Kanunda Değişiklik Yapılmasına Dair Kanun," 2011.

[2] International Renewable Energy Agency (IRENA), *IRENA (2018), Renewable capacity statistics 2018*. 2018.

[3] International Renewable Energy Agency, *Renewable Energy Statistics 2017*. 2017.

[4] E. Muljadi, V. Gevorgian, and M. Singh, "Understanding Inertial and Frequency Response of Wind Power Plants Preprint," *2012 IEEE Power Electronics and Machines in Wind Applications (PEMWA)*, no. July, pp. 1–8, 2012.

[5] J. Eto, J. Undrill, P. Mackin, R. Daschmans, B. Williams, B. Haney, R. Hunt, J. Ellis, H. Illian, C. Martinez, M. OMalley, K. Coughlin, and K. Hamachi-LaCommare, "Use of Frequency Response Metrics to Assess the Planning and Operating Requirements for Reliable Integration of Variable Renewable Generation," no. December 2010, pp. LBNL–4142E, 2010.

[6] TEİAŞ, "Yük Tevzi Raporları," 2019.

[7] J. B. Ekanayake, N. Jenkins, and G. Strbac, "Frequency Response from Wind Turbines," *Wind Engineering*, vol. 32, no. 6, pp. 573–586, 2008.

[8] I. Erinmez, D. Bickers, G. Wood, and W. Hung, "NGC experience with frequency control in England and Wales-provision of frequency response by generators," *IEEE Power Engineering Society. 1999 Winter Meeting (Cat. No.99CH36233)*, vol. 1, pp. 590–596 vol.1, 1999.

[9] TEIAS, "TEIAS Transparency Platfrom," 2019.

[10] P. M. Anderson and A. A. Fouad, *Power System Control and Stability*. 2 ed., 2003.

[11] European Commission, "Communication from the Commission to the European Parliament, the Council, the European economic and social Committee and the Committee of the Regions - 20 20 by 2020 - Europe's climate change opportunity," *COM (2008) 30 final*, p. Brussels, 2008.

[12] European Parliament, "Directive 2009/28/EC of the European Parliament and of the Council of 23 April 2009," *Official Journal of the European Union*, vol. 140, no. 16, pp. 16–62, 2009.

[13] Eurostat, "Renewable energy in the EU-newsrelease," Tech. Rep. January, 2018.

[14] REN21, *Renewables Global Futures Report*. 2017.

[15] IRENA, "A Renewable Energy Roadmap," Tech. Rep. June, 2014.

[16] H. Klinge Jacobsen and E. Zvingilaite, "Reducing the market impact of large shares of intermittent energy in Denmark," *Energy Policy*, vol. 38, no. 7, pp. 3403–3413, 2010.

[17] M. Zipf and D. Most, "Impacts of volatile and uncertain renewable energy sources on the German electricity system," *International Conference on the European Energy Market, EEM*, 2013.

[18] A. Ipakchi and F. Albuyeh, "Grid of the future," *IEEE Power and Energy Magazine*, vol. 7, no. 2, pp. 52–62, 2009.

[19] D. Gautam, L. Goel, R. Ayyanar, V. Vittal, and T. Harbour, "Control strategy to mitigate the impact of reduced inertia due to doubly fed induction generators on large power systems," *IEEE Transactions on Power Systems*, vol. 26, no. 1, pp. 214–224, 2011.

[20] J. Van De Vyver, J. D. M. De Kooning, B. Meersman, L. Vandevelde, and T. L. Vandoorn, "Droop Control as an Alternative Inertial Response Strategy for the Synthetic Inertia on Wind Turbines," *IEEE Transactions on Power Systems*, vol. 31, no. 2, pp. 1129–1138, 2016.

[21] G. Lalor, J. Ritchie, S. Rourke, D. Flynn, and M. O'Malley, "Dynamic frequency control with increasing wind generation," *IEEE Power Engineering Society General Meeting, 2004.*, pp. 1–6, 2004.

[22] J. Ekanayake, "Control of DFIG wind turbines," *Power Engineer*, vol. 17, no. 1, pp. 28–32, 2003.

[23] J. Ekanayake and N. Jenkins, "Comparison of the response of doubly fed and fixed-speed induction generator wind turbines to changes in network frequency," *IEEE Transactions on Energy Conversion*, vol. 19, no. 4, pp. 800–802, 2004.

[24] J. Morren, S. de Haan, W. Kling, and J. Ferreira, "Wind Turbines Emulating Inertia and Supporting Primary Frequency Control," *IEEE Transactions on Power Systems*, vol. 21, no. 1, pp. 433–434, 2006.

[25] J. Morren, J. Pierik, and S. W. de Haan, "Inertial response of variable speed wind turbines," *Electric Power Systems Research*, vol. 76, no. 11, pp. 980–987, 2006.

[26] X. Wang, W. Gao, J. Wang, Z. Wu, W. Yan, V. Gevorgian, Y. Zhang, E. Muljadi, M. Kang, M. Hwang, and Y. C. Kang, "Assessment of system frequency support effect of PMSG-WTG using torque-limit-based inertial control," in *2016 IEEE Energy Conversion Congress and Exposition (ECCE)*, pp. 1–6, IEEE, sep 2016.

[27] X. Wang, S. Member, W. Gao, S. Member, J. Wang, S. Yan, M. Kang, S. Member, M. Hwang, S. Member, Y. Kang, S. Member, and E. Muljadi, "Inertial Response of Wind Power Plants : A Comparison of Frequency-based Inertial Control and Stepwise Inertial Control," pp. 0–5, 2016.

[28] J. Zhu, C. D. Booth, G. P. Adam, A. J. Roscoe, and C. G. Bright, "Inertia emulation control strategy for VSC-HVDC transmission systems," *IEEE Transactions on Power Systems*, vol. 28, no. 2, pp. 1277–1287, 2013.

[29] J. C. Hernández, P. G. Bueno, and F. Sanchez-sutil, "Enhanced utility-scale photovoltaic units with frequency support functions and dynamic grid support for transmission systems," vol. 11, pp. 361–372, 2017.

[30] J. F. Conroy and R. Watson, "Frequency response capability of full converter wind turbine generators in comparison to conventional generation," *IEEE Transactions on Power Systems*, vol. 23, no. 2, pp. 649–656, 2008.

[31] F. Gonzalez-Longatt, E. Chikuni, and E. Rashayi, "Effects of the Synthetic Inertia from wind power on the total system inertia after a frequency disturbance,"

Proceedings of the IEEE International Conference on Industrial Technology, pp. 826–832, 2013.

[32] K. Clark, N. W. Miller, and J. J. Sanchez-gasca, "Modeling of GE Wind Turbine-Generators for Grid Studies Prepared by :," tech. rep., 2010.

[33] Enercon, "Grid Integration and Wind Farm Management," tech. rep., 2018.

[34] F. Gonzalez-Longatt, A. Bonfiglio, R. Procopio, and D. Bogdanov, "Practical limit of synthetic inertia in full converter wind turbine generators: Simulation approach," in *2016 19th International Symposium on Electrical Apparatus and Technologies, SIELA 2016*, 2016.

[35] P. Kundur, *Power System Stability and Control*. McGraw-Hill,Inc.

[36] J. Machowski, J. W. Bialek, and J. R. Bumby, *Power system dynamics: stability and controlJohn Wiley & Sons,*. 2011.

[37] T. P. Chen, "Dual-modulator compensation technique for parallel inverters using space-vector modulation," *IEEE Transactions on Industrial Electronics*, vol. 56, no. 8, pp. 3004–3012, 2009.

[38] T. Ackermann, *Wind Power in Power Systems Wind Power in Power Systems Edited by*, vol. 8. 2005.

[39] S. Heier, *Grid Integration of Wind Energy*. 3 ed., 1998.

[40] Q. Wang and L. Chang, "An Intelligent Maximum Power Extraction Algorithm for Inverter-Based Variable SpeedWind Turbine Systems," *IEEE Transactions on Power Electronics*, vol. 19, no. 5, pp. 1242–1249, 2004.

[41] M. Barakati, M. Kazerani, and D. Aplevich, "Maximum Power Tracking Control for a Wind Turbine System Including a Matrix," vol. 24, no. Mc, p. 4244, 2009.

[42] T. Thriringer and J. Linders, "Control by Variable Rotor Speed of a Fixed Pitch Wind," *IEEE Transactions on Energy*, vol. 8, no. 3, pp. 520–526, 1993.

[43] S. M. Barakati, *Modeling and Controller Design of a Wind Energy Conversion System Including a Matrix Converter*. PhD thesis, University of Waterloo, 2008.

[44] W. Lu and B. T. Ooi, "Multiterminal LVDC system for optimal acquisition of power in wind-farm using induction generators," *IEEE Transactions on Power Electronics*, vol. 17, no. 4, pp. 558–563, 2002.

[45] Q. Zeng, L. Chang, and R. Shao, "Fuzzy-logic-based maximum power point tracking strategy for PMSG variable-speed wind turbine generation systems," *Canadian Conference on Electrical and Computer Engineering*, no. 1, pp. 405–409, 2008.

[46] W. M. Lin, C. M. Hong, and C. H. Chen, "Neural-network-based MPPT control of a stand-alone hybrid power generation system," *IEEE Transactions on Power Electronics*, vol. 26, no. 12, pp. 3571–3581, 2011.

[47] H. Polinder, J. A. Ferreira, B. B. Jensen, A. B. Abrahamsen, K. Atallah, and R. a. McMahon, "Trends in Wind Turbine Generator Systems," *IEEE Journal of Emerging and Selected Topics in Power Electronics*, vol. 1, no. 3, pp. 174–185, 2013.

[48] J. Ukonsaari and N. Bennstedt, "Wind Turbine Gearboxes: Maintenance Effect on Present and Future Gearboxes for Wind Turbines," tech. rep., 2016.

[49] M. P. Kazmierkowski, R. Krishnan, and F. Blaabjerg, *Control in Power Electronics—Selected Problems*. New York: Academic, 2002.

[50] F. Blaabjerg, R. Teodorescu, M. Liserre, and A. V. Timbus, "Overview of control and grid synchronization for distributed power generation systems," *IEEE Transactions on Industrial Electronics*, vol. 53, no. 5, pp. 1398–1409, 2006.

[51] M. Chinchilla, S. Arnaltes, and J. C. Burgos, "Control of permanent-magnet generators applied to variable-speed wind-energy systems connected to the grid," *IEEE Transactions on Energy Conversion*, vol. 21, no. 1, pp. 130–135, 2006.

[52] T. Orłowska-Kowalska, F. Blaabjerg, and J. Rodríguez, *Advanced and intelligent control in power electronics and drives*. 2014.

[53] H. Brantsæter, Ł. Kocewiak, A. R. Årdal, and E. Tedeschi, *Passive filter design and offshore wind turbine modelling for system level harmonic studies*, vol. 80. Elsevier B.V., 2015.

[54] R. Eriksson, N. Modig, and K. Elkington, "Synthetic inertia versus fast frequency response: a definition," *IET Renewable Power Generation*, vol. 12, pp. 507–514, 2017.

[55] F. M. Gonzalez-longatt, "Activation Schemes of Synthetic Inertia Controller on Full Converter Wind Turbine (Type 4)," no. Type 4, 2015.

[56] F. Wu, P. Zheng, Y. Sui, B. Yu, and P. Wang, "Design and experimental verification of a short-circuit proof six-phase permanent magnet machine for safety critical applications," *IEEE Transactions on Magnetics*, 2014.

[57] Turkish Wind Energy Association, "Turkish Wind Energy Statistic Report," tech. rep., 2018.

[58] F. M. Gonzalez-Longatt, "Activation Schemes of Synthetic Inertia Controller for Full Converter Wind Turbine Generators,"

[59] National Grid Electricity Transmission, "Firm Frequency Response Tender Rules and Standard Contract Terms," 2016.

[60] K. Smethurst and V. Walsh, "Testing Guidance For Providers Of Firm Frequency Response Balancing Service," *National Grid*, no. November, p. 3, 2017.

[61] Federal Energy Regulatory Commission, "18 CFR Part 35-Frequency Regulation Compensation in the Organized Wholesale Power Markets," 2011.

[62] NEC Energy Solutions, "Application: Frequency Regulation (US)," tech. rep., Westborough, 2014.

Appendix A

P.M. ANDERSON TEST CASE PROPERTIES

Loads	Location (Bus Number)	Active Power (MW)	Reactive Power (MVAr)
Load A	5	125	50
Load B	6	90	30
Load C	8	100	35

Table A.1: Load Data of the P.M. Anderson Test System

From Bus	To Bus	Resistance (R) (pu)	Reactance (X) (pu)	Susceptance (B/2) (pu)
4	5	0.0100	0.8500	0.0880
4	6	0.0170	0.0920	0.0790
5	7	0.0320	0.1610	0.1530
6	9	0.0390	0.1700	0.1790
7	8	0.0085	0.0720	0.0745
8	9	0.0119	0.1008	0.1045

Table A.2: Line Data of the P.M. Anderson Test System

Parameter	Location (Bus Number)	Active Power (MW)	Reactive Power (MVAr)
Nominal Apparent Power (MVA)	247.5	192	128
Nominal Voltage (kV)	16.5	18	13.8
Nominal Power Factor	1	0.85	0.85
Plant Type	hydro	steam	steam
Rotor Type	salient	round	round
Nominal Speed (rpm)	180	3600	3600
x_d (pu)	0.146	0.8958	1.3125
x'_d (pu)	0.0608	0.1198	0.1813
x_q (pu)	0.0969	0.8645	1.2578
x'_q (pu)	0.0969	0.1969	0.25
x_l (pu)	0.0336	0.0521	0.0742
τ'_{d0} (s)	8.96	6	5.89
τ'_{q0} (s)	0	0.535	0.6
Stored Energy at nominal speed (MWs)	2364	640	301
Inertia (s)	9.5515	3.3333	2.3516

Table A.3: Generator Data of the P.M. Anderson Test System

Transformers	From Bus	To Bus	High Voltage Side (kV)	Low Voltage Side (kV)	Reactance (pu)
Transformer 1	1	4	230	16.5	0.0576
Transformer 1	2	7	230	18	0.0625
Transformer 1	3	9	230	13.8	0.0586

Table A.4: Transformer Data of the P.M. Anderson Test System